THE CONTROL OF THE PROPERTIES OF POLYETHYLENE THROUGH ITS POLYMERISATION

A thesis submitted to
the University of Southampton
in support of candidature for
the degree of
Doctor of Philosophy

by

Philippe Jean-Marie MATHIEU, Maitre-es-Sciences, D.E.S.T.

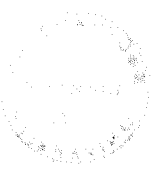

October 1981

Acknowledgements

I would like the following people to find here the expression of my most sincere gratitude:

Dr. P.J. HENDRA for supervision, guidance and encouragement during this project.

Dr. A.D. CAUNT and Mr. M.E.A. CUDBY of I.C.I. Limited for fruitful discussions and supervision during my stays at Welwyn Garden City.

Dr. R.D. SANG for proof-reading the manuscript.

My thanks are also due to all the people I met during my stay in Southampton and who made my life enjoyable.

Finally, S.R.C. for financial support and I.C.I. Plastics Division for the provision of experimental facilities.

CONTENTS

UNIVERSITY OF SOUTHAMPTON

ABSTRACT

FACULTY OF SCIENCE

Doctor of Philosophy

THE CONTROL OF THE PROPERTIES OF POLYETHYLENE THROUGH ITS POLYMERISATION

by Philippe Jean-Marie Mathieu

In order to understand correlations between structural models of polymers and observed properties, various unusual polymerisations of ethylene were carried out. A detailed description of the polymerisation equipment and procedure is given. The effect of the major polymerisation parameters is reported and a selection of our own polymers is described.

Molecular characterisation (light scattering, G.P.C. and infrared) examination were made on our polymers as well as commercial ones. Melt viscosity was studied using a cone and plate rheometer. Mechanical property studies were made by impact and tensile experiments. Crystallisation studies were made by density determination of the degree of crystallinity and lamellar thickness by Raman Spectroscopy.

Molecular characterisation revealed that some samples prepared here have relatively high molecular weight values (about 8 to 10 times those of commercial grades used as comparisons). The melt and mechanical properties are very different from the comparisons. Some of the differences can be explained through molecular weight grounds alone but it is not sufficient. It is known that an increase in molecular weight causes mechanical properties to change because networks occur. This is due to molecular entanglements which inevitably occur in the longest chains. It is considered that the improved properties cannot fully be explained on this basis alone. It is suggested that the explanation comes from the original polymerisation reaction. In order to make the polymers, polymerisation reactions were carried out such a way that the growing chains could easily entangle with each other. It is suggested that this idea should be further studied.

Some evidence was also found that some of the entanglements are destroyed during the working up of the polymers after they have been made.

In the conclusion of the thesis, it is suggested that the project has to be enlarged to maximise the presence of entanglements which might lead to the creation of new polymeric grades which could even become gels in the molten state.

CHAPTER I

INTRODUCTION

I.1 Amorphous and crystalline polymers

Polymers can be divided into two categories: those which are wholly amorphous and those which are partly crystalline. Some polymers, such as atactic polystyrene are wholly amorphous under almost all conditions; other polymers which are partly crystalline may be amorphous under certain conditions, e.g. above their melting point, or if quickly quenched from their molten condition into the glassy state. Polyethylene terephtalate (PET) is an example of the latter type.

The two categories are very readily distinguished from each other by X-ray diffractometry. The amorphous polymers show the same type of diffuse halo in their diffractograms as do simple liquids. The local structure of an amorphous polymer or of a simple liquid does not have the high degree of spatial order which is characteristic of crystals. From the point of view of longer range order, the structure of an amorphous polymer might be considered as comparable to the contents of a bowl of spaghetti. The spaghetti-like molecules, are in a state of wriggling motion whose amplitude and speed depend on temperature.

The X-ray diffractograms of crystalline polymers show a series of sharp rings superposed on some diffuse scattering. The diffuse scattering comes from the amorphous regions of the polymers; the sharp rings come from regions of crystalline orders (crystallites) embedded in the amorphous matrix. The individual crystallites are small, typically 100 Å x 200 Å x 200 Å. The individual crystallites generally group together in large aggregates called spherulites, which are often of a

size easily visible by optical microscopy when viewed between crossed polarisers (Fig. I.1).

The regularity of the polymer chain is the main factor which makes the polymer amo rphous or crystalline. For example atactic polystyrene (in which the configuration of the phenyl groups in the "up" and "down" position along the chain is random) is completely amo rphous, whereas isotactic polystyrene (in which the phenyl groups along the chain are all in the "up" position or all in the "down" position) is generally obtained in a partly crystalline condition (about 50% crystallinity).

Polyethylene is normally crystalline. However, it has been proved recently that it is possible to obtain P.E. in its glassy state (1, 2). High density polyethyline (H.D.P.E.) which has a structure close to linear polymethylene has a high degree of crystallinity (about 90%) and a melting temperature (Tm) $\simeq$ 137°C. One of the low density polyethylenes (L.D.P.E.) which contains roughly an average of two butyl and one ethyl side groups per 100 carbon chain atoms has a lower degree of crystallinity (about 50%) and a melting temperature (Tm) $\simeq$ 110°C. The density of linear polyethylene is typically 0.97; the density of branched polyethylene is around 0.92. It only requires eight ethyl or butyl groups per 100 carbon chain atoms to destroy completely the crystallinity of polyethylene (3).

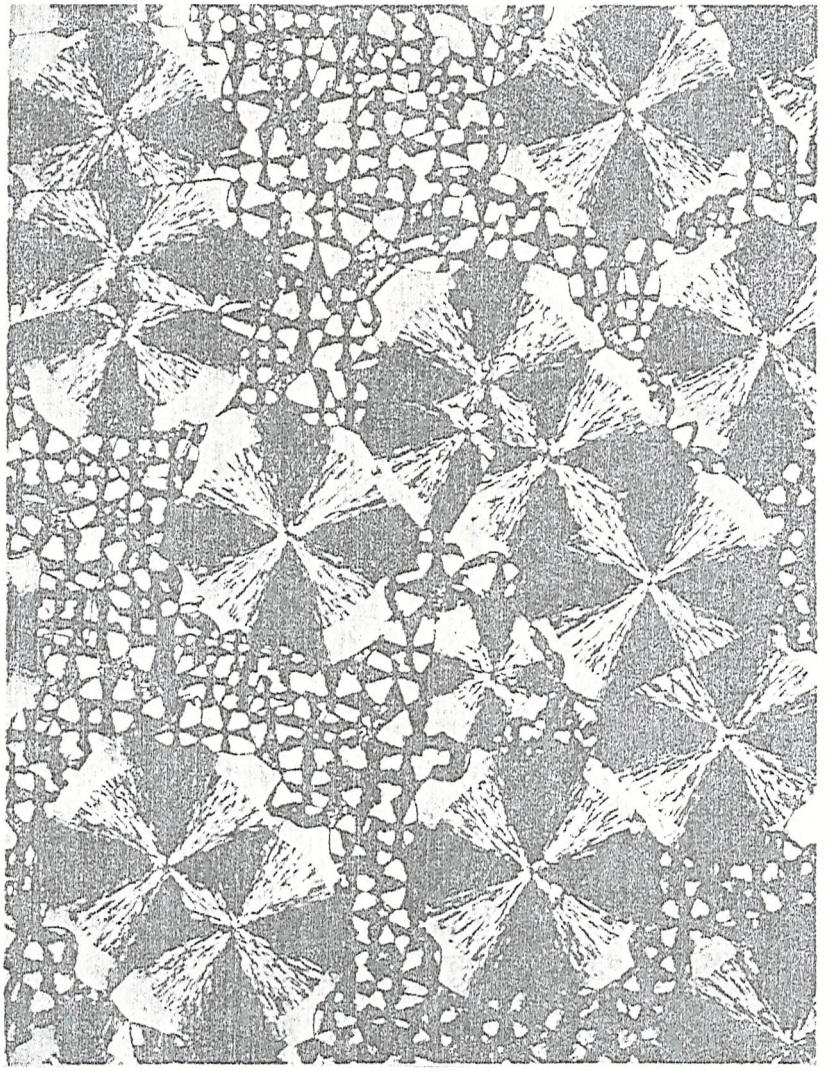

Figure I.1 SPHERULITE STRUCTURE OF A CRYSTALLINE POLYMER VIEWED BETWEEN CROSSED POLAROIDS

I.2 Crystalline polymer morphology

I.2.1 Fringed micelle model

In the early X-rays diffraction studies of polymers (including polyethylene (4)) both sharp and diffuse diffraction effects were reported (5, 6).

The first structural model to explain this observation was the "Fringed micelle" structure (Fig. I.2). It was suggested that the solid consist of well ordered regions or "micelles" (in which the chains lie parallel to each other along their axis) embedded in a matrix of disordered regions. The polymer chains were supposed to meander through both ordered and disordered regions. Using this model X-ray patterns could be interpretated in terms of crystalline and amo rphous regions and the relative contribution of crystalline material could be expressed as the "degree of crystallinity".

This model was abandoned when it was found possible to grow single crystals of polymer from dilute solutions and with the observation that the spherulites produced by polymer crystallised from the melt contain this lamellar structure (see the following sections).

I.2.2 Single crystals

During their studies on polymer crystallisation Keller (7), Fisher (8) and Till (9) independently reported in 1957 that single crystals of polyethylene could be grown from dilute solution in xylene. The examination of the material prepared in this way revealed the existence of thin

Figure I.2 THE "FRINGED MICELLE MODEL" OF SEMICRYSTALLINE POLYMERS (33)

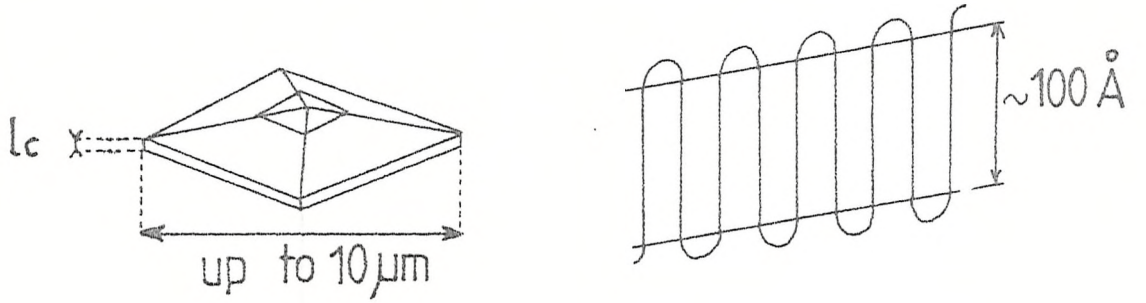

(a) (b)

Figure I.3

(a) lamellar crystal (schematic representation)

(b) chain orientation in a lamellar crystal

platelets or "lamellar" crystals.

These crystals were found to be roughly 100 Å thick and up to several microns in lateral dimensions. Keller (7) determined that the orientation of the molecules was perpendicular (or almost) to the lamellar surfaces (Fig. I.3). As the chain length is at least 100 times longer than the lamellar thickness it was assumed (7) that the chain must re-enter the lamellae several times and adopt a chain folded structure.

Single crystals of various polymers have now been grown from solution, e.g. polypropylene (10, 11), some polyethers (12), polyamides (13) and polyesters (14).

The nature of the fold surface has been of considerable interest, and in particular the degree of disorder present on the fold surface. Use of atomic models shows that at least 5 carbon atoms are required to complete the sharp fold (19), a type of folding which has been observed for the cyclic alkane $C_{34}H_{68}$ (20).

Degradation of the crystalline core is a much slower process (21). Measurement of the lengths of the chain segments thus removed is found to contain a narrow distribution around C_{11} (C_9 to C_{13}). This strongly favours the presence of loose loops rather than adjacent re-entry.

The various models which have mainly been put forward are represented in Fig. I.4.

It has been noted by Keller and O'Connor (15) that when single crystals are held for a period of time just below their melting temperature their thickness increases with the formation of holes in the lamellae during this

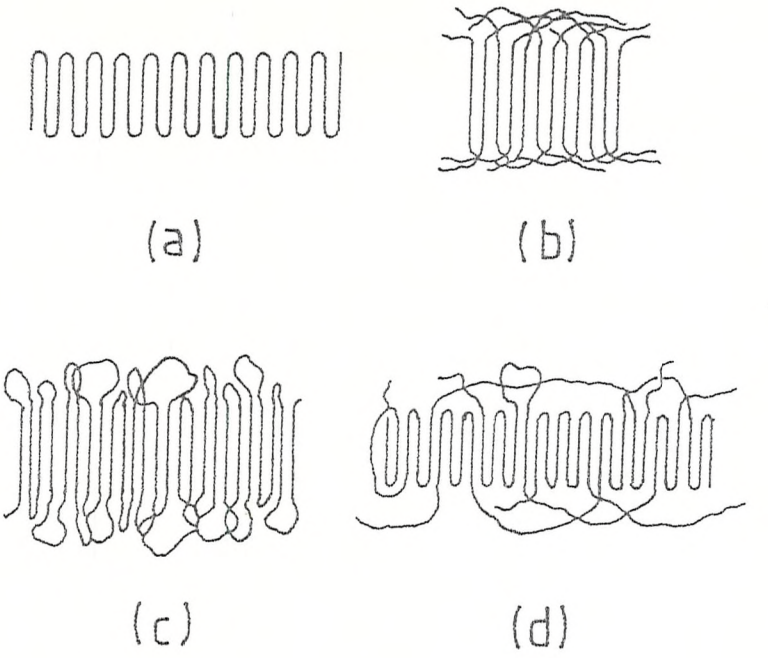

Fig I.4 TWO DIMENSIONAL REPRESENTATION OF MODELS OF THE FOLD SURFACE IN POLYMER LAMELLAE

(a) sharp folds (22)

(b) loose loops with adjacent re-entry (23)

(c) switchboard model (24)

(d) a composite model (25)

process (16) (annealing process). Several mechanisms have been put forward to explain this phenomenon (17, 18).

I.2.3 Melt crystalline polymers

It is well established that polyethylene crystallises from the melt through the growth of spherulites. Crystallisation starts at various nuclei and spreads out in a spherical fashion until the growth fronts of adjacent nuclei touch each other (Fig. I.5).

The fracture surfaces of polyethylene observed by electron microscopy reveal stacks of lamellae twisted around the radial direction . These lamellae have the same dimensions as those in single crystals produced from dilute solutions. Annealing experiments reveal that their thickness increases as shown for single crystals (19, 26, 27).

It is therefore very attractive to relate the structural models of both solution grown and melt crystallised polyethylene.

The controversy which arises over the structure of the surface of the lamellae is of considerable interest. This controversy mainly comes from the different type of crystallisation models put forward by two categories of scientists.

On one hand, those who support Flory think that in the melt the molecules adopt a random coil structure identical to that of the polymer in solution (28, 32). During crystallisation the chains tend to lie parallel to each

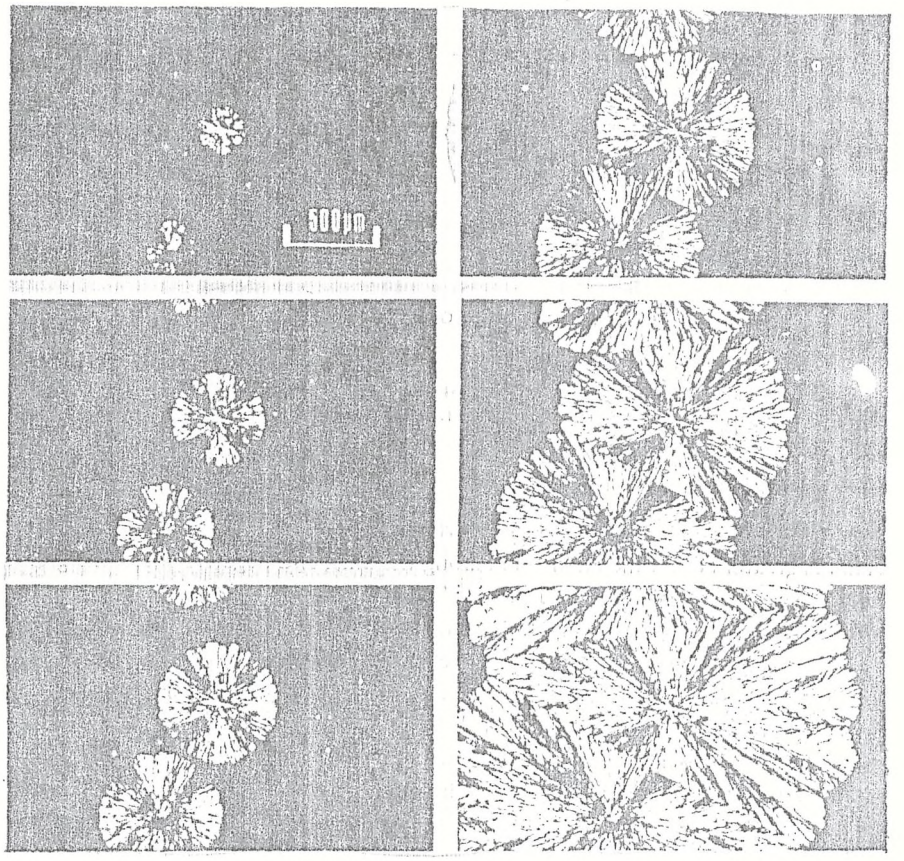

Figure I.5

Sequence of photographs taken, under polarized light, over a period of about 1 min, showing the growth of poly(ethylene oxide) spherulites from the melt. From top left to bottom right; initially discrete spherulites with spherical symmetry are observed but the growing fronts eventually impinge on one another to form an irregular matrix.

other around a nucleus (which could be impurity, dust, single crystal, ... anything but a discontinuity in density). Then the final picture of the solid state is like the one given in Fig. I.6a, for which re-entry of a given lamellae, although of frequent occurence, is not generally at the site adjacent to its emergence from the crystal lamella. Some chains translate from one lamella to another and there are interconnections between the amo rphous and crystalline phase (29).

Conversely, others (including De Gennes and Hoffman) believe that in the molten state some chains are embedded in a pipe formed by other chains (30) (Fig. I.7). When crystallisation occurs the former chains are sucked out from their tube (reptation model) and reeled-in to form a crystalline core. Also the surface of the lamellae is regular with only adjacent re-entries. Between the lamellae lies the amo rphous phase with no interconnection with the crystalline phase (Fig. I.6b).

Many consider that the mobility of chains in the melt is far too sluggish to permit reeling-in of the chain to the growing crystal front. In a recent paper (31), De Gennes describes his reptation model as unsatisfying.

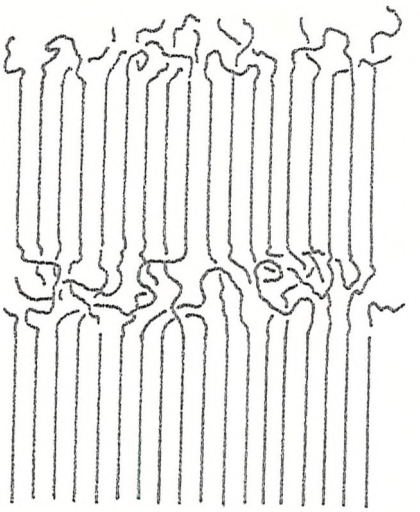

(a)

Molecular arrangements in a lamellar semicrystalline polymer in which different molecules are extensively interwined. Re-entry of a given lamella, although of frequent occurrence, is not generally at the site adjacent to its emergence from the crystal lamella.

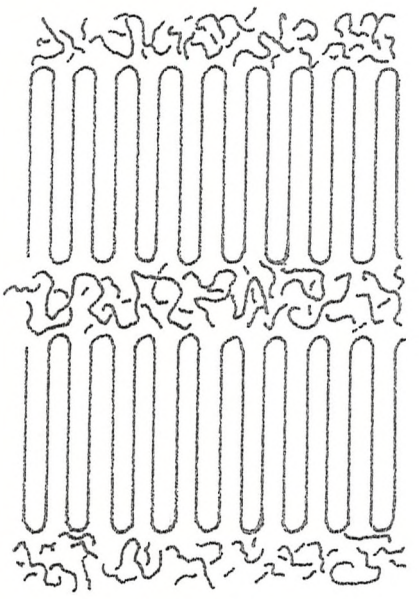

(b)

The regularly folded model for a semi-crystalline polymer. The amorphous interlayers are represented without commitment on the interconnections between the two phases.

Figure I.6

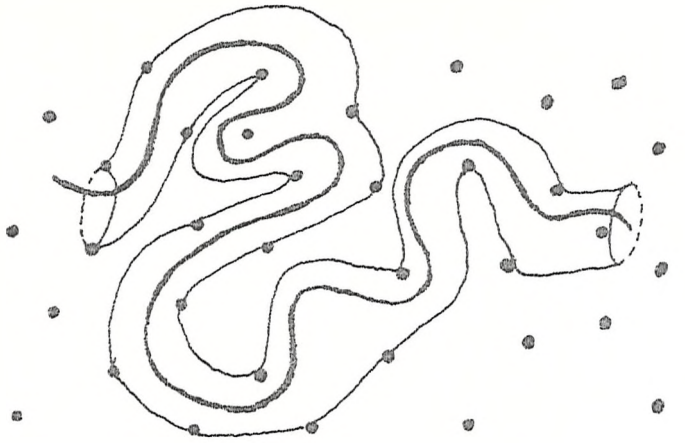

Fig I.7 DE GENNES' MELT MODEL

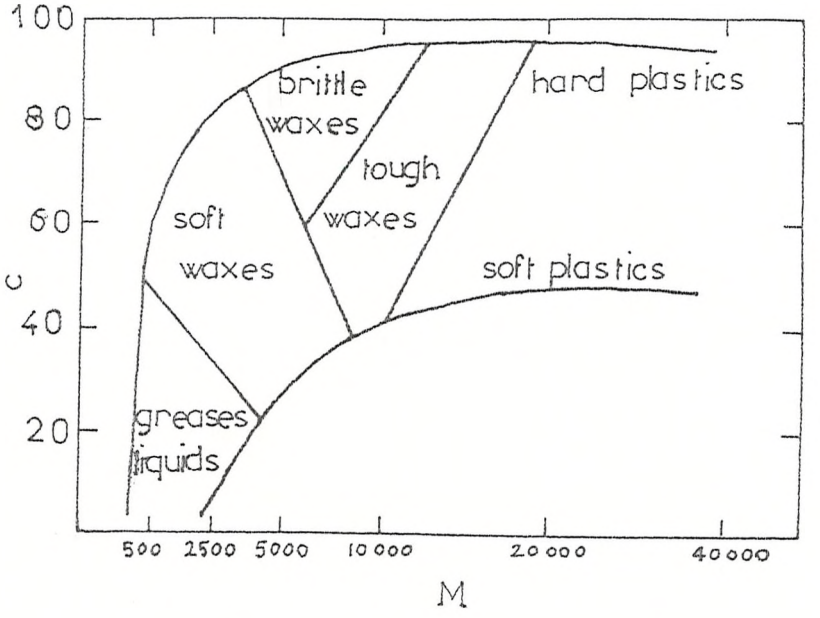

Figure I.8 INFLUENCE OF CRYSTALLINITY AND ON THE PHYSICAL PROPERTIES OF POLYETHYLENE

(the percentage crystallinity 'c' is plotted against molar mass 'M')

I.3 Mechanical properties of polymers

The constant increase on use of synthetic polymers by industry to replace or supplement traditional materials such as wood, metals, ceramics, etc. has stimulated the search for more versatile polymeric structures covering a wide range of properties.

A discussion of the mechanical properties of crystalline polymers requires their classification into several categories depending upon their physical properties and characteristics; among these, there is information about the fine structure i.e. the type of monomer used and/or whether more than one type of monomer is used (copolymerisation), these are the chemical level information, the knowledge of the architectural aspect, e.g. the structure of the conformation of the polymer backbone, i.e. linear, branching, cross-linking, rigidity ..... , the molecular weight characteristics and the degree of crystallinity.

Furthermore, temperature is also important when discussing mechanical properties. Well below the glass transition temperature Tg, molecular motion is essentially absent and the material behaves as a hard, glassy solid with the presence or absence of crystallinity making little difference. Above the melting point, crystallinity plays no part in the properties of the amo rphous melt.

Importance of crystallinity

In Fig. I.8 is reported the influence of crystallinity and chain length on the properties of polyethylene (34). In Table I.1 a classification of crystalline polymers has been made according to the temperature range and the degree of crystallinity.

Although it would be ambitious to describe completely the properties of crystalline polymers some general rules can be defined.

Polymers with low crystallinity such as poly (vinyl chloride) and elastomers polyamides behave like lightly cross-linked amo rphous polymers. The visco-elastic properties of these polymers are more like these of amo rphous polymers except that the transition region between glassy and liquid behaviour is considerably broadened on the temperature scale.

At very low extensions ($< 1\%$) polymers with intermediate degrees of crystallinity (e.g. low density polyethylene) behave much like those with very low crystallinity.

At higher extensions, these polymers exhibit the phenomena of a yield stress and cold drawing with changes in crystalline morphology. Polymers of intermediate degree of crystallinity are characteristically leathery or horny in texture and show good impact resistance which is in many cases retained even below Tg.

The major effects of a further increase in crystallinity to very high values are an increase in modulus and the onset of a tendency towards brittleness. Such polymers, of which high-density polyethylene is typical can be cold drawn only

with difficulty. Tensile failure occurs at or slightly beyond yield stress.

Table I.1 Classification of crystalline polymers

Predominant Properties in Temperature Range	Degree of crystallinity		
	Low (5 - 10%)	Intermediate (20 - 60%)	High (70 - 90%)
Above Tg	Rubbery	Leathery, Tough	Stiff, hard brittle
Below Tg	Glassy, brittle	Hornlike, Tough	Stiff, hard brittle

I.4 Generalities on the flow properties of the polymer melts

Importance of the molecular weight and molecular weight distributions

As it has been shown previously, these characteristics influence the properties of crystalline polymers, but they can in addition drastically change the flow characteristics of the polymer melt. It is therefore very important to know the molecular weight and molecular weight distribution (MWD) when discussing flow properties of the melt.

Only some of the properties relevant to the melt behaviour will be discussed here as it would be too ambitious to attempt to describe them all; the general rules are as follows:

- at low shear stress, the higher the molecular weight the higher the viscosity (lower is the M.F.I.). (The M.F.I. is defined as the mass of polymer extrudated through a standard die under a standard stress at a standard temperature. These values are established by A.S.T.M. (35).. Of all the family of capillary flow systems used, the Melt Flow Indexer is the cheapest and the most widely used.)

- at low shear stress, the broader the molecular weight distribution the higher the viscosity.

At higher shear stress these effects are reversed.

Flow occurs when polymer molecules slide each other. The ease of flow will depend on the mobility of the molecular chains and the forces holding the molecular chains together. In this respect branching is another important factor playing a determining role in the flow properties of polymer melts.

I.5 Morphology - properties correlations

I.5.1 Preliminary

Two approaches to polymer rheology are discernible: that of the theoreticians, who are concerned with a fundamental description of what would happen if certain idealised criteria were met; and that of the practitioner, who is concerned with the results of what is actually happening. To theoreticians, the manipulation of notional equations of state by tensors is of great significance. To practitioners, the fact that an idea works, or does not, overrides all other considerations.

I.5.2 Morphology - properties correlations

Although considerable knowledge regarding the physical characteristics of polymers, such as molecular weight, crystallinity, etc., and correlations between these and their properties are to some extent known and established, a need persists to investigate more in this field taking into account particularly the morphology of the polymer chains either in the melt or in the solid state depending upon the case in question.

Indeed, several theories regarding the micro-morphology or texture of the chains have been put forward but so far no model has been universally accepted. As a consequence, it is difficult to establish correlations between morphology and properties.

In this respect, it is valuable to consider the influence of all the various structural regions present in the melt crystalline material.

For example, although it is well established that brittleness increases with the degree of crystallinity, one has to consider as well the quality of the crystals and the amount of defects in them, as these could drastically modify the brittleness of the material. Secondly, the amo rphous phase between the crystalline lamellae must play a significant role regarding the mechanical behaviour of these materials. Although brittleness is directly related to crystallinity the amo rphous zones are of great interest. However, lack of knowledge of the morphology of the amo rphous phase especially with the controversy over the existence or not of chains translating from one crystalline core to another prevents us advancing any general explanation regarding the mechanical behaviour of crystalline polymers. Thirdly, during melt crystallisation the spherulites grow and spread out from nuclei in a spherical fashion until the growing fronts of two neighbour spherulites meet (Fig. I.5). The front edges, because of the sudden change of morphology, are to some extent susceptible to initiate failure in the polymer is under mechanical stress. Fourthly, the zones in which low molecular weight material, monomer molecules, impurities and defects are rejected into, are again for the same reason as above susceptible to fail under stress.

As a result of the great complexity of the structure and our relatively limited knowledge of it, it is really

difficult to make any attempt at explanation of the mechanical behaviour of crystalline polymers. As a first stage one can list the various characteristics of the polymer versus its mechanical properties. If some relationships seem to be apparent and suggest bridges between theory and practice one must bear in mind that the foundations are not secure.

One example is to consider the crystallinity present in the solid state of a "crystalline" polymer. It is of interest to know how this crystallinity is spread out throughout the material. For a given degree of crystallinity (say 50%) one can derive several pictures of the solid state. Thus one may imagine a structure in which the lamellae are very thick and the amo rphous phase between them very thick too. Alternatively one could envisage crystalline cores that are only layers separated by thin amo rphous phases. Finally one could propose something between these two models. In the two extreme models (Fig. I.9 (a) and (b)) the degree of crystallinity remains the same but the number of interfaces (lamellae amo rphous phase) varies considerably. It is then of interest to study some mechanical properties (for example elongation to break) against the number of interfaces per unit volume. In the study reported here, lamellar thickness measurements are indispensable in addition to the determination of the degree of crystallinity. It has been shown that for melt crystallised polymers (36) these characteristics are interdependent with the melt temperature and the cooling rate.

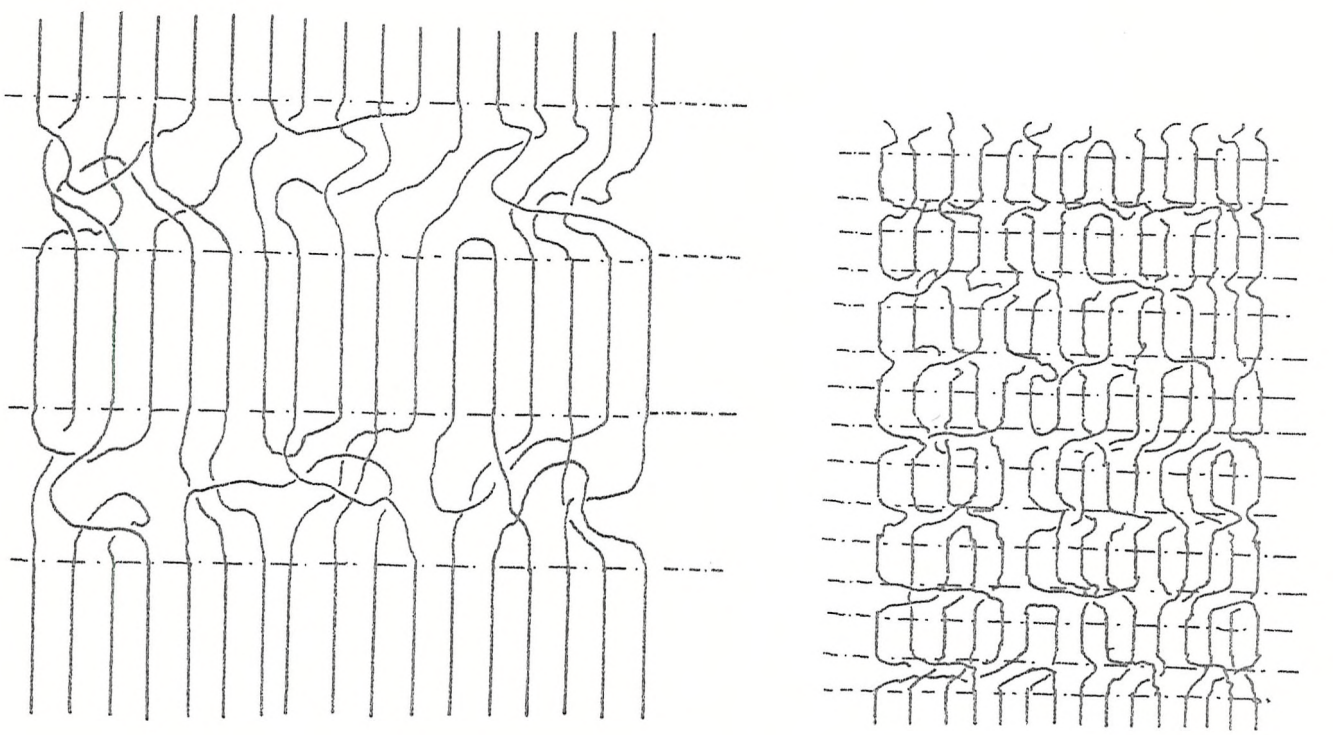

Figure I.9

It has been demonstrated that the morphology of the melt crystallised material is to some extent related to that of the melt from which it is produced (37). It is therefore of interest to know the structure and the characteristics of the melt and all the parameters which can modify its properties. In this respect, it is well established that the molecular weight plays a great role regarding the flow properties of the melt. Assuming that the chains adopt a random coil structure in the melt as they do in solution (28) it is inevitable that the mass formed is very confused and entangled; it seems obvious that the longer the chains the more entangled the mass. A study of the materials crystallized from these melts is of interest in particular to check if polymer melts with different viscosities (or M.F.I.) can crystalline differently when they are cooled down.

To conclude, it is clear that the properties are related to the morphology but this relationship is still unknown. The disagreement between structural models and mechanical properties observed is a proof. Polyethylene, for example, is far less tough than one could hope. All this lack of knowledge is certainly an obstacle in producing better quality polyethylene.

I.6 Reasoning behind project

The basis of this thesis is to answer the following question: can two polymers made differently but apparently identical (same monomer, identical molecular weight characteristics, etc.) behave very differently when they are processed; are their mechanical properties very different from one another? This is extremely important for industrial reasons (use of polymers) of course, but indispensable also for our general knowledge of polymer science.

Basically all the polymers available on the market are made under commercial conditions. This means that a compromise of quality, efficiency and repeatability has been chosen to produce such polymers. The idea of this present project was to demonstrate that polymerisations of a monomer carried out under conditions very different from one another could modify the structure and change the mechanical and rheoligical properties of the polymers produced.

It was therefore decided to produce special polymers which would be compared with commercial ones. The ideal was to produce polymers under extreme conditions in high enough yield for all the experiments and tests necessary to study them. To allow a good comparison between our polymers and the commercial one chosen as a reference, the molecular weight of all the materials had to be in the same range.

All the studies reported here and others not referred to include molecular weight determinations, infrared

examination, rheological behaviour of the polymer melts, mechanical properties of the melt crystallised materials and crystallisation studies (lamellar thickness and crystallinity) of the solid state.

I.7 Choice of polyethylene

For this project which implies fabrication of polymers under particular polymerization conditions, it was decided to carry out this study with polyethylene. The reasons for this are numerous and easily explained.

Polyethylene is the polymer which has the simplest chemical formula - $(CH_2)_n$ -; thanks to its simplicity there is no problem of tacticity, or stereogularity, which one comes across using other polymers. However, there remains the possibility of branching but this can be completely eliminated with high molecular weight material (H.D.P.E.). In that case polyethylene becomes close to polymethylene.

For the experimental practical point of view, it is relatively cheap, easy and safe to produce several batches of polyethylene in the laboratory. It is possible to "play" at will with the polymerization conditions such as catalyst concentrations, temperature, solvent, ... to obtain different types of polymer.

The last important factor is that polyethylene is a universal polymer in today's world; therefore there is a large range of commercial polyethylenes available, with various molecular weight to compare with those produced by our own means.

CHAPTER II

MOLECULAR CHARACTERIZATION

II.1 Average molecular masses and molecular weight distribution

One of the most important features distinguishing a high polymer from a simple molecule is its lack of an exact molecular weight. This is a consequence of the fact that during the polymerization process the length of the polymer molecule is entirely determined by random reactions events. Therefore some chains are longer than others and to characterize the polymer one needs to use average values of molecular weights. Several average values are defined, the most important ones being:

the number average molecular mass

$$\overline{Mn} = \frac{\sum Ni\ Mi}{\sum Ni} = \frac{\sum Wi}{\sum (Wi/Mi)}$$

the weight average molecular mass

$$\overline{Mw} = \frac{\sum Ni\ Mi^2}{\sum Ni\ Mi} = \frac{\sum Wi\ Mi}{\sum Wi}$$

where Ni is the number of molecules of species i of molecular weight Mi and

$Wi = NiMi/N_A$ where N_A is Avogadro's number.

Depending on the techniques used, either $\overline{Mn}$ or $\overline{Mw}$ is obtained. For example ebulliosopy, cryoscopy and osmotic pressure techniques lead to $\overline{Mn}$, light scattering technique leads to $\overline{Mw}$.

A fairly recent technique, gel permeation chromatography (G.P.C.) allows us to determine the relative amount of each species i of molecular weight Mi. (A brief description of the method is given below).

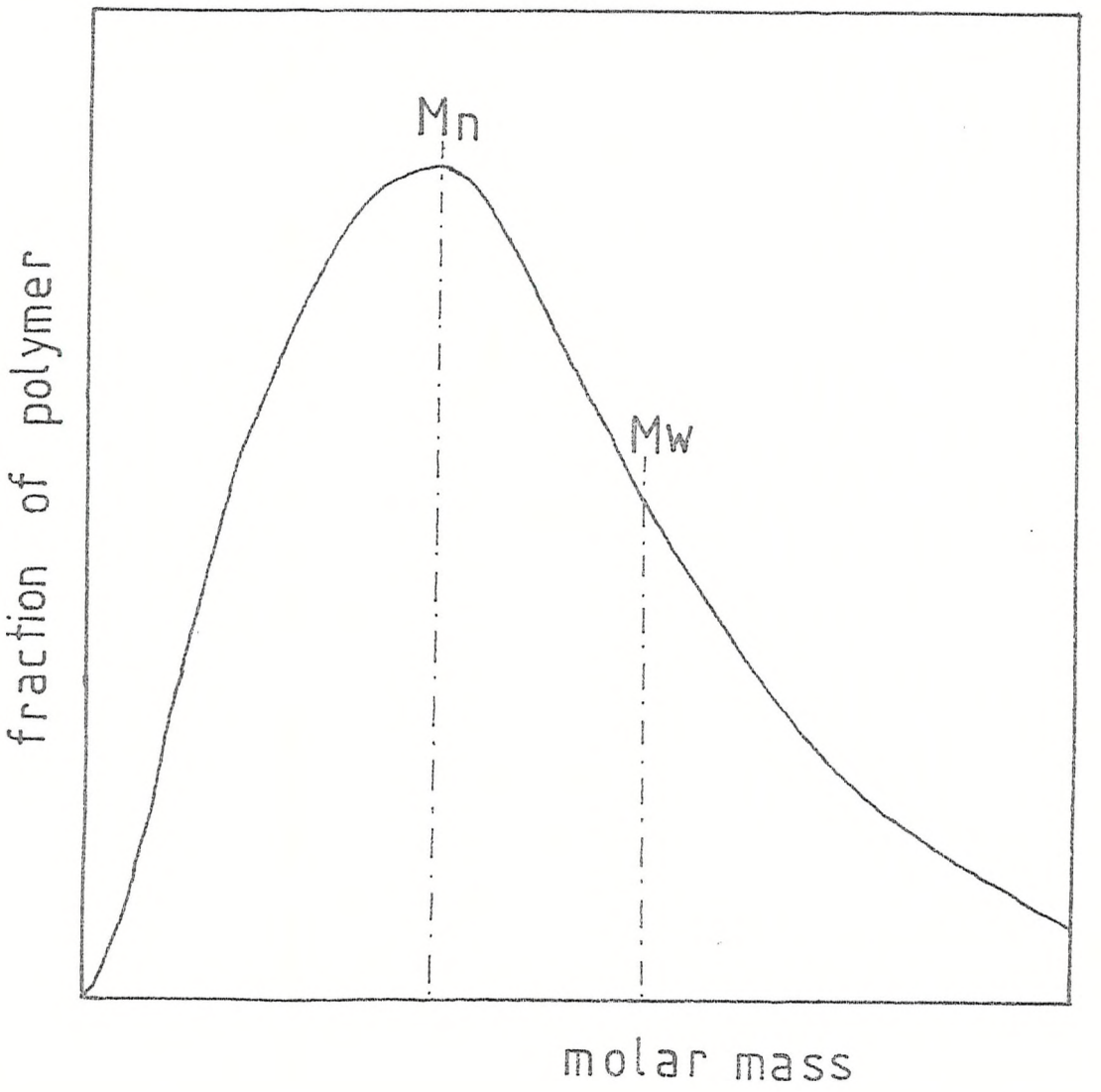

Fig II.1 TYPICAL DISTRIBUTION OF MOLAR MASSES FOR A SYNTHETIC POLYMER SAMPLE

In Fig. II.1 is given a typical distribution of molar masses for a synthetic polymer.

The width of the distribution, the polydispersity, is often estimated by establishing the ratio ($\overline{Mw}/\overline{Mn}$).

II.1.1 Gel permeation chromatography

The determination of the molecular weight distribution (M.W.D.) using several techniques giving $\overline{Mn}$ and $\overline{Mw}$ is time consuming and expensive. A new technique was developed in the 60's (39) which allows us to determine directly the molecular weight distribution as well as $\overline{Mn}$ and $\overline{Mw}$, by a computer-based routine.

The principle of this technique is to separate the molecules according to their molecular size. This separation takes place in a chromatographic column filled with a non-ionic stationary phase of beads of a rigid porous "gel" (often beads of cross-linked polystyrene). The pores in this gel are the same size range as the molecular dimensions of the polymer to be analysed.

A sample of the dilute polymer solution is introduced in a solvent stream flowing through the column. As the dissolved polymer molecules flow past the porous beads, they can diffuse into the internal pore structure of the gel to an extent depending on their size and the pore-size distribution of the gel. Larger molecules can either enter only a small fraction of the internal pores of the gel, or are completely excluded; smaller molecules penetrate a larger fraction of the interior of the gel.

The larger the polymer molecule the less time it spends inside the gel and the sooner it flows through the column. The different molecular species are eluted from the column according to their molecular size (38) and are separated according to their molecular weight, the largest emerging first, Fig. II.2.

No theory predicting retention times or volumes as a function of molecular size has appeared for gel permeation chromatography. A specific column or set of columns (with gels of different pore size) is empirically calibrated to give such a relationship, using standard polymers of known molecular weight (usually narrow-distribution polystyrene). For a particular polymer a calibration curve giving molecular weight vs retention volumes can be established, but as the technique appears to depend on the volume of the molecule, attempts to construct a universal curve have been made. The most successful approach is to plot the product (intrinsic viscosity x molecular weight) $[\eta] \times M$, against the elution volume V. The product $[\eta] \times M$ is proportional to the hydrodynamic volume of the polymer molecule in solution. Therefore a measure of the retention time coupled with a measure of the viscosity of the eluted fraction leads to molecular weight .

Gel permeation chromatography has proved extremely valuable for both analytical and preparative work with a wide variety of systems ranging from low to very high molecular weights. The method can be applied to a wide variety of solvents and polymers according to the type of gel used. With polystyrene gels the common solvents are

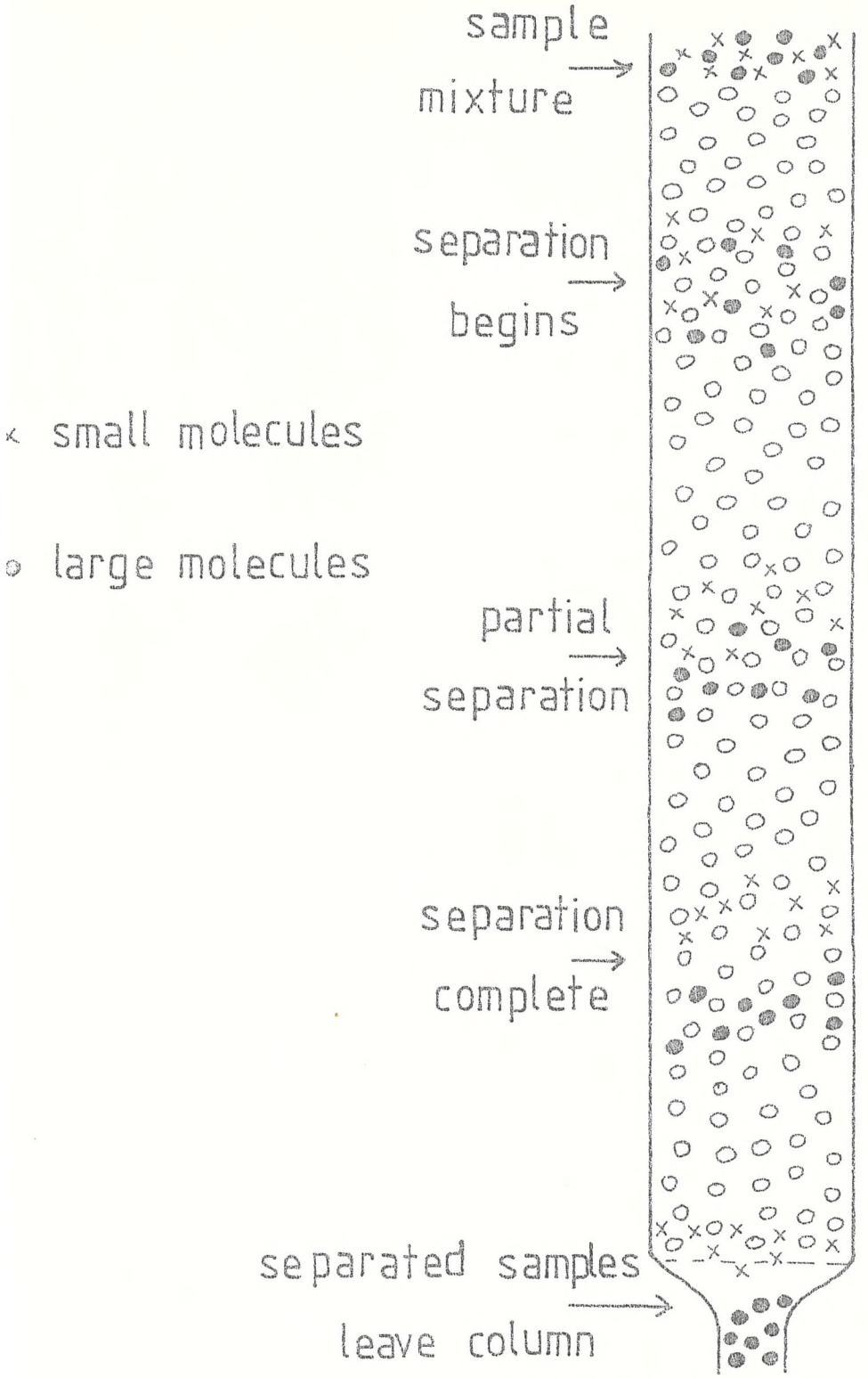

Fig. II.2 PRINCIPLE OF THE SEPARATION OF MOLECULES ACCORDING TO SIZE BY GEL PERMEATION CHROMATOGRAPHY

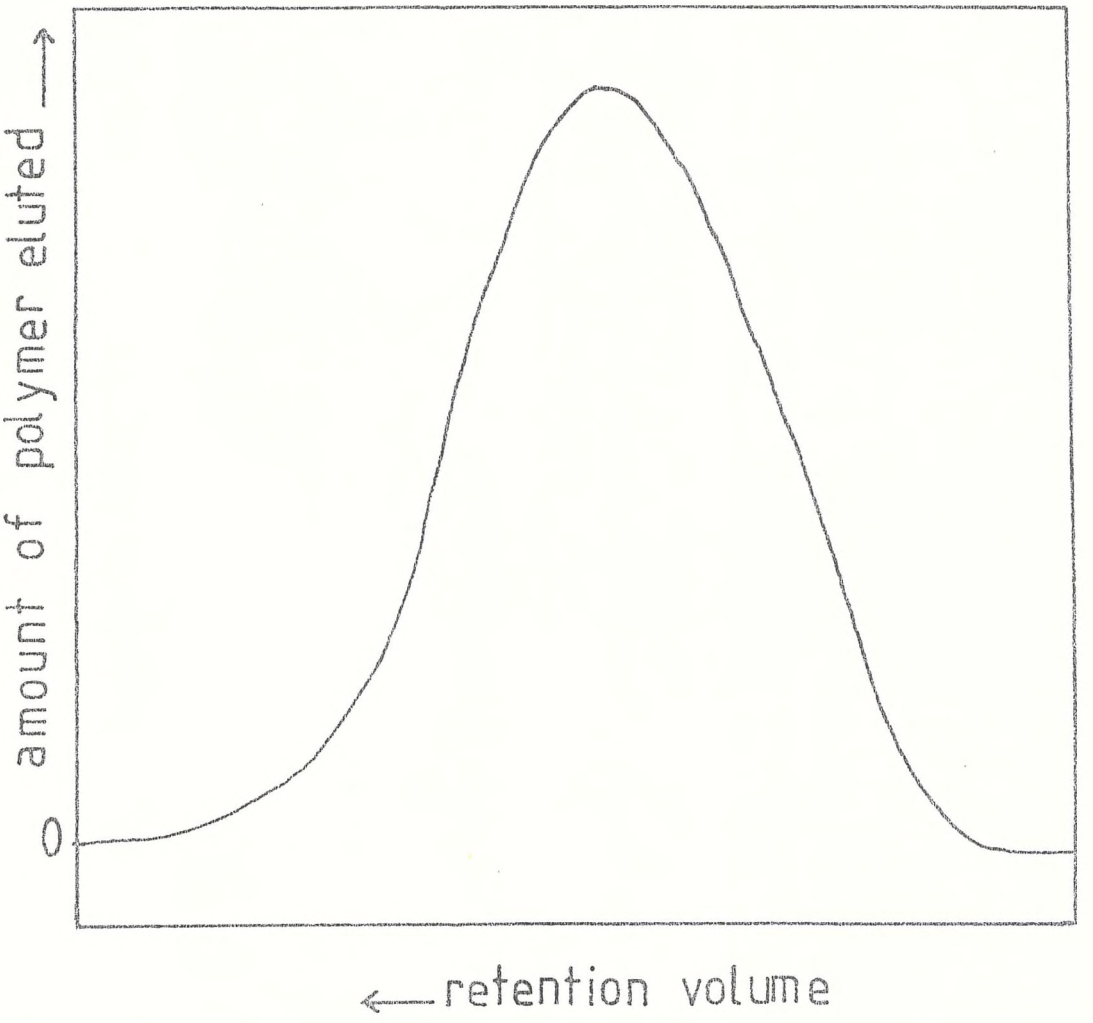

Fig II.3 A TYPICAL GEL PERMEATION CHROMATOGRAM

(Polystyrene in tetrahydrofuran Mw/Mn = 2.9)

tetrahydrofuran (T.H.F.), toluene or, at high temperatures, o-dichlorobenzene. The analytical work requires a few milligrams of sample and the work is typically complete in 2 - 4 hours. An extensive bibliography on gel permeation chromatography has been compiled (40).

II.1.2 Light scattering:

II.1.2.1 Theory of light scattering

The phenomenon of light scattering is familiar to all of us; the blue colour of the sky, the poor penetration of car headlights in fog. In the last example the light is scattered by the water droplets which form the fog.

Lord Rayleigh established the fundamentals of light scattering during his studies on gases in 1871 (41, 42). Light is an electromagnetic wave, produced by the interaction of a magnetic and electric field, both oscillating in phase at a right angle to one another along the direction of propagation. When the light strikes matter, the electrons present in the atoms or molecules of the medium are excited. Vibrations are induced in phase with the incident light wave. Light then propagates in all directions, with the same wavelength as the exciting beam.

For gases, Rayleigh showed that the reduced intensity of the scattered light and the molar mass M of the gas are related as follows:

$$R_\theta = (2\pi^2/NA\,\lambda^4)\,(d\tilde{n}/dc)^2\,(1 + \cos^2\theta)\,Mc$$

where R_θ is the Rayleigh ratio defined as $i_\theta r^2/Io$ with Io intensity of incident beam; i_θ the quantity of light scattered per unit volume by one centre at an angle θ to the incident beam

r the distance of the centre from the observer,

and where λ is the wavelength of the light used

c is the concentration

$d\tilde{n}/dc$ is the specific refractive increment.

For liquids and solutions the theory is more complex especially for scattering from large solute particles (43, 44). In the case when the dimensions of the polymer chains are greater than $\lambda/20$, scattered light emitted from two or more centres arrive considerably out of phase at the observation point (Fig. II.4). The scattering envelope is then dependant on the molecular shape.

A measure of the dissymetry coefficient $Z + R_\theta/R\,(\pi - \theta)$ gives a rough idea of the molecular size. Z is equal to unity for small particles and becomes greater for larger ones. The particle scattering factor $P(\theta)$ which is the ratio of the scattering intensity in the absence of interference, measured at the same angle θ measures the angular attenuation of scattering.

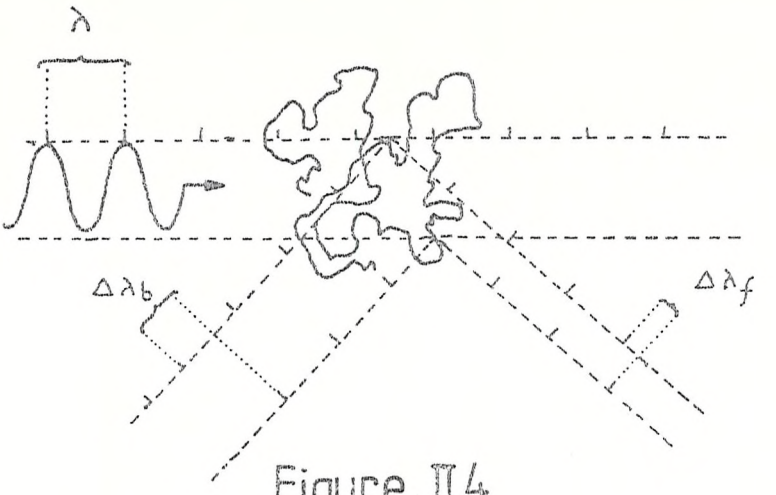

Figure II.4

Destructive interference of light scattered by large particles. Waves arriving at the forward observation point are $\Delta\lambda_f$ out of phase and those arriving at the backward point are $\Delta\lambda_b$ out of phase.

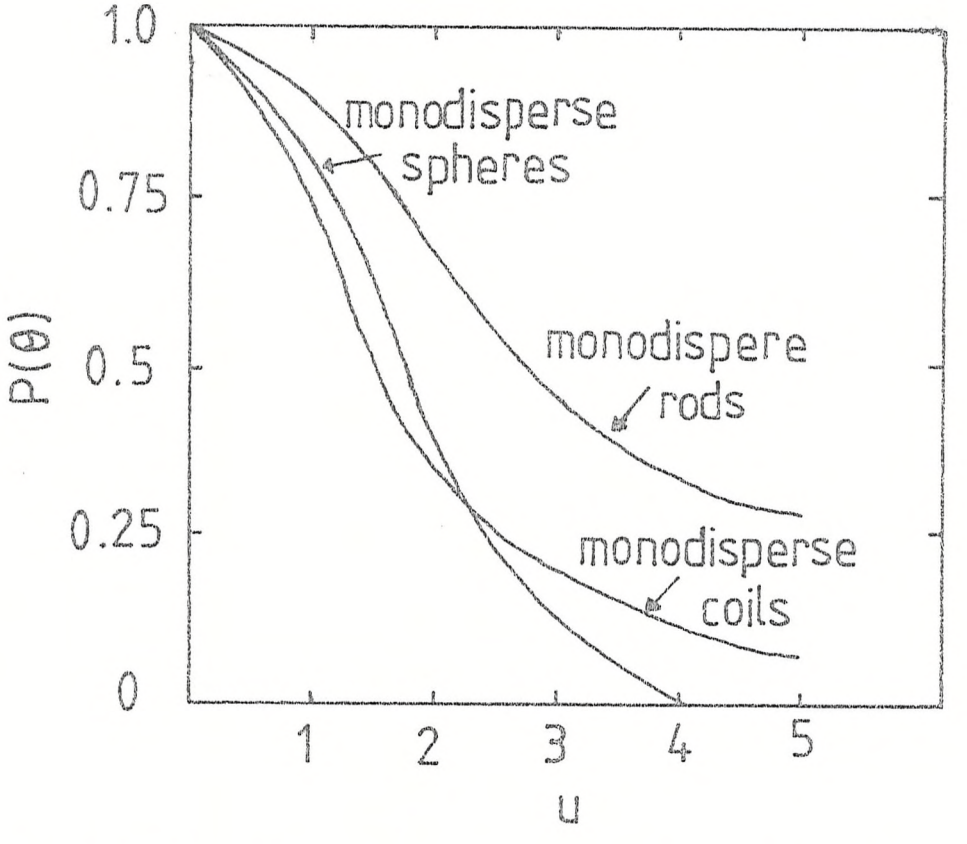

Fig II.5 P(θ) as a function of u for three model shapes : coils, spheres

The function P(θ) is size dependant and can be related to the polymer coil size by

$$P(\theta) = (2/u^2)\left\{e^{-u} - (1 - u)\right\}$$

$$\text{with } u = \left\{(4\pi/\lambda) \sin(\theta/2)\right\}^2 \langle \bar{s}^2 \rangle$$

in which $\langle \bar{s}^2 \rangle^{\frac{1}{2}}$ is the radius of gyration of the molecule, i.e. the average distance from the centre of gravity of the molecule to the chain end.

The shape of the molecule in solution can be related to P(θ) as shown in Fig. II.5.

II.1.2.2 Equipment

Various types of instruments are available commercially. The schematic diagram Fig. II.6 shows the main features of a typical model.

Light is obtained from a water cooled mercury vapour lamp(1) and one of three wavelengths 365, 436 or 546 nm is selected with an appropriate filter(2). The light beam, which may be polarized or not, is collimated before passing through the sample cell(4). This cell is immersed in a liquid bath which can be thermostated at temperatures between 273 and 400°K. Scattered light is detected by a photomultiplier(5), revolving from step to step round the cell and the intensity is recorded on a galvanometer. The 90° scattering R_{90^o} is plotted as $(K'c/R_{90})$ against the concentration and the linear extrapolation for c = o leads to Mw.

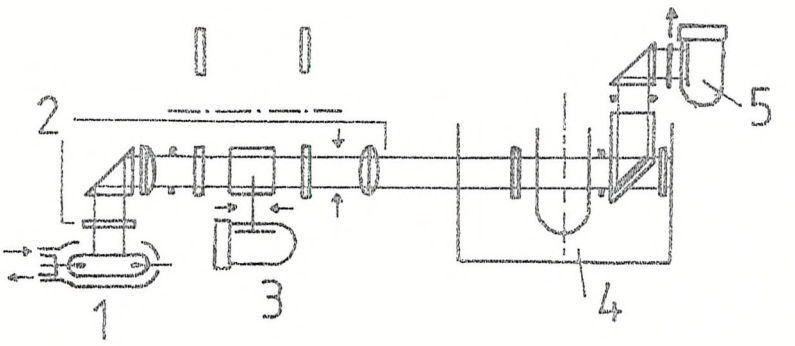

1. The light source, a water cooled mercury vapour lamp
2. Path of incident beam through a system of filters, polarizers, and a variable slit
3. Reference photomultiplier
4. Thermostat
5. Photomultiplier

Fig II.6 SCHEMATIC REPRESENTATION OF THE OPTICS OF A LIGHT SCATTERING INSTRUMENT

II.1.2.3 Sample preparation

The preparation of the sample is of considerable importance. The polymer is dissolved in a suitable solvent at an appropriate temperature. Better results are favoured by the proper choice of solvent. The difference in refractive index between polymer and solvent should be as large as possible.

Scattered light from impurities such as dust, are frequently larger than that from the polymer molecules, i.e. it may easily outweigh the scattering from the polymer solution. The solutions must be therefore free of impurities, clarified by filtration or centrifugation.

II.1.2.4 Molecular weight determinations

Two methods, briefly exposed below, can be used to determine the molecular weight Mw.

i) Zimm plot (45)

The idea is based on the fact that since the scattering at $\theta = 0$ is independant of size, $P(\theta)$ is unity when $\theta = 0$. To overcome the difficulty of measuring the scattered light at a such angle an extrapolation procedure has been devised using the following form of equation for large particles:

$$Kc/R\theta = 1/Mw\ P(\theta) + 2\ A_2\ C + ...$$

substituting for $P(\theta)$ leads to

$$Kc/R\theta = 1/Mw + (1/Mw)\left\{(16\pi^2/3\lambda'^2)\sin^2(\theta/2)<\bar{s}^2>\right\} + 2A_{2c} + ...$$

The Zimm plot is a graph of $(Kc/R\theta)$ against $\left\{\sin^2 (\theta/2) + k'c\right\}$ where k' is an arbitrary constant chosen to provide a convenient spread of the data. Measures are made for several concentrations and at various angles of observation. A double extrapolation is then carried out by joining all the points of equal concentration and extrapolating to $\theta = 0$ and all the points of equal angle and extrapolating to $c = 0$ (Fig. II.7). Both lines on extrapolation to the axis, should intersect at the same point. The intersection point is 1/Mw; the slope of the $\theta = 0$ line yields to the second virial coefficient (A_2), whereas $\langle \bar{s}^2 \rangle^{\frac{1}{2}}$ is obtained from the initial slope of the $c = 0$ line.

ii) <u>The dissymetry method</u>

The Zimm method previously described is certainly the best one to use for Mw determinations providing the Zimm diagram obtained from the experimental measurements is similar to the one shown on Fig. II.7.

However, for some polymers (including polyethylene) the plot of the experimental data gives a Zimm diagram distorted at high angles of observation, as shown on Fig. II.8. In these cases although it is still possible to extrapolate as previously, the molecular weight Mw (Zimm) obtained takes too much account of high molecular weight 'tail'. A correction for the dissymetry observed between measurements made at θ and $(\pi - \theta)$ needs then to be applied. Usually this correction can be made using 45°, 90° and 135° scatterings only. To make the calculations possible,

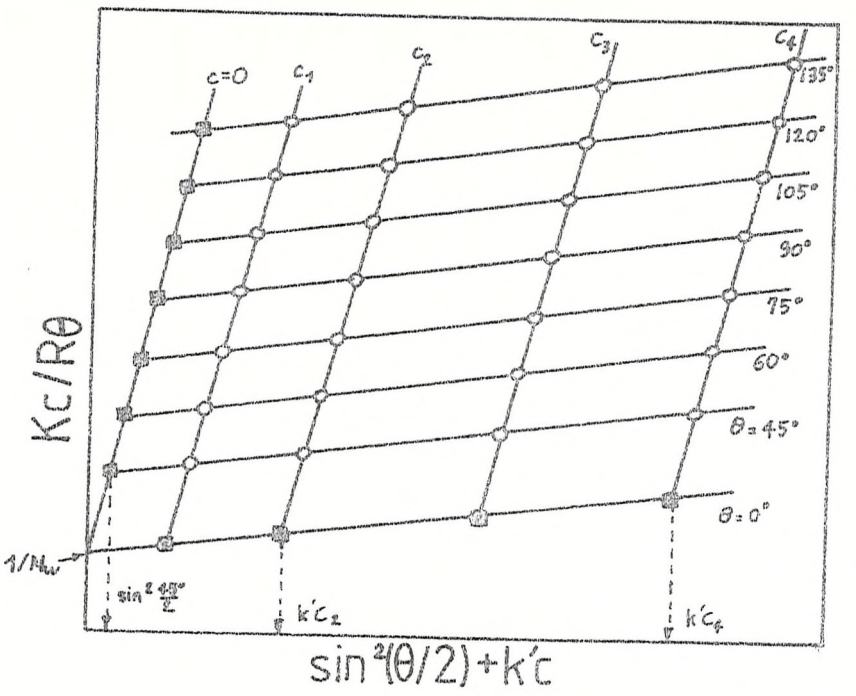

o experimental points

■ extrapolated points

Figure II.7 TYPICAL ZIMM PLOT

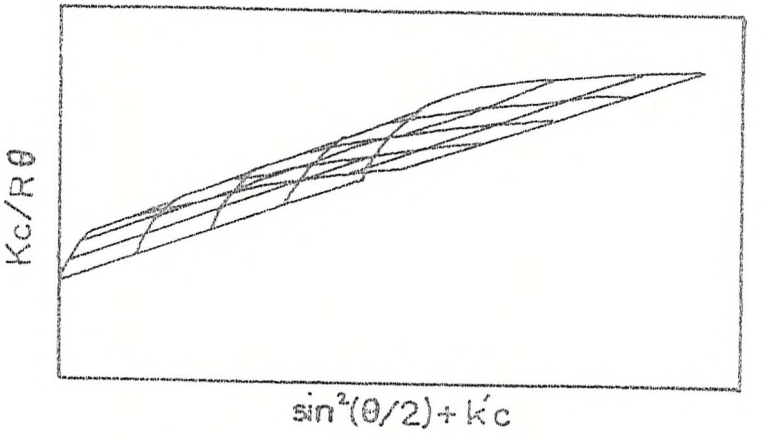

Figure II.8 ZIMM PLOT FOR POLYETHYLENE

coefficients have been tabulated (46); they take into account the shape of the molecule in solution (sphere, coil or rod). Doty and Steiner (47) have calculated values of P (θ) for the random coil model (e.g. for polyethylene) and these values must be used when dealing with unfrationated materials.

The dissymetry coefficient z ($z = i(\theta)/i(\pi - \theta)$) is concentration dependant and so it is necessary to extrapolate the data to zero concentration. From this extrapolated value $\overline{Mw}_{(90^o)}$ is obtainable.

A more complete and detailed description of the Zimm and the dissimetry methods can be found in the literature (48, 49).

Range of applicability

In practice, polymer molecular weights in the range of 10,000 - 10,000,000 can readily be measured with the possibility of extending the range in either direction in favourable cases.

It has long been assumed that information on particle shape could be determined from measurement of the angular dissimetry of light scattering. Benoit (50) demonstrated that except under very favourable circumstances this view point should be abandoned.

iii) Polymer dimensions

The most important parameters regarding the polymer molecule in solution are the radius of gyration and the second virial coefficient. These two values respectively denoted $\langle \bar{s}^2 \rangle^{\frac{1}{2}}$ and A_2 are obtainable from the Zimm plot as has been briefly mentioned earlier.

The radius of gyration is, by definition, the average of the root mean square distances of a chain element from the centre of gravity of the coil in the molecular population. This value gives therefore an idea of the size of the molecule in solution. In the notation $\langle \bar{s}^2 \rangle^{\frac{1}{2}}$ the angular brackets denote averaging due to chain polydispersity in the sample and the bar indicates averaging for the many conformational sizes available to chains of the same molar mass. In theory, this value is simply related to the average root mean square distance between the chain ends $\langle \bar{r}^2 \rangle^{\frac{1}{2}}$ by the relationship

$$\langle \bar{s}^2 \rangle^{\frac{1}{2}} = \frac{1}{6} \langle \bar{r}^2 \rangle^{\frac{1}{2}}$$

The second virial coefficient is related to the polymer solvent interaction and the molar mass. Deviations from ideal solutions are expressed in terms of virial expansions, and for solutions, sufficiently accurate results can be described by the terms up to the second virial coefficient while neglecting higher terms. The value of A_2 is a measure of solvent-polymer compatibility, as the parameter reflects the tendency of a polymer segment to exclude its neighbours from the volume it occupies. Thus a large positive value indicates a good solvent while a

low value (sometimes even negative) shows that the solvent is relatively poor.

The dependance of A_2 on M can often be predicted, for good solvents, by a simple equation

$$A_2 = K M^{-\gamma}$$

where γ vary from 0.15 to 0.4 depending on the system and K is a constant.

II.2 Vibrational Spectroscopy

In a molecule, the atoms are in constant oscillation around an equilibrium position. The molecule exhibits a complex set of motions involving translations, rotations and vibrations. If the number of atoms in a molecule is N, the system has a total of 3N degrees of freedom, 3 of these being associated with the translation of the whole molecule, 3 others with its rotation (2 if the molecule is linear). There are therefore 3N - 6 (3N - 5) vibrational degrees of freedom leading to the same number of normal modes of vibration. Each of these, since it is a true vibration, results in a normal coordinate q_k . The "random" movements of a molecule can always be interpreted in terms of its normal modes of vibration.

Since the number of atoms in a polymer molecule is extremely large so is the number of its normal modes of vibration one would expect a very complicated spectrum. Actually the spectra are relatively simple since whole classes of vibrations have almost identical frequencies.

Although Infrared and Raman Spectroscopy are different techniques they are both useful in the study of the structure of polymer molecules. In fact because the basic principles behind each phenomenon lead to different selection rules covering the activity of the normal vibrational modes (e.g. the rule of mutual exclusion in centrosymmetric molecules) the techniques are complementary since they both measure vibration frequencies.

If Infrared Spectroscopy has been used since the early days of polymer science, the technical difficulties associated with Raman Spectroscopy have, until the mid 60's, limited its use to an insignificant number of polymer molecules (51). Since the introduction of multiple monochromators and lasers providing powerful monochromatic light which is the ideal source for Raman Spectroscopy, this technique has developed rapidly and is now a major technique in the study of polymer structure.

II.2.1 Infrared Spectroscopy (52, 53)

If a molecule in its equilibrium position has an electric dipole moment (which is the case for any non centro-symmetric molecule), this dipole moment will, in general, change with the relative position of the nuclei. Therefore, if a molecule vibrates, its dipole moment varies periodically with a frequency which is that of the vibration. In classical electrodynamics, this results in the emission of light at the frequency ν vib. Conversely, the oscillator could be set in vibration by absorption of light of frequency ν vib.; this phenomenon is the basis of infrared spectroscopy. In other words, a radiation of frequency correponding to one of the normal modes of vibration of the molecule will be only absorbed if the dipole moment changes during that vibration, i.e. if

$$\left(\frac{\partial \mu}{\partial q_k}\right)_{q_k=0} \neq 0$$

In quantum mechanics, a transition moment between two stationary energy levels a and b is defined

$$[\mu]_{ab} = \int \Psi_b^* \mu \Psi_a \, d\tau$$

where $[\mu]_{ab}$ is the transition moment

Ψ_a and Ψ_b are the wave functions respectively associated with the initial and final energy states.

μ is the dipole moment of the molecule (here considered as an operator).

The probability of a transition between a and b, and therefore the spectral intensity, is proportional to the square of the transition moment integral. The condition for $[\mu]_{ab}$ to be non-zero, i.e. for the vibration to be active in the infrared, is for the function in the integral to be an even one. The activity of a normal mode of vibration is thus governed by symmetry considerations.

II.2.2 Raman Spectroscopy (52, 53, 54)

When a transparent sample is illuminated with light, a small amount of the light is scattered in all directions. If the incident light has a discrete spectrum (monochromatic) an analysis of the scattered light shows that it contains radiation of the same frequency as the incident light but also much weaker radiation at additional frequencies. Scattering of light at the same frequency as the exciter originates from the Tyndall effect (diffusion due to inhomogeneities within the sample) or

from Rayleigh Scattering. Scattering at different frequencies was theoretically predicted by Smekal (55) and first observed by Raman (56) and is now named the RAMAN effect.

In the classical treatment, if a light wave of frequency ν falls on a molecule, it creates around it a varying electric field:

$$E = E_o \sin 2\pi\nu t$$

This field induces a varying dipole moment in the molecule, its magnitude being $|P| = \alpha |E|$ where α is called the "polarizability tensor of the molecule":

$$\text{and } \alpha = \begin{vmatrix} \alpha_{xx} & \alpha_{xy} & \alpha_{xz} \\ \alpha_{yx} & \alpha_{yy} & \alpha_{yz} \\ \alpha_{yx} & \alpha_{zy} & \alpha_{zz} \end{vmatrix}$$

If a molecule is vibrating, the polarizability tensor may well be varying periodically, and, hence the resulting dipole moment will also be affected. For a vibration occuring at a frequency ν vib, the polarizability can be approximated to:

$$\alpha = \alpha_o + q_k \left(\frac{\partial \alpha}{\partial q_k}\right)_{q_k = 0}$$

where α_o is the polarizability of the molecule in its equilibrium position,

and $\left(\frac{\partial \alpha}{\partial q_k}\right)_{q_k=0}$ is the change of polarizability during the transition.

The induced dipole moment can then be expressed by:

$$P = \alpha_o E_o \sin 2\pi\nu t + q_k \left(\frac{\partial \alpha}{\partial q_k}\right)_{q_k=0} E_o \sin 2\pi\nu t \cdot \sin 2\pi\nu_{vib.} t$$

which becomes after a trigonometric transformation:

$$P = \underbrace{\alpha_o E_o \sin 2\pi\nu t}_{\text{Rayleigh scattering}} + q_k \left(\frac{\partial \alpha}{\partial q_k}\right)_{q_k=0} \underbrace{\left(\underbrace{\cos 2\pi(\nu-\nu_{vib})t}_{\text{stokes}} - \underbrace{\cos 2\pi(\nu+\nu_{vib})t}_{\text{anti-stokes}}\right)}_{\text{Raman scattering}} \frac{E_o}{2} q_{k_o}$$

It can be seen that the induced dipole moment changes with the frequency of the incident light ν and also with the frequencies $\nu - \nu_{vib}$ and $\nu + \nu_{vib}$; hence emission of light occurs at these frequencies if $\left(\frac{\partial \alpha}{\partial q_k}\right)_{q_k=0} = 0$ only the Rayleigh scattering will be present. In other words, according to this classical treatment, the condition for Raman activity is that the polarizability of the molecule changes during the vibration.

In a quantum mechanical explanation of Raman Scattering a photon of energy $h\nu$ colliding with a molecule can either be scattered elastically (Rayleigh scattering) or inelastically (i.e. it can take or give part of its energy to the scattering system). In the latter case, the light quantum can only give or take amounts of energy corresponding to the difference between two stationary states of the system. If ΔE is the

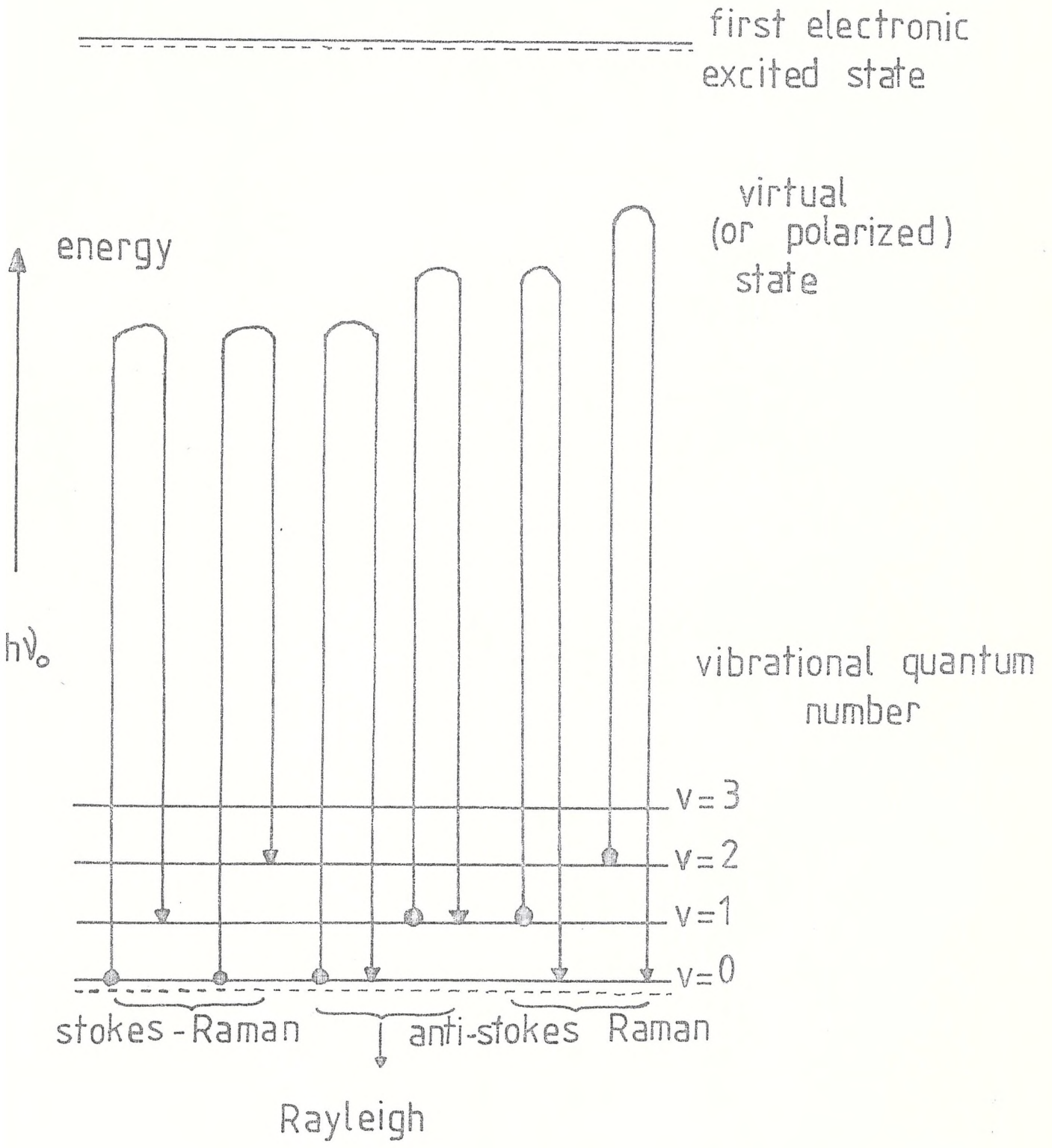

Figure II.9 SCHEMATIC ILLUSTRATION OF THE RAMAN EFFECT

difference between the two states involved the scattered photons will have the frequencies $\nu + \frac{\Delta E}{h}$ and $\nu - \frac{\Delta E}{h}$ (with h = Planck's constant).

When the incident light strikes a molecule, there is a pertubation of the whole system which reaches a virtual state of higher energy; light is scattered when the system returns to one of its stationary states which can be the same as the initial state (Rayleigh scattering) or one of higher or lower energy (respectively Stokes and anti-Stokes lines). At normal temperatures, the vibrational levels of lower energy are more populated hence the Stokes lines, i.e. those corresponding to the molecule undergoing a transition to a higher energy level will be more intense than the anti-Stokes lines. Another consequence resulting in the differences in the populations of the energy levels is that the intensity of the anti-Stokes lines decreases with the increase of Raman Shift. Since in any case the Raman effect is very weak, (I Raman $< 10^{-8}$ I source) Raman spectra are usually recorded on the Stokes side of the Rayleigh line.

In a similar manner to infrared absorption, the mathematical formulation of the Raman effect leads in quantum mechanics to the definition of another space integral

$$[\alpha]_{ab} = \int \psi_b^* \alpha_{ij} \psi_a \, d\tau$$ where $[\alpha]$ is now an operator.

Application of Raman Spectroscopy to polymer science: the L.A. mode

The only application of Raman Spectroscopy involved in this project is the measure of lamellar thickness from the low frequency Raman band observable in many polymers. This band, due to the longitudinal acoustic (sometimes "accordian") mode (L.A. mode), was first observed in the spectrum of n-alkanes (57). The first polymer observed to exhibit a similar band was polyethylene (58). The vibration involves an accordian-like vibration of the crystalline stems of the lamellae. Assuming the stem behaves like an elastic rod, the frequency (ν) of the vibration is inversely related to the length of the stem and is given by the following equation:

$$\nu = \frac{m}{2L}\sqrt{\frac{E}{\rho}}$$

where m is the mode order
L is the lamellar core thickness
E is Youngs modulus along the chain axis
and ρ is the density.

There have been many studies undertaken to discover if the amourphous phase at the surfaces of the lamellae, contributes to the vibration (59, 60). However, it seems clear that, for polyethylene at least, the vibration is terminated by the first gauche unit at the end of the all trans $-CH_2-CH_2-$ sequence (61), although the coordinate will translate a methyl chain branch (62). As a consequence, the Raman measurement gives the length of the all trans CH_2

sequence, i.e. the thickness of the crystalline core, whereas the low angle X-ray diffraction experiment gives the distance between the centres of adjacent stacked lamellae. The other main advantage of the Raman technique over low angle X-ray diffraction is that the data can be obtained fairly quickly, typically in 10 minutes, compared to L.A.X.D. experiments taking up to two days.

For a lamellar core thickness of 10 - 20 nm, the L.A. mode in polyethylene has a frequency of 30 - 15 cm^{-1}, a region that can be easily accessed by modern Raman spectrometers.

CHAPTER III

EXPERIMENTAL PART AND RESULTS

III.1 Polymerisations

III.1.1 Introduction

As explained at the end of Chapter I we needed to produce our own polymers to carry out this project. Several types of polymerisations are known for producing polyethylene and each type requires particular equipment and facilities.

The only facilities readily accessible were for low-pressure polymerisations using Ziegler-Natta catalysts. Although this restricted the work considerably, the main difficulties regarding our polymerisations has been to find the right conditions to obtain interesting material in sufficient quantities to study their mechanical and rheological properties.

One of the most important characteristics of the polymers produced is their molecular weight and molecular weight distribution. It required several test polymerisation reactions in order to control these parameters so that reproducible polymers could be produced.

A considerable number of polymerisations (70 - 80) were carried out during this project to find the most satisfactory experimental conditions (nature of catalyst system, its concentration, temperature, solvent, etc.) to obtain the most acceptable material. The effect of each parameter upon the polymer obtained is described below.

Choice of catalyst

Although the range of catalysts available for low-pressure polymerisation of ethylene is very wide it was decided to choose a Ziegler-Natta one. Ziegler-Natta catalysis involves a mixture of a transition metal compound and a metal alkyl. These catalysts can be divided into two categories: homogeneous catalysts (which are soluble in the solvent) and heterogeneous catalysts.

Most of the polymerisations made have been carried out with an homogeneous catalyst system, a mixture of Vanadylchloride ($VOCl_3$) and an alkyl aluminium dihalide. It is known (63) that this catalyst system favours the creation of high molecular weight polyethylene with a fairly narrow molecular weight distribution. The rate of reaction with such a catalyst system is quite high at the beginning of the polymerisation and then decreases with time, according to Figure III.5. (N.B. The ordinate represent a quantity proportional to the consumption of monomer). It is assumed that the number of active centres present in the system decreases with time and consequently the activity of the catalyst, likewise decreases.

Some polymerisations were made with an heterogeneous catalyst system, a mixture of α titanium trichloride ($TiCl_3$ Al Cl_3, Stauffer A A), and a dialkyl aluminium halide. This catalyst system was abandoned because the quantity of polymer obtained was far too low to undertake any mechanical or rheological experiments. However, it was noted that, contrary to the homogeneous catalyst system previously described, the rate of reaction was fairly steady

with time and the amount of polymer obtained was roughly proportional to the duration of the polymerisation. This result has also been observed with the polymerisation of propylene (64); in this case the heterogeneous catalyst system is essential if control of tacticity is required as is normal.

As the largest amount of polyethylene available was very desirable for the project, the homogeneous catalyst system was therefore used most of the time.

However, if this study has to be enlarged in the future the heterogeneous catalyst system cannot be neglected.

Effect of the concentration of catalyst

There is obviously a relationship between the amount of catalyst put into the reaction vessel and the quantity of polymer produced, but there is no real proportionality. The quantity of catalyst used is fairly low, typically in the order of 0.1 to 10 millimoles for 1 litre of solvent.

It might be expected that with a high concentration of catalyst (therefore a large number of active centres) the chance that a chain which is growing from one active centre might "meet" another growing chain from another active centre is much greater than with a low concentration of catalyst. This hypothesis was one of the most important bases of this work. It has been found, as will be described later, that polymerisations which differ only in the catalyst concentration lead to polymers with different properties from one another.

Effects of reaction temperature

The study of the effect of the polymerisation temperature on the resulting polymer was made at the first stage of this work and revealed interesting results (65). The rate of reaction is very dependant upon temperature. The higher the temperature, the lower the rate of reaction and the lower the yield. This is due in part to the poor solubility of the gaseous monomer in the solvent at elevated temperatures. Another contributing cause of lower activity at high temperatures stems from the fact that Ziegler catalysts commonly begin to loose their activity above 60°C.

Polymers prepared at different temperatures (with all other conditions identical) revealed different properties from one another. Although it is not possible at this stage to define a precise relationship it was noticable that at higher polymerisation temperatures the mechanical properties exhibited by the polymer produced were better.

The temperature chosen as a compromise between quality and quantity was 65°C. It has to be pointed out that the accuracy of control in the temperature quoted is not very important since noticable differences are only detected for temperatures differing by about 5°C.

Nature of monomer. Effect of partial pressure

Polymerisations have been made only at atmospheric or low pressures using the equipment described in Figures III.1, III.2, III.3, and III.4. It is, however, possible to vary

at will the partial pressure of monomer by diluting it with an inert gas; nitrogen was used in this case.

With the use of homogeneous catalyst systems the effect of partial pressure has no noticable effect upon the amount of polymer produced, if the duration of the polymerisation is greater than 3 - 4 hours.

It was thought that by reducing the proportion of ethylene in the ethylene-nitrogen mixture, a control of the rate of reaction could be obtained. It was proposed that consequently chains would have more time to meander through the solution as they were formed slowly. This hypothesis is of considerable interest and has been tested by varying the partial pressure in many polymerisations. The procedure for mixing ethylene with nitrogen is explained later.

One of the major problems to overcome was to reduce the molecular weight of the samples first produced. The values in early polymerisation reactions were typically in the range 10^7 - 10^8. Thus the polymer melts were far too viscous to be readily studied and processed. The use of a chain transfert agent, typically hydrogen, can control the molecular weight of the polymer (63). Whilst the necessary proportion of hydrogen may be determined by experiment and is dependant on the particular type of catalyst used, it has been found that using our preferred procedure a relatively small proportion of hydrogen is effective, typically some 1.5% by volume of the monomer/nitrogen mixture.

Choice of solvent

Although this parameter is of interest, this aspect has not been investigated at this stage.

All the polymerisations (except one made in xylene at 110°C, which did not "work" well) were made with aliphatic diluents, typically heptane. The important characteristics of the solvent are its boiling point and its volatility. These properties are of consequence, not in the polymerisation itself, but for the cleaning and drying operations applied after preparation.

Other parameters

The effect of stirring has also been considered to some extent; some polymerisations were carried out by bubbling the gas mixture through the solution without any stirring. These polymerisations needed modifications to the equipment and did not allow a measurement of the rate of polymerisation (the feeding and counting systems were disconnected). No noticable differences were detected in the resulting polymers and this procedure was then abandoned.

III.1.2 Typical polymerisation procedures

Figures III.1, III.2, III.3, and III.4 show the typical polymerisation arrangement.

At the beginning of the polymerisation, the vessel must be scrupulously clean and dry.

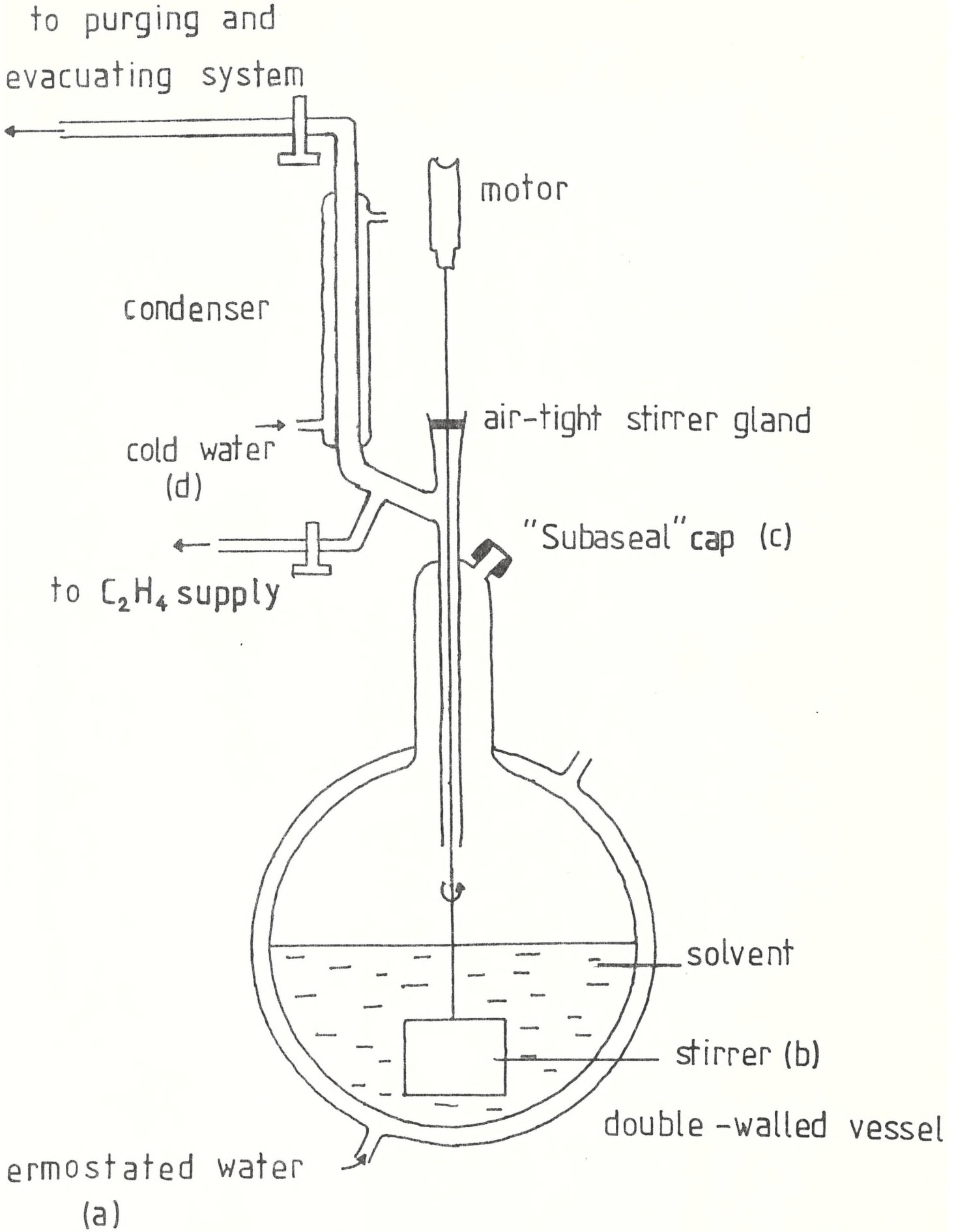

Fig III.1 DILUENT POLYMERISATION APPARATUS

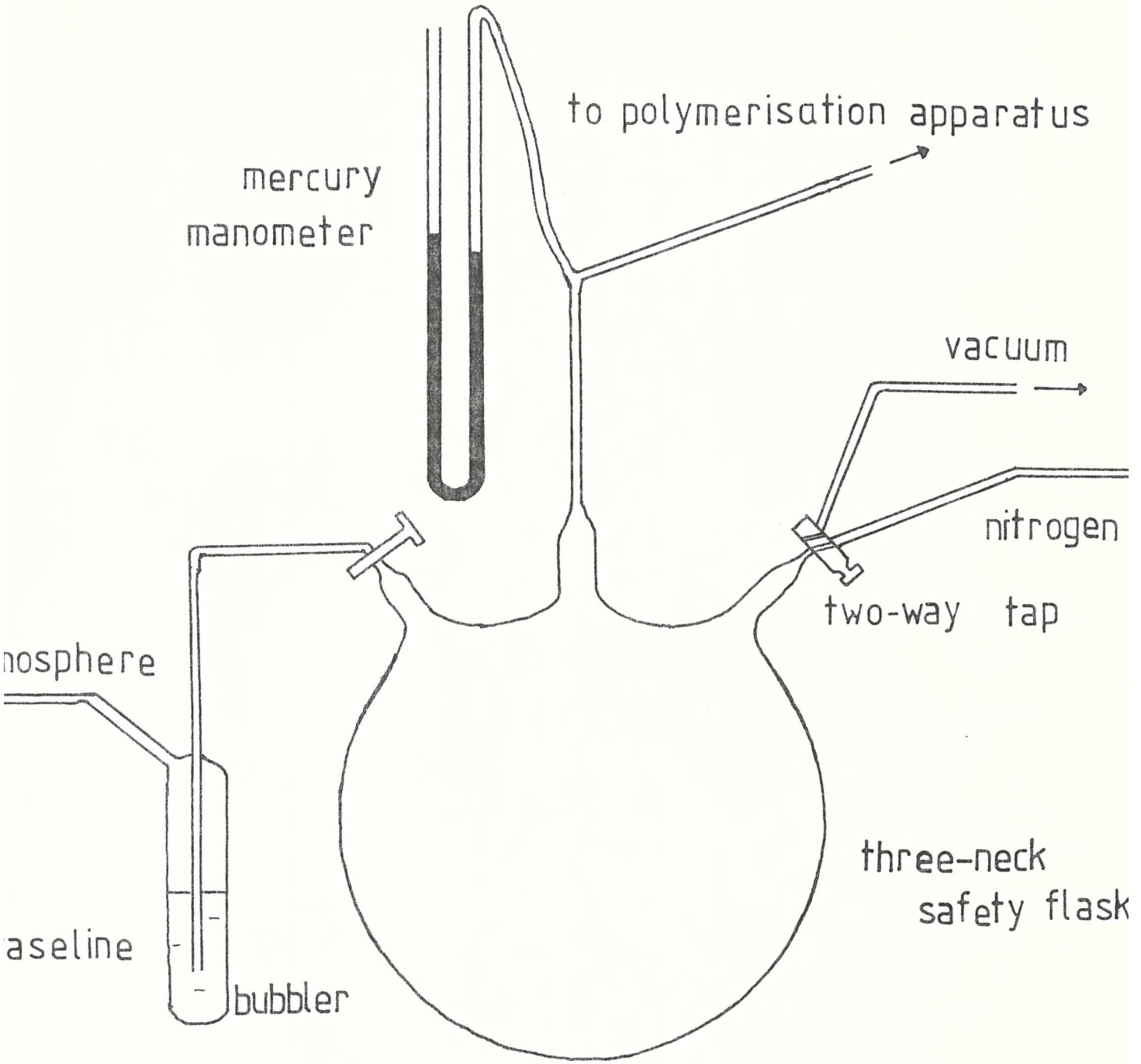

Fig III.2 PURGING AND EVACUATING SYSTEM

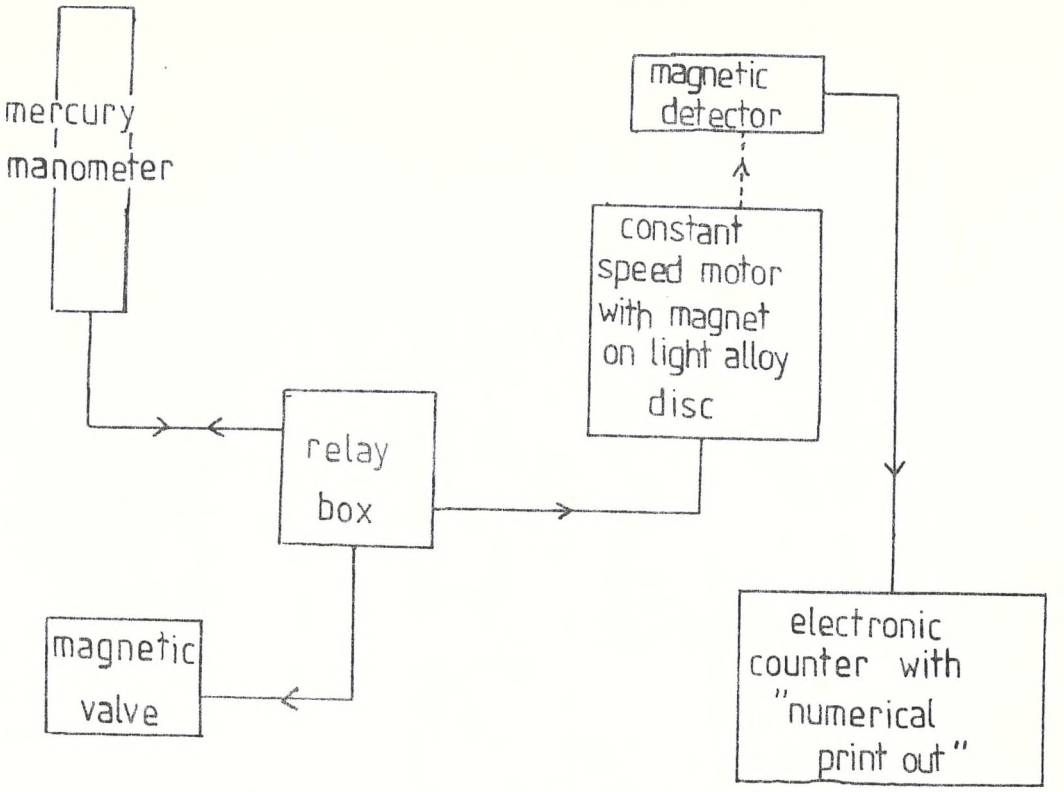

Fig III.3 BLOCK DIAGRAM OF "COUNTING" CIRCUIT

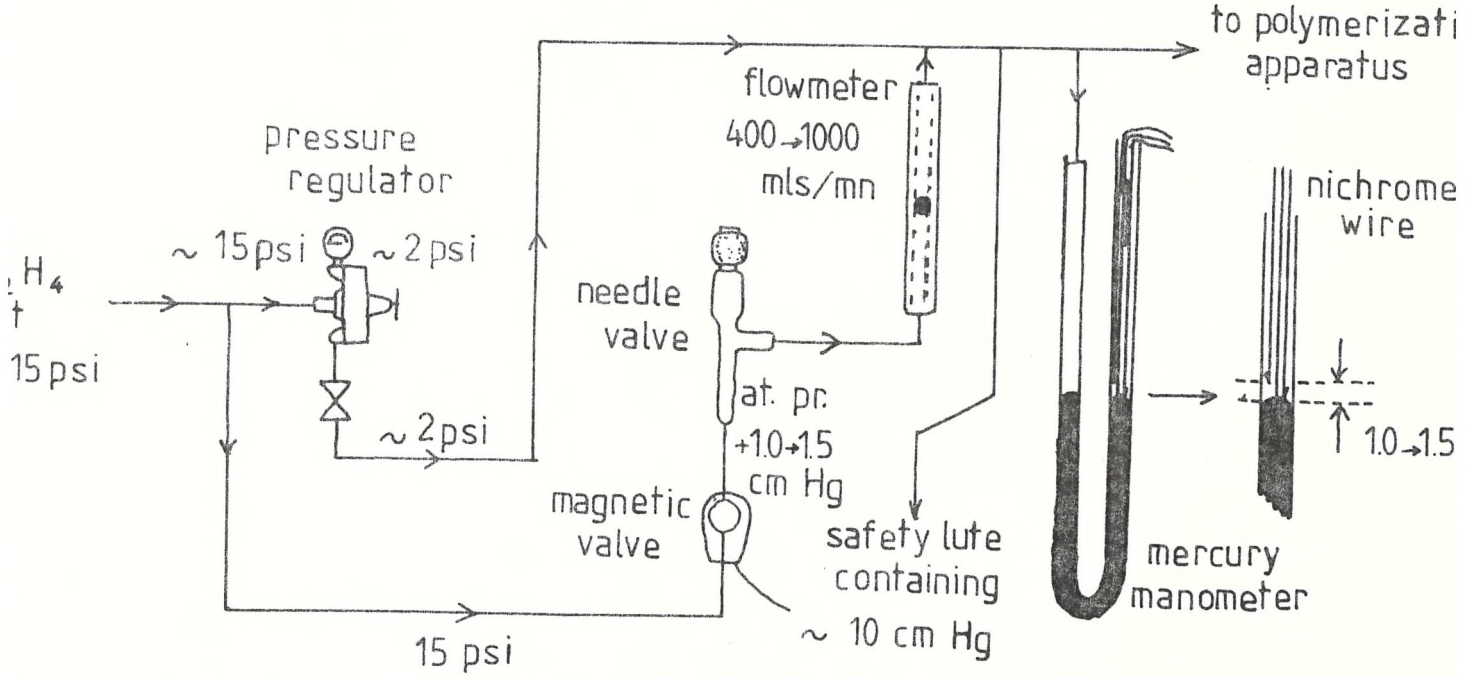

III.4 DIAGRAM OF ETHYLENE SATURATION AND FEEDING SYSTEM

- The thermostated circulating water system (a) is first switched on and adjusted to the desired temperature typically 65°C. The double-walled vessel is then put under vacuum for a few minutes to remove all the remaining oxygen and any droplets of water which remain in the reactor. The vacuum line is switched off for a quarter of an hour and the air-tightness checked with a mercury manometer connected to the apparatus. This is very important for preventing air from penetrating into the reactor during polymerisation and monomer escaping into the laboratory. The reactor is then purged with high purity nitrogen. Both these operations are repeated at least three times.

- The predetermined quantity of solvent (typically one litre) is then introduced into the vessel. The reactor at this stage is under an excess of nitrogen pressure therefore the "Subaseal" cap (c) is removed. The solvent is introduced with a funnel while a nitrogen blanket is maintained in the reactor. The "Subaseal" cap is then replaced. The stirrer (b) is also turned on.

- Once again the polymerisation apparatus is evacuated and purged three times with nitrogen. This operation has the effect of removing all the water and air contained in the solvent. It is not possible to put the reaction under very low vacuum because at a temperature of 65°C the aliphatic solvent boils easily. To minimise the escape of solvent the cooling water system (d) is turned on to condense the diluent vapour.

- The next stage is to saturate the reactor and the solvent with the monomer or monomer-nitrogen mixture, depending upon

the type of polymerisation being undertaken. The apparatus is once again evacuated and the vacuum line turned off. For polymerisations with a mixture of monomer and nitrogen, nitrogen is introduced first until the right pressure is obtained. This operation is controlled by using the mercury manometer. Ethylene is introduced into the reactor until the total pressure inside the vessel reaches 1 atmosphere. The gas feeding system is then automatically turned off. For polymerisations with non-diluted ethylene, the monomer is introduced after the apparatus has been under vacuum. Using the feeding and counting systems (Figures III.3 and III.4) it is possible to follow the consumption of monomer required to saturate the solvent. It usually left about 5 minutes to reach saturation of the aliphatic diluent.

- The catalyst mixture is then introduced into the reactor. This operation is carried out in two separate parts.

Firstly, the introduction of the alkyl aluminium dihalide, typically Et Al Cl_2. This reagent inflames in air and must be kept under inert gas (nitrogen). It was handled as a 3.5 molar solution in heptane. The use of a micro-syringe facilitates the manipulation of this material without danger. It is introduced into the polymerisation apparatus by introducing the needle of the syringe through the "Subaseal" cap.

Secondly, usually five minutes later, the other part of the catalyst mixture is introduced using the same procedure. This is really when the polymerisation begins. As soon as the second part is introduced, the supply system is automatically switched on in response to the lack of monomer

inside the vessel. The electronic counter can be programmed to print out counts proportional to the amount of monomer consumed by the reaction (e.g. every four minutes). Although it is very difficult to know precisely the real quantity of ethylene used, these counts give an idea of the rate of the reaction with time. The polymerisation proceeds at a regulated total pressure of 1 atmosphere.

- The final operation is to stop the polymerisation. After usually 3 - 4 hours from the beginning of the polymerisation the reaction is stopped by introducing a few millimoles of an alcohol such as isopropanol or butanol. This "kills" the activity of the catalyst system. The ethylene is then turned off and the reactor is left under a stream of nitrogen for about half an hour.

The stirrer is then turned off and the reactor emptied. The polymer obtained, usually small white particles, needs to be cleaned and dried before use.

Although a lot of polymerisations have been carried out, only five of them will be reported and described here, as it is unnecessary to describe them all with detailed experimental conditions (which varied from one experiment to another). Nevertheless, it should be understood that a great part of the time spent on this project has been expended in researching the optimal polymerisation conditions. The simple rules given earlier (effect of temperature, catalyst concentration .....) were obtained from all these optimisation experiments.

Note: The numbers associated to our own polymers are run numbers, and not related to characteristics of the polymers concerned.

Polymerisation conditions for sample 28

The typical general polymerisation procedure described earlier was applied for this polymerisation with the following details:

Solvent:	1 litre of heptane
Temperature:	65°C
Cocatalyst:	Et Al Cl_2 (5 mmols)
Monomer:	C_2H_4/H_2 1.5% mixture at 1 atmosphere pressure
Catalyst:	$VOCl_3$ (1 mmol)

At the end of the polymerisation after 4 hours and the introduction of isopropranol (to kill the catalyst activity) the mixture polymer + solvent was left under nitrogen for about 10 mins, and allowed to cool down. The reactor was then emptied into a Buckner funnel and the polymer filtered. Petroleum spirit was used first to rinse the polymer, then methanol. In order to reduce the catalyst residues content, the polymer was left overnight in a 50:50 HCl-methanol mixture with stirring. The polymer was rinsed several times with methanol and again filtered on a Buckner funnel. It was then dried in a vacuum oven set at 70°C. The weight of polymer obtained was 25g and its appearance was white and powdery.

Polymerisation conditions for sample 54

The typical polymerisation procedures described earlier were applied for this polymerisation.

Solvent:	3 litres of heptane
Temperature:	65°C
Cocatalyst:	Et Al Cl_2 (15 mmols from stock solution in heptane)
Monomer:	C_2H_4/H_2 1.5% mixture at 1 atmosphere pressure

The introduction of 0.3 mmols of $VOCl_3$ (from a 1 M solution in heptane) was made at time t = 0. As the polymerisation "died" shortly afterwards, further quantities of $VOCl_3$ were added as follows:

0.3 mmols at t = 1 hr 20 mins

0.3 mmols at t = 2 hrs 18 mins

0.3 mmols at t = 3 hrs

0.3 mmols at t = 3 hrs 23 mins

The effect of several additions of $VOCl_3$ upon the reaction and its rate is shown on Fig. III.5.

At t = 4 hours the reaction was terminated by evacuation of monomer, introduction of nitrogen and addition of 150 cm^3 of isopropanol to "kill" the catalyst activity.

The polymer in suspension formed a "thick porridge" and most of it was transferred under nitrogen to the cleaning vessel, maintained at 65°C, with a further 500 cm^3 of heptane.

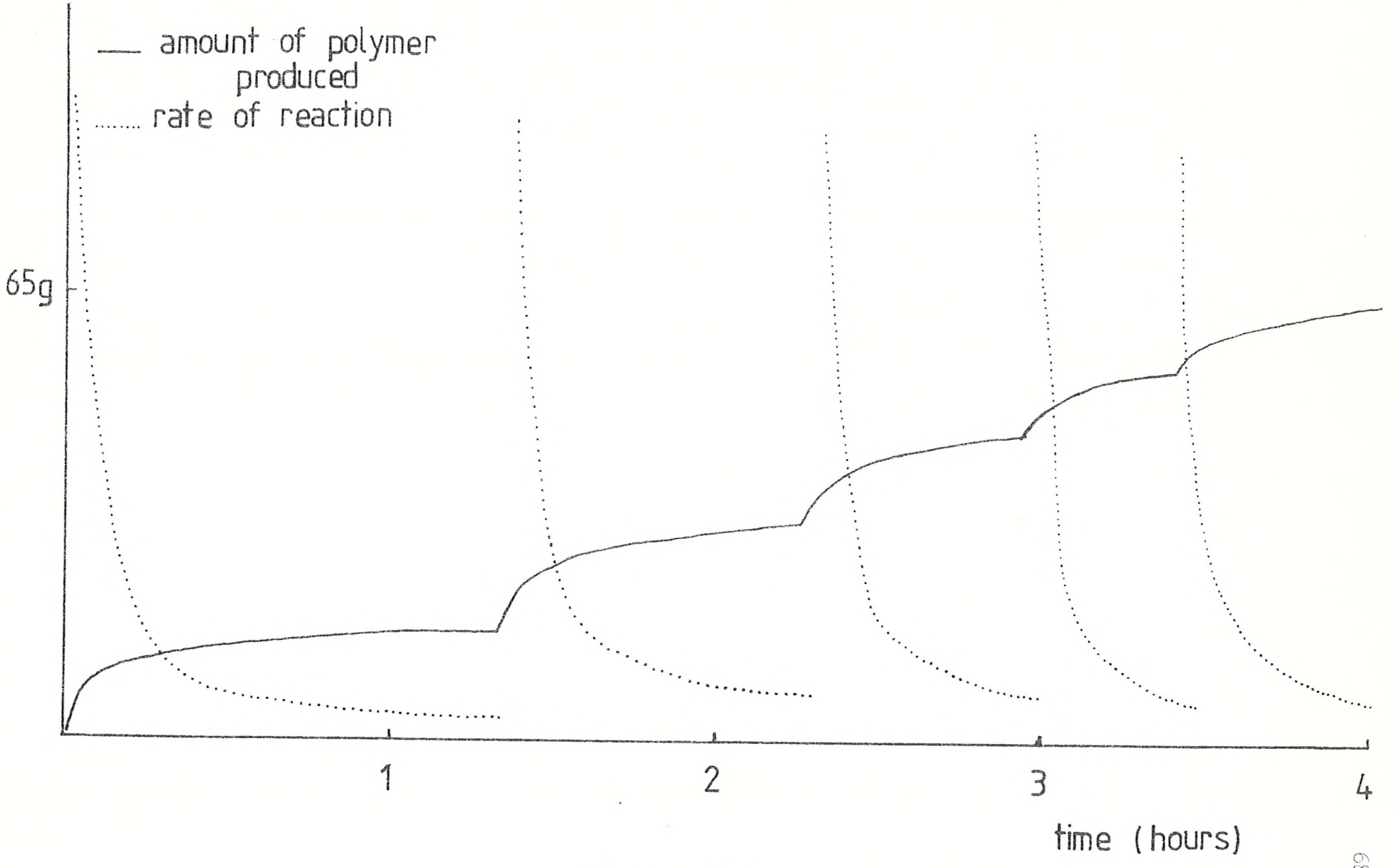
amount of polymer produced
rate of reaction
65g
1
2
3
4
time (hours)

Figure III.5

After stirring for a few minutes the mixture was allowed to settle down and about 1100 cm^3 of light green liquid was removed. In order to remove most catalyst residues a mixture of 100 cm^3 of 1 $\bar{M}$ HCl + 400 cm^3 of methanol was introduced. After stirring, the mixture was once again allowed to settle down and 1600 cm^3 of liquid was removed. The polymer was rinsed four times with methanol (about 1000 cm^3). At each stage the volume of liquid taken out was higher than the amount of methanol introduced as some polymerisation diluent came out with it. At the end, the polymer was transferred into a Buckner funnel and pressed down to eliminate as much as possible of solvent. It was then dried off in a vacuum oven, set at 80°C, to constant weight. The yield for this particular polymerisation was 65 grammes. Samples from dried polymer were taken for catalyst residues analysis and molecular weight determination.

Polymerisation conditions for sample 55

Solvent, temperature and monomer were the same as above for sample 54.

Cocatalyst:	Et Al Cl_2 15 mmols from a 3.65 $\bar{M}$ solution
Catalyst:	Single injection of 0.3 mmols of $VOCl_3$ from a 1 $\bar{M}$ solution.

The procedure was the conventional one and the run was terminated in an identical manner as for 54, 4 hours after the introduction of $VOCl_3$. The yield of the polymerisation was 22.9 g.

Polymerisation conditions for sample 56

Same as for 55 except that the reaction was terminated 35 mins after the introduction of $VOCl_3$. The yield of the polymerisation was 15.3 g.

Polymerisation conditions for sample 57

Identical to 54 with 5 injections of $VOCl_3$. The amount of polymer obtained was 64 g.

Summary and observations (cf Table III.1)

From this set of polymerisations it can be concluded that:

(a) the reaction slows down rapidly after the introduction of $VOCl_3$. This observation has been reported elsewhere (83). Several introductions of catalyst reactivate the reaction as shown on Fig. III.5 increasing therefore the amount of polymer produced.

(b) if a polymerisation is left for four hours it is reasonable to assume that 70% of the polymer obtained is created within the first 30 mins. (comparison of samples 55 and 56).

(c) polymerisations 54 and 57 give the same result in term of yield.

Table III.1 Polymerisation conditions for experimental samples.

Sample	Solvent (Heptane)	$VOCl_3$ mmols	Et Al Cl_2 mmols	Time	Yield (g)
28	1 litre	0.1	5	4 hrs	25
54	3 litres	1.5 in 5 injections	15	4 hrs	65
55	3 litres	0.3	15	4 hrs	22.9
56	3 litres	0.3	15	35 mins	15.3
57	3 litres	1.5 in 5 injections	15	4 hrs	64

III.2 Molecular Weight Determination

III.2.1 Light scattering

III.2.1.1 Sample preparation

As explained earlier (Chapter II) this method is based on a measurement of the intensity of light scattered by a solution (polymer under characterisation + solvent) at several angles of incident light and for several concentrations of polymer in solution.

One of the main difficulties to overcome in obtaining valid results is to prepare very clean solutions. α - chloro naphtalene was the solvent used in this research. Its refractive index at 160°C (temperature at which the measurements were made) is $\tilde{n} = 1.57$. The value of the specific refractive index increment ($d\tilde{n}/dc$) for the polymer + solvent system is - 0.182 cm^3 g with high density polyethylene (66).

It was found very difficult to dissolve our samples. In some cases ten hours refluxing at 200°C were required to achieve complete dissolution at a concentration of 2.5 mg/ml. Antioxidant (1%) had been added to the solution to prevent degradation with temperature. The antioxidant used was "Topanol O" which is a butylated hydroxy toluene. This antioxidant is known to be very efficient (67). Before being analysed, the solutions were filtered through glass fibre filters of pore size approximately 0.5 μm. No success was achieved with filters of pore size of 0.2 μm.

III.2.1.2 Apparatus and operations

The equipment used was home-made by I.C.I.; a full description, diagrams and comments about the apparatus can be found in the literature (68).

The source used was a high pressure mercury lamp and an appropriate filter was used to select radiation at 546 nm. The incident beam was vertically polarized and the measurement of the intensity of the scattered light was made in the vertical component. Typically measurements were made at angles from 30° to 135° in steps of 15 or 30°; 3 to 5 solutions were used with their concentration varying from 1 to 5 mg/l, except for the samples which were very difficult to dissolve.

III.2.1.3 Results and discussion (Cf Table III.2)

Rigidex 9 is specified by its manufacturers (British Petroleum Chemicals Limited) to have a molecular weight $\overline{Mw}$ of 179×10^3. This value is more comparable to our $\overline{Mw}$ (90°) value (139×10^3) rather than $\overline{Mw}$ (Zimm) (450×10^3). This is not surprising as we have already seen (Chapter II) that $\overline{Mw}$ (Zimm) is very sensitive to a high molecular weight "tail". As a result, the molecular weight values reported through this thesis for correlation with other properties will be the $\overline{Mw}$ (90°) figures.

Except for sample 28, samples 54 - 57 have higher values of $\overline{Mw}$ (either Zimm or 90°) than the others; significant differences are also shown among these four samples.

Table III.2 Light scattering data

Samples	$\overline{Mw}$ (Zimm) (1)	$\overline{Mw}$ (90°) (2)	Rg (nm)	A_2 measured	A_2 calculated (3)
Rigidex 9	450,000	139,000	-	-	-
Rigidex 2000	320,000	178,000	-	-	-
Sample 28	200,000	99,000	-	-	-
54	1,250,000	1,160,000	119	6.7×10^{-4}	4.46×10^{-4}
55	5,000,000	4,600,000	238	6×10^{-4}	2.8×10^{-4}
56	1,180,000	800,000	123	6.05×10^{-4}	4.5×10^{-4}
57	1,250,000	960,000	98	6.7×10^{-4}	4.46×10^{-4}

Note: $\overline{Mw}$ (Zimm), $\overline{Mw}$ (90°), Rg (radius of gyration) and A_2 have been defined and presented in Chapter II.

(1) $\overline{Mw}$ (Zimm) was obtained by least squares reduction of the concentration variation data at each angle in turn to obtain the zero concentration intercept, followed by by least squares reduction of the zero concentration intercepts as a function of angle to obtain the zero c, zero intercept giving the molecular weight.

(2) Obtained from the 90^{o} scatter with a correction for dissymmetry assuming random coil configuration.

(3) Calculated from $\overline{Mw}$ using the formula A_2 = 0.06 $\overline{Mw}$ (Zimm) - 0.35.

However, these results are very debatable for two main reasons:

i) On cooling, the solutions of these samples form a coherent gel rather than the fragmented precipitate usually observed. Normally when such solutions are allowed to cool down (at concentrations of 2.5 mg/ml) polymer precipitates and floats above the remainder of the polymer solution. For our samples 54 - 57 the precipitate was spread out through all the solution, suggesting that even in the solution there is some entanglement of molecules (70). In other words, it is possible that in solution the molecules do not adopt the random coil model configuration expected for H.D.P.E. chains and that a single molecule may not be isolated. If this is so, the molecular weight may be artificial and refer to connected groups of molecules rather than individuals.

ii) Also for samples 54 - 57 the second virial coefficients A_2 (as defined in Chapter II) are higher than would be expected for linear polymers of such molecular weights. Effectively, the observed value of 6×10^{-4} is that expected for linear polymer of Mw = 3.5×10^5. This also suggests that the measured molecular weight is higher than it should be. This observation is more acute for sample 55 where $\overline{Mw}$ (90°) = 4,600,000 and A_2 is measured at 6×10^{-4}, almost identical to 6.05×10^{-4} for sample 56 where Mw (90°) is 800,000.

As a result, we propose that the behaviour of our polymers in solution is not what would be expected for typical linear polyethylene and that the molecular weight data obtained from light scattering have to be considered with care. The ratio $\bar{M}w$ (Zimm)/$\bar{M}w$ (90°) which gives an indication of the importance of the high molecular weight tail suggests that for sample 54 - 57 the presence of high molecular material is far less important than in samples 28 and Rigidex.

III.2.2 Gel permeation chromatography

III.2.2.1 Sample preparation

As with light scattering, very clean solutions of polymers must be prepared before injecting the sample through the columnsof the G.P.C. apparatus.

The solvent used was 1-methyl-naphthalene. This solvent has good chromatographic properties and is a good solvent for polyethylene. Its boiling point is 246°C, its refractive index at 165°C (the temperature at which measurements have been made) is 1.6.

The solutions were automatically prepared and filtered using an equipment designed and built by I.C.I. The concentrations were 0.25% and the filtration was carried out on a coarse filter of pore size of about 50 μm. (This filtration is only a pre-filtration as there is at the head of each column a filter of 10 μm pore size). Some antioxidant (1% Topanol-O as used in light scattering measurements) was added to the solutions to prevent degradation of the polymer.

III.2.2.2 Apparatus and operations

The equipment used has been designed and built by I.C.I.; a full description with diagrams and comments can be found in the literature (69).

The apparatus is fitted with four columns; the stationary phase is porous silica, the pore size range varies from 30 Å up to 10000 Å.

The detector measures the difference of refractive index between pure solvent and solution. The intensity of the signal is proportional to the concentration of polymer of molecular weight M in the eluted solution.

The amount of solution introduced through the columns is 2 mls.

III.2.2.3 Results and discussion

The calibration of the columns was made with linear polyethylene standard samples from the National Bureau of Standard. This calibration is a plot of molecular weight vs elution time (or volume).

Unfortunately, measurements were possible only on samples of Rigidex 2000 and 28, and on samples of 25 and 27 which are not mentioned elsewhere in this thesis because the amount of polymer obtained prevented melt flow and mechanical properties. In table III.3 G.P.C. data are given.

Except for Rigidex 2000, the chromatogram obtained was less intense than expected. In other words, the amount of polymer detected after elution is very much lower (half to one third) of what would be expected for a conventional injection of 2 mls at 0.25% concentration. Although the exact reasons are unknown several hypothesis may be suggested as follows:

(a) the samples are not completely dissolved, therefore the real concentration is less than 0.25% (which would be obtained using the automatic dissolving machine) consequently the chromatographic signal is diminished. This is likely to happen; as already observed in the light scattering experiments, the samples are very difficult to dissolve.

(b) irreversible interaction has occurred between the polymer and the stationary phase which contain polar sites. Some polymer may then stay in the stationary phase and is not eluted.

(c) finally the behaviour of our samples may not be the conventional behaviour in G.P.C., i.e. the usual rules put forward to explain the elution process (volume of polymer molecule compared with the pore size of the stationary phase, see Chapter II) are not applicable for our samples.

Because of possible explanation (b) which could lead to a degradation of the G.P.C. columns and affect their qualities of separation, no other samples were accepted for molecular weight characteristics determination. This is the reason why the sample 54 - 57 mentioned through this thesis have not been treated by G.P.C.

Results shown in Table III.3 clearly indicate that the main difference between Rigidex 2000 and our samples is the molecular weight distribution M.W.D. (which is characterised by the ratio of $\overline{Mw}$ and $\overline{Mn}$ as defined in Chapter II). Our

samples have definite narrower M.W.D. (3 to 5) compared with Rigidex 2000's (7.5).

Table III.3 G.P.C. molecular weight measurements

Sample	$\overline{Mw}$ (1)	$\overline{Mn}$ (1)	$\overline{Mw}/\overline{Mn}$ (1)
Rigidex 2000	147,000	20,000	7.4
Rigidex 9*	179,000	9,800	18.2
25	170,000	35,500	4.8
27	263,000	121,000	2.2
28	100,000	37,500	2.7

(1) determined by computer from gel permeation chromatogramm

* From British Petroleum Chemical technigram

The other relevant point from Table III.3 is the fairly good agreement between $\overline{Mw}$ and $\overline{Mw}$ (90^{o}) for Rigidex 2000 and sample 28. This strongly indicates once again that $\overline{Mw}$ (Zimm) is not the proper $\overline{Mw}$ value to take into account for correlation with other properties.

Although samples 54 - 57 have not been tested by G.P.C., we can confidently assume that the narrow molecular weight distribution found for samples 25, 27, and 28 persists for them also, because the polymerisation conditions were not varied dramatically from one set of syntheses to another. Further, $VOCl_3$ polymerisations usually favour the creation of linear polyethylene with a narrow M.W.D. (63). Light

scattering measurements (ratio of $\overline{Mw}$ (Zimm)/$\overline{M}w$ (90°)) also give evidence that the molecular weight distribution is narrower for samples 54 - 57 than for Rigidex, especially in the case of the highest molecular weight range.

III.3 Infrared Examination

Infrared examinations were made in order to estimate the methyl content in our polymers.

This was carried out by pressing some polymer at 150°C and 15 tons load for less than 1 minute using a hot press. Polymers were then cooled down using the water cooling system of the press. Films obtained were about 70 μm thick.

The Infrared Spectrum was recorded for each sample on a 580 Perkin-Elmer Infrared Spectrometer. The region of interest for this determination is the region between 1400 cm^{-1} and 1300 cm^{-1}. The band due to methyl groups is at 1377 cm^{-1} and appears on the edge of a block of absorption maxima at 1366 cm^{-1} and 1351 cm^{-1}, the latter arising from $-CH_2-$ groups.

Various methods are used to determine precisely the methyl content in polyethylene (71). Although the 1377 cm^{-1} band is very sensitive to methyl groups it was not detectable for any of our samples. It was therefore concluded without any risk that the methyl content was in all cases less than 1 group per 1000 carbon atoms.

From this measurement it was concluded that none of our samples are branched, and that polymers produced are linear polyethylene. This result is in agreement with the high molecular weight of our samples.

III.4 Melt viscosity measurements - The cone and plate rheometer

III.4.1 Introduction

Rotational viscometers are commonly used to measure rheoligical properties of polymer melts (72). There are many variations which differ widely according to the system and the parameters to be studied. A requirement for an apparatus to measure melt properties at low shear rates (less than $1\,s^{-1}$) to complement capillary rheometers measurements at higher shear rates (73) lead to the construction of this equipment. It is based on the cone and plate geometry originally suggested by Higginbotham (74) and developed by Weissenberg (75) and others.

III.4.2 Principle of the measurement

A truncated cone is mounted with its axis perpendicular to a fixed plate. The separation between cone and plate is such that the imaginary apex of the cone lies in the plane of the plate. The sample is contained in the narrow gap ($\alpha \leqslant 5^{\circ}$) between cone and plate where α is the angle between the sides of the cone and the plane of the plate. These small values of α produce an approximately uniform shear rate through the sample when the cone is rotated. This cone and plate geometry also makes it easy to introduce the sample and to clean the apparatus. If the cone is driven at angular velocity ω, the shear rate in the sample $\dot{\gamma} = \omega/\alpha$. The viscosity of the sample is then

$$\eta = \frac{\sigma}{\dot{\gamma}} = \frac{3}{2\pi R^3} \frac{\alpha}{\omega} T$$

where σ is the shear stress in the sample, R is the cone radius and T is the torque measured by the dynamometer attached to the plate.

III.4.3 Description of apparatus

A schematic diagram of the apparatus is shown in Figure III.6. The cone is driven by a series of synchronous motors. The torque transmitted to the plate through the sample is measured by a dynamometer: the variation of torque with time is displayed on a recorder. The dynamometer is calibrated in situ by the addition of known weights to the string and pulley system between the dynamometer and the plate. The cone and plate contain separate heaters each with its own temperature controller. The surrounding insulation jacket may be used to maintain an inert atmosphere over samples which are subject to oxidative degradation. The vertical position of the cone is fixed. The plate may be raised and lowered on a micrometer screw. In operation it is placed at a distance from the cone equivalent to the truncation of the cone. Emphasis has been given to rigidity of structure and isolation of the apparatus from stray vibrations.

More details on the construction of this apparatus can be found in the literature (76).

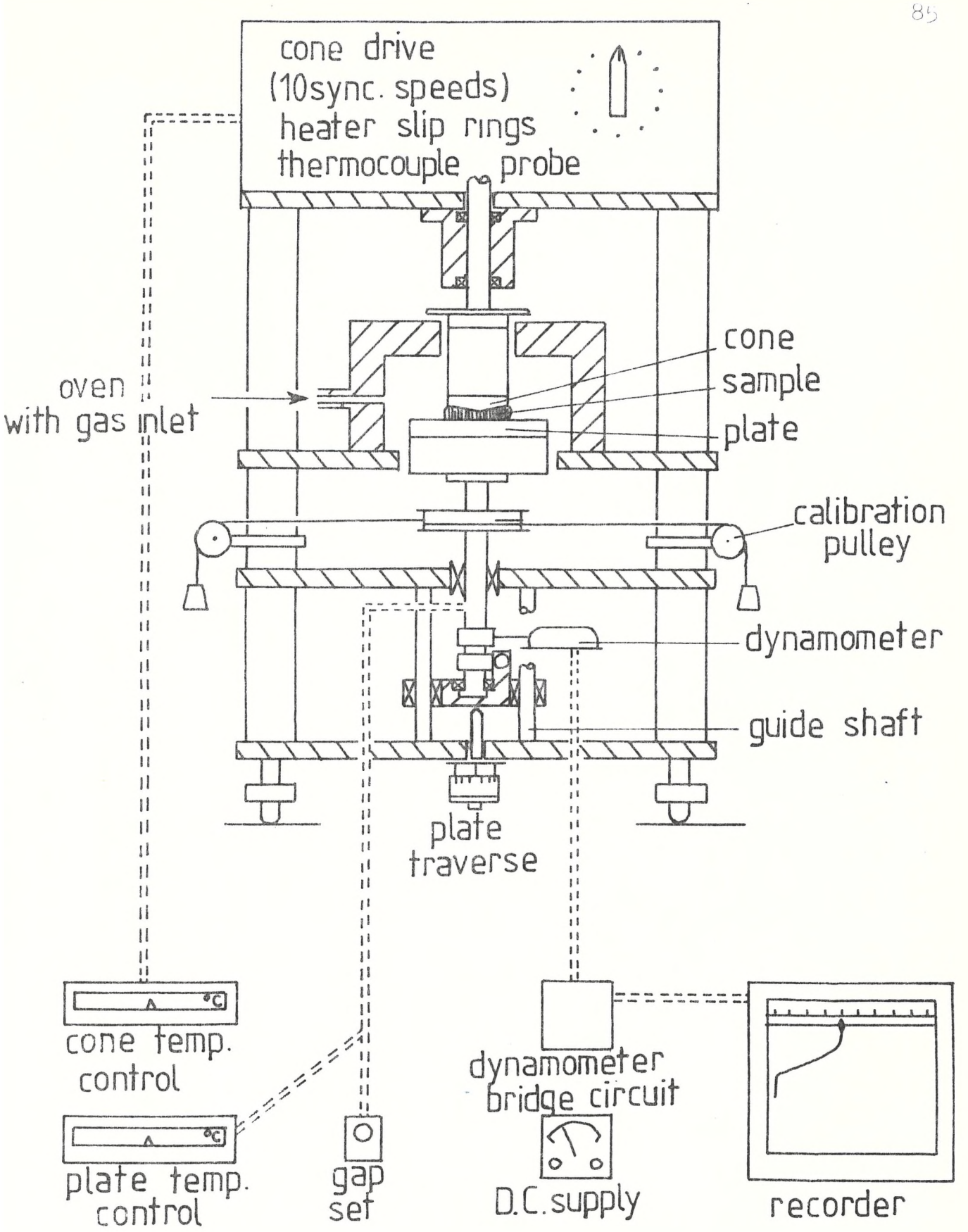

Figure III.6 CONE AND PLATE RHEOMETER

(schematic representation)

III.4.4 Operation of the apparatus

Once the cone and plate have reached the desired temperature, the sample is inserted as powder or chips. A further 5 - 15 minutes is allowed for temperature equilibration. The plate is then raised until the gap between the cone and plate is 0.010 in, equivalent to the truncation depth of the cone. The motor is run at the slowest speed (the speeds vary from 1 rev per 20 h to 1.2 rev per min corresponding for a 5^{o} cone to a shear rate range of 10^{-3} to 1.44 s^{-1}) until a steady flow condition is achieved as indicated by a constant torque. Then a change of speed is effected.

III.4.5 Experimental conditions and results

The temperature chosen to measure the viscosity of our samples was $170^{o}C$. This temperature is commonly used for high density polyethylene viscosity measurement and allows us to compare our results to reference specimens.

The amount of sample used for each experiment was about 4 grammes. No antioxidant was added as previous experiments had shown that for our samples viscosity is not time dependant and that polymer did not degrade in the time required to make the measurement. Pellets were used for Rigidex and powder for the experimental polymers. Some measurements were also carried out on samples taken from polymeric sheets prepared for mechanical testing (tensile or impact charging measurements). No formation of bubbles was observed on following the instructions

previously mentioned. The reproducibility of measurements obtained was checked and several experiments gave the same results. The correlation between this type of rheometer and capillary instruments is known to be excellent (77).

The results are usually shown as a graph of viscosity vs shear stress. Figure III.7 shows the various curves obtained for our samples. When the viscosity of the sample was too high (e.g. sample 56) it was not possible to obtain many experimental points because of the limitation of the apparatus to a shear stress of about 2×10^4 N/m^2. One can readily observe from Figure III.7 that the materials tested behave very differently from one another. A full discussion of these results related to molecular weight characteristics will be given later.

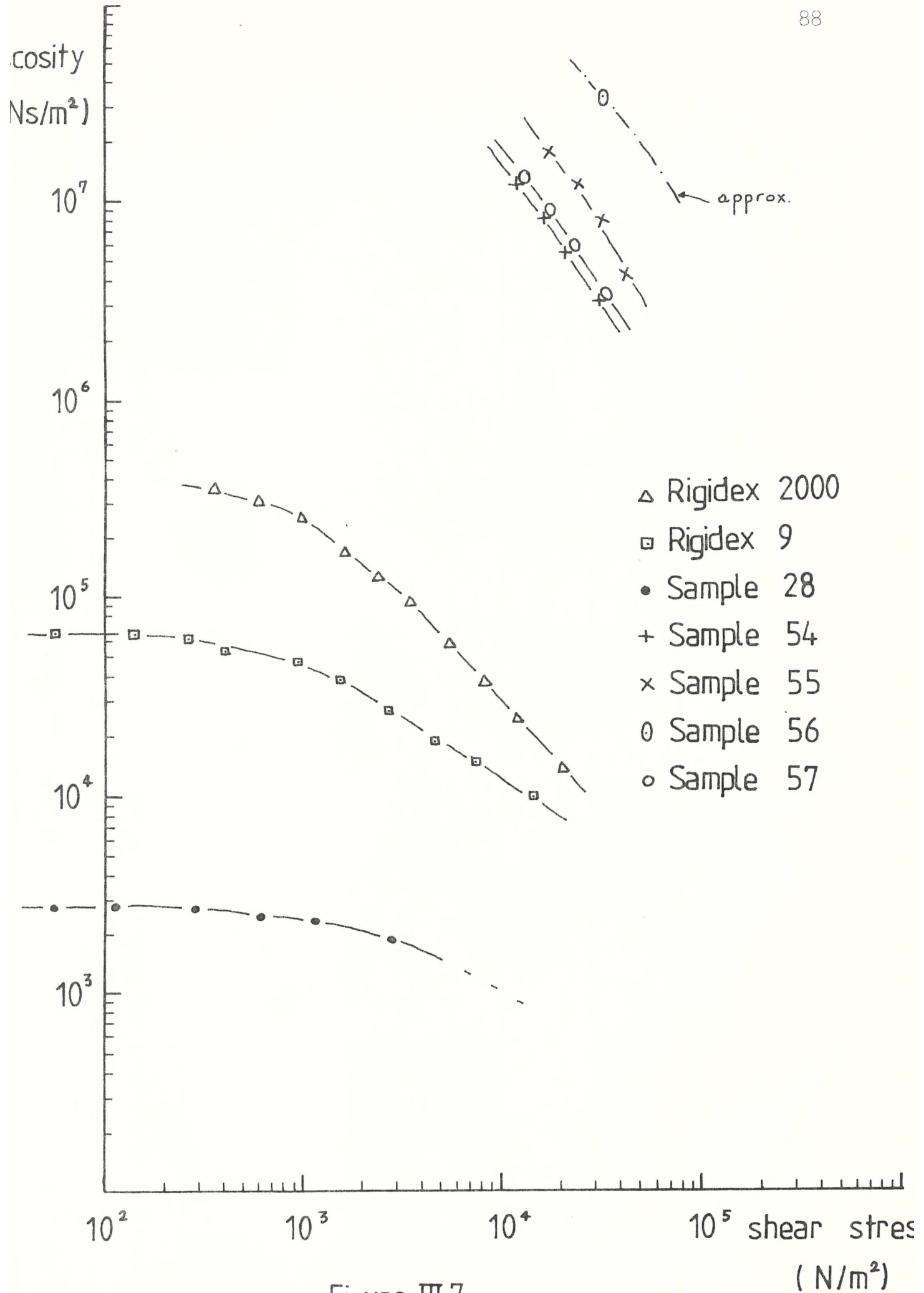
cosity
Ns/m²)
10⁷
10⁶
10⁵
10⁴
10³
10²
10³
10⁴
10⁵ shear stres
(N/m²)
approx.
Rigidex 2000
Rigidex 9
Sample 28
Sample 54
Sample 55
Sample 56
Sample 57

Figure III.7

III.5 Mechanical properties

III.5.1 Impact measurements - The instrumented falling weight impact machine (78)

III.5.1.1 Introduction

The determination of the impact behaviour of a plastics component is an important part of any assessment of a material's behaviour in service. Various methods have been used in the past, none of which can be said to give a complete picture of the impact phenomenon. Each method is highly labour-intensive since a large number of specimens needs to be tested and the specimens themselves often require careful machining. In an attempt both to reduce the labour-intensive aspect of impact testing and to obtain as much information as possible from a test on a single specimen, the traditional falling weight impact test was instrumented in such a way as to record the load-deformation characteristics of a plastic component under impact, i.e. under high rates of loading.

By using an excess of energy in the impactor, it is ensured that the specimen always exhibits some kind of failure phenomenon. Figure III.9(b) shows various types of failure for a given specimen at various temperatures. We then obtain from the instrumented falling weight device a record of the load (W) against deflection (y) behaviour of a test specimen as it deforms to failure. From the trace of W against y we can measure the load, deflection and energy absorbed at any stage of the deformation process and in particular at yield and break. The equipment is interfaced to a computer so that an immediate record of the values of

energy, load and deformation at yield and break are obtained.

The advantages of the Instrumented Falling Weight Device are as follows:

1) Sample preparation is reduced to a minimum since whole mouldings, or specimens roughly cut from the whole, can be tested.

2) The number of specimens required for a given material evaluation is reduced since each specimen under test fails and the details of each failure are recorded.

3) The distinction between brittle and ductile behaviour is more clearly defined than in other tests since any yielding of the material can be observed from the load deflection details for each specimen. This is a very important feature of the test.

4) The test will seek out the "weak" directions in a component and failure will occur in these directions.

5) Whole mouldings with different geometries can be tested to assess the effects of corners, ribs, etc.

III.5.1.2 Apparatus

The details of the instrumented falling weight impact machine are shown in Figure III.8. The specimen support shown is an annular ring of diameter 50 mm on which the specimen (plate or disc) is placed. The size of the support can be changed or adapted for other specimen geometries.

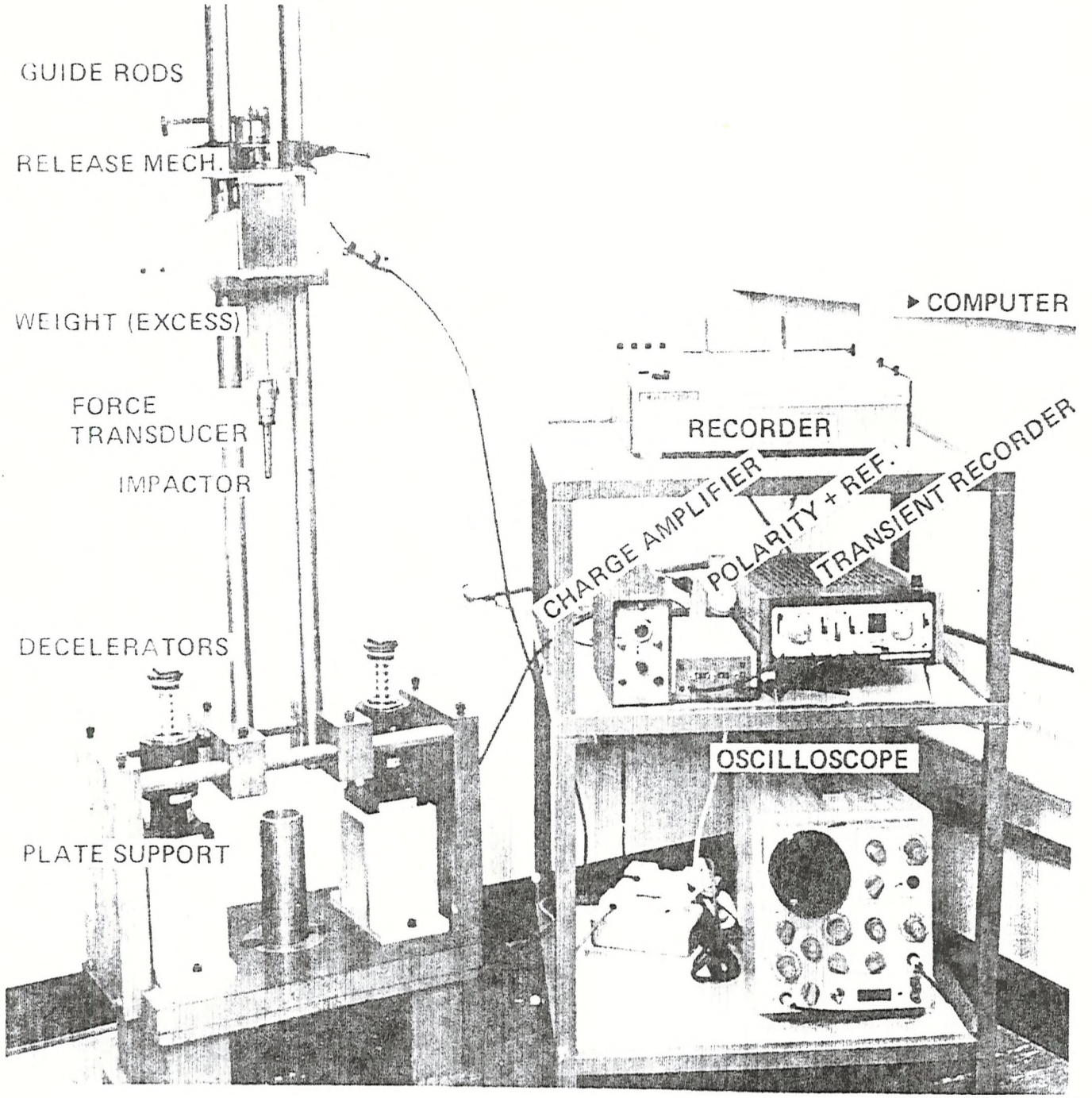

Fig III.8 INSTRUMENTED FALLING WEIGHT IMPACT EQUIPMENT

The weight ($\sim$ 10 Kg) is released from a height such that the velocity at impact is known (usually 3 or 5 m/s). A force transducer is connected to the impactor (usually a "nose" of radius 12 mm, but other shapes and sizes are available) which gives a record of the load on the specimen during the time it is deformed by the impactor. This information is stored and displayed on an oscilloscope as a load-time curve. At the press of a switch this information is fed to a computer which prints out the salient load-deflection details. A permanent record of the load deformation behaviour is simultaneously obtained on the chart recorder.

Results

A typical load-deflection trace obtained on a ductile material is shown on Figure III.9(a). From it we can distinguish the various important aspects of the deformation behaviour. As the impactor strikes the specimen the load of the specimen begins to rise in an approximately linear curve from which an assessment of the "stiffness" can be obtained. The slope of this part of the curve is calculated by the computer and printed out. For a brittle material (e.g. 'Perspex' at room temperature), failure will occur in this linear region and the load falls to zero. For a ductile material (e.g. H.D.P.E. at room temperature), the curve shows a "peak" corresponding to a "yield" after which the load falls off as the material deforms around the impactor

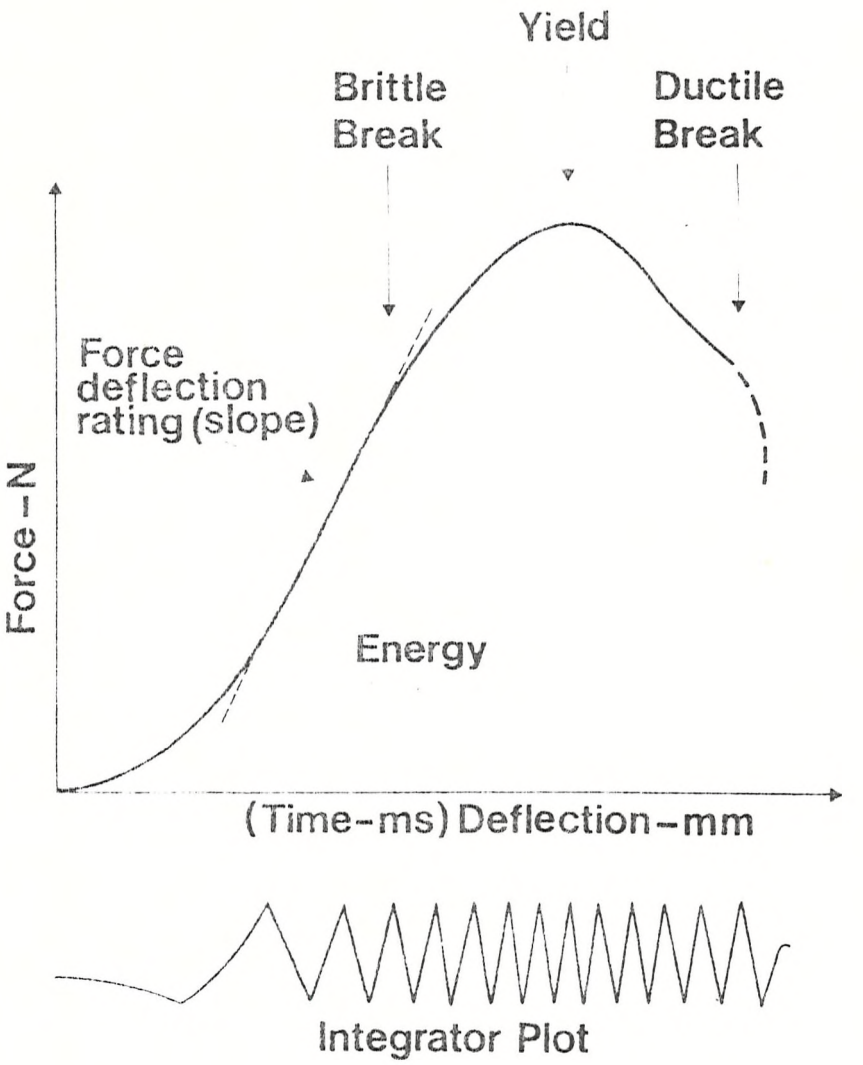

Fig. III.9a TYPICAL FORCE DEFLECTION CURVE

DUCTILE/BRITTLE TRANSITION OF A POLYMER

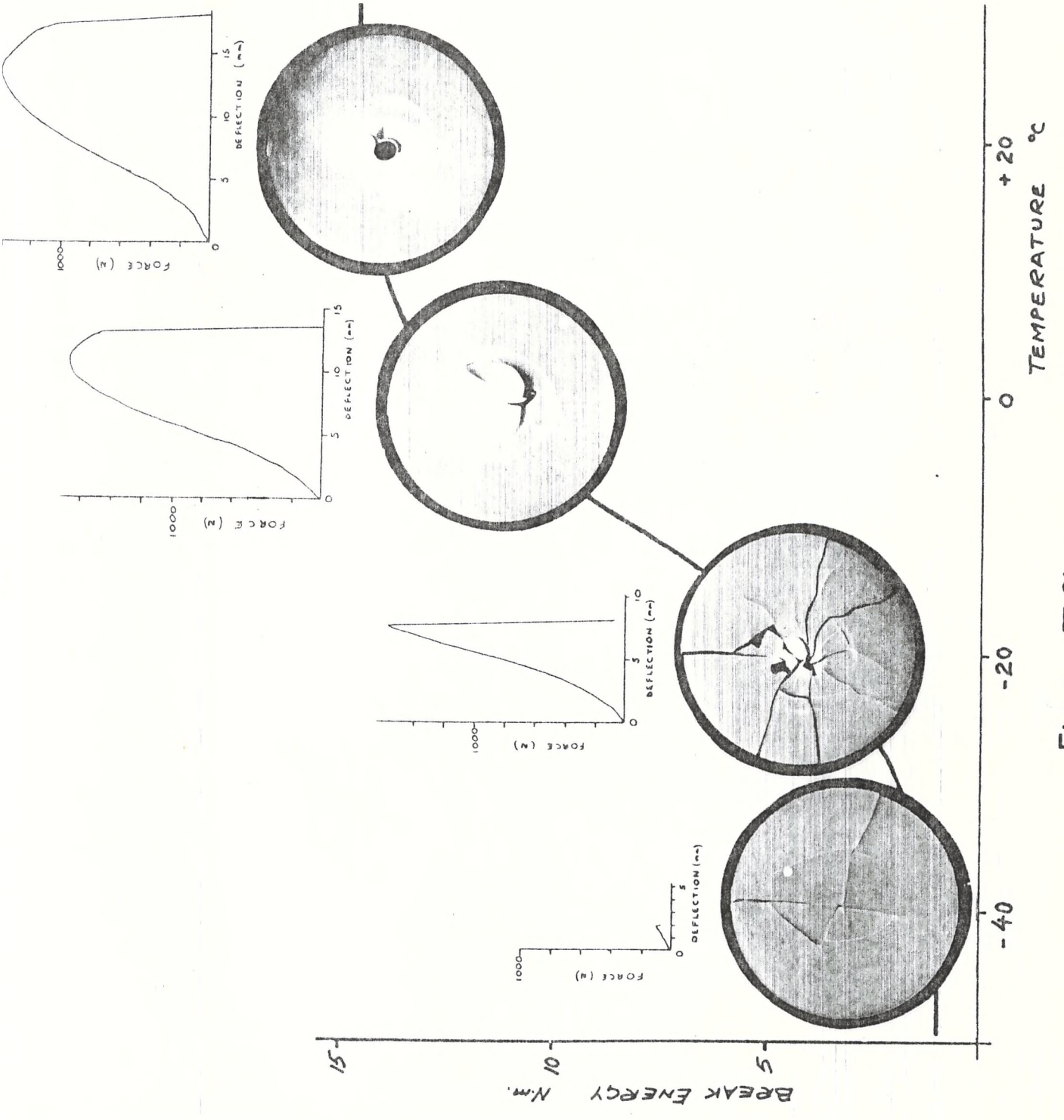

Figure. III.9b

until the "nose" finally penetrates the specimen. The computer calculates the load, deflection and energy absorbed at this final break point, as well as at the yield point.

III.5.1.3 Sample preparation

The sample for test is usually a plate or a disc bigger than the support diameter (typically 50 mm). The sample must be thick enough to remain on the support when the weight goes through it.

The test samples were moulded using a hot press. About 8 g of bulk polymer (powder for the experimental polymers or pellets for Rigidex) were placed between two plates coated with P.T.F.E. To obtain the right shape and thickness a circular mould was used between the plates. The polymer was pressed and melted for 3 mins at 170 - 180°C and at 15 tons. The sample was then cooled down to 40°C, still under pressure, using the water cooling system of the hot press. The cooling rate thus achieved is about 65°C/min. The samples obtained were discs of about 70 mm diameter and 1 mm thickness. This type of specimen is then ready to be placed on the annular ring for testing.

III.5.1.4 Results

Because some samples were tougher than expected, series of tests have been carried out on a 40 mm diameter support instead of the conventional 50 mm one. In the latter case

the sample was sometimes pushed into the ring, the impactor did not go through the sample and no proper results could then be obtained. The modification of the support, slightly affects the data and these will be discussed later.

The impactor was positioned so that its speed when it reached the sample was $\sim 5 m/s$. All samples tested, including Rigidex 2000 and Rigidex 9 showed a failure of the ductile type.

Depending upon the amount of polymer available, it was sometimes possible to carry out several tests for the same material. This was also done where possible to check the reproducibility of the experiment.

In the two tables below (Table III.4 and Table III.5) the data obtained from the instrumented falling weight machine are quoted. A typical force-deflection curve for ductile material is shown in Figure III.10 and the individual results are discussed below.

From the first series of data (Table III.4) it appears that there is only a slight difference between Rigidex 9 and Rigidex 2000. One can see that Rigidex 9 has a gradient value slightly higher than Rigidex 2000, (108 N/mm compared to 100; the average value of the three measurements). This material can therefore be assumed to be stiffer than Rigidex 2000. However the failure energy is just a bit lower (583 Nm compared to 593). No real comment can be made as the experimental error on these data is of the order of the difference between the two values. Nevertheless, the comparison between Rigidex 2000 and Rigidex 9 confirms the well known fact that stiffness and toughness are two

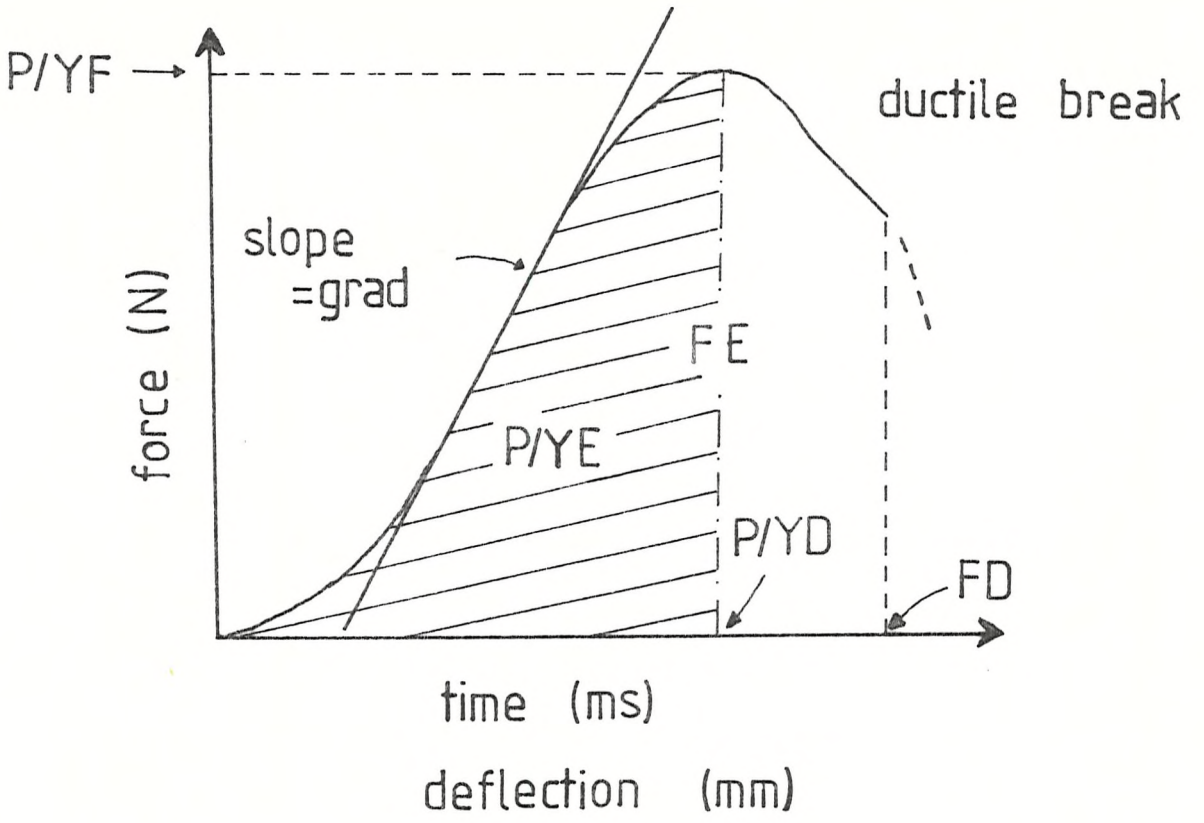

Figure III.10

Grad: Slope of the leading edge of the peak; this parameter is directly connected to the stiffness.

P/YF: Force at yield.

P/YD: Deflection at yield.

P/YE: Energy at yield; area under the peak before yield takes place.

FD: Failure deflection.

FE: Failure energy; area under the peak until failures take place.

Table III.4 Impact data for experiments carried out on a 50 mm diameter support

Sample	Gradient (N/mm)	Force at Yield (N)	Deflection at Yield (mm)	Energy at Yield (Nm)	Failure deflection (mm)	Failure energy (Nm)
Rigidex 9 a	108	750	10.5	4.49	13.0	5.88
Rigidex 9 b	108	767	10.5	4.53	13.0	5.78
Rigidex 2000 a	103	727	12.7	4.23	15.8	5.84
Rigidex 2000 b	97	773	12.6	4.44	15.6	6.19
Rigidex 2000 c	99	734	12.9	4.25	15.6	5.76
54 a	93	832	12.5	5.94	15.9	8.10
54 b	94	824	12.4	5.80	15.6	7.85
54 c	93	836	12.3	5.84	15.6	7.91

Table III.5 Impact data for experiments carried out on a 40 mm diameter support

Sample	Gradient (N/mm)	Force at Yield (N)	Deflection at Yield (mm)	Energy at Yield (Nm)	Failure deflection (mm)	Failure energy (Nm)
Rigidex 9	116	758	11.6	4.26	14.6	5.56
54 a	103	836	13.7	5.69	17.8	8.17
54 b	108	891	13.9	5.89	18.3	8.72
55	108	941	15.9	7.67	20.9	11.3
56	112	1039	15.0	7.82	19.0	10.8
57 a	110	930	13.5	6.42	17.6	9.11
57 b	112	953	13.7	6.63	17.9	9.43
57 c	110	922	13.8	6.30	17.8	8.96

properties which are difficult to improve at the same time.

Since the differences between Rigidex 2000 and Rigidex 9 are so small, it will be assumed that they are identical and, to simplify the analysis of the data, other samples will be compared with Rigidex 9 only. This sample has also the advantage of having been tested on a 40 mm diameter support as well as on a 50 mm diameter one.

The comparison between Table III.4 and Table III.5 gives some idea of the normalisation of the data required for the change of diameter support from 50 mm to 40 mm. It can be observed that with a smaller diameter the gradient value goes up by roughly 8 - 10% whereas the values on the deflection of the specimen are increased by about 12% either at yield or at break. However the energy values remain identical within experimental error. It can also be observed from the Tables III.4 and III.5 that this type of experiment is quite reproducible when the same polymeric material is tested several times. The fluctuation of the results is well below 10%.

The analysis of the second series of data gives precise information on our own materials compared to Rigidex 9. For all our samples the gradient valuesare lowered by 5 to 10% but all the other data are significantly higher. For simplicity, only the failure energy of the various samples will be compared. This is the best representative figure being the most characteristic one describing the toughness of the sample considered.

It will be noted from the failure energy column that the energy absorbed by the material before it breaks is 50%

higher for sample 54 and up to 90% higher for sample 55 compared with Rigidex 9.

As a whole, one can conclude that although the same type of ductile failure is observed for all the samples, our materials are less stiff but definitively tougher than 'normal'.

A discussion of the significance of impact and other data and properties will be given later in the appropriate chapter.

III.5.2 Tensile Measurements

III.5.2.1 Introduction

This type of measurement allows us to study the deformation of a material when it is subjected to a tensile load. This method is complementary to the impact one previously described. By applying both methods one can characterise the mechanical properties of polymers.

III.5.2.2 Apparatus

The equipment used is a Universal Testing Instrument 100 Kg capacity Model 1101 manufactured by Instron Limited (see Figure III.11).

Samples with a predetermined shape (see later) are placed between the two clamps of the machine. The top clamp is fixed while the bottom one moves downwards at a predetermined speed. The range of speed available on this machine is quite large and varies from 5mm/min to 1000mm/min. The speed usually used is 10 mm/min. The top clamp is connected to an interchangeable load cell which detects and records the load on the sample which is under test. The load cell is essentially an electrical sensing device, using foil strain gauges, which produces signals, corresponding to load variations, which operates in turn the pen of a high speed chart recorder. The accuracy of the load weighing system is better than $\pm$ 0.5% under all conditions (79). As the load detected on the sample under stress is dependant on its cross-sectional area the recorder unit is supplied with an area compensator.

Model 1101

Universal Testing Instrument
100 kg capacity

INSTRON

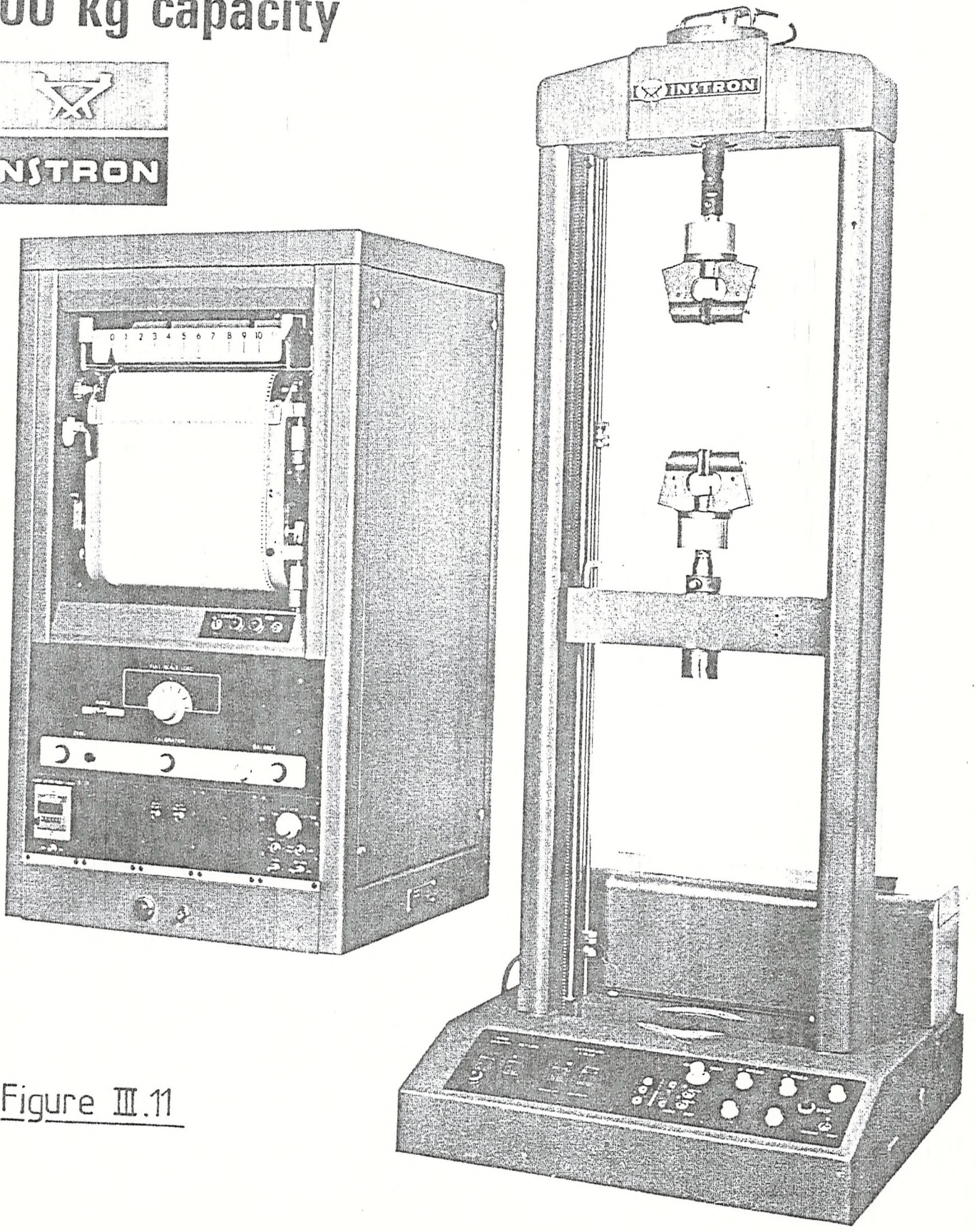

Figure III.11

Results

The data derived from tensile stress strain measurements on plastics are important from a practical viewpoint, providing information on the modulus, the brittleness and the ultimate and yield strengths of the polymer. A typical stress strain curve is given in Figure III.12.

The shape of such a curve is dependant on the rate of testing; consequently, this must be specified if a meaningful comparison of data is to be made. The initial portion of the curve is linear and the tensile modulus E can be obtained from its slope. The point L represents the stress beyond which a brittle material will fracture and the area under the curve to this point is proportional to the energy required for brittle fracture. If the material is tough no fracture occurs and the curve then passes through a maximum or inflection point Y, known as the yield point. Beyond this, the ultimate elongation is eventually reached and the polymer breaks at B. The area under this part of the curve is the energy required for tough fracture.

In Figure III.13 is given the different stress-strain curves for different types of polymeric materials.

III.5.2.3 Sample Preparation

Thin sheets of polymeric material were obtained by pressing and heating bulk polymer (either powder or pellets) with a hot press. The experimental conditions were the same as those for the impact samples except that thickness

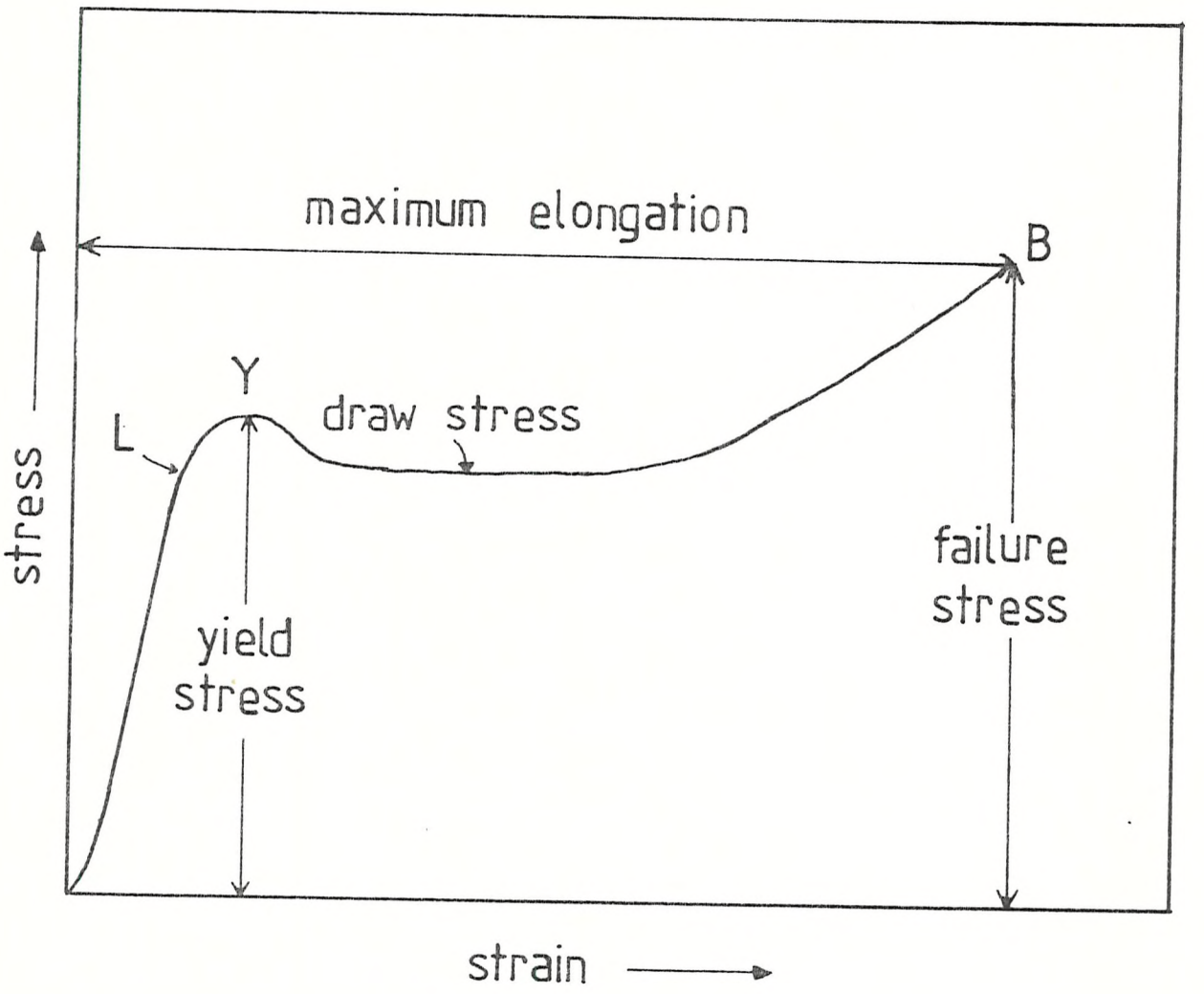

Figure III.12 GENERALIZED TENSILE STRESS-STRAIN CURVE FOR PLASTICS.

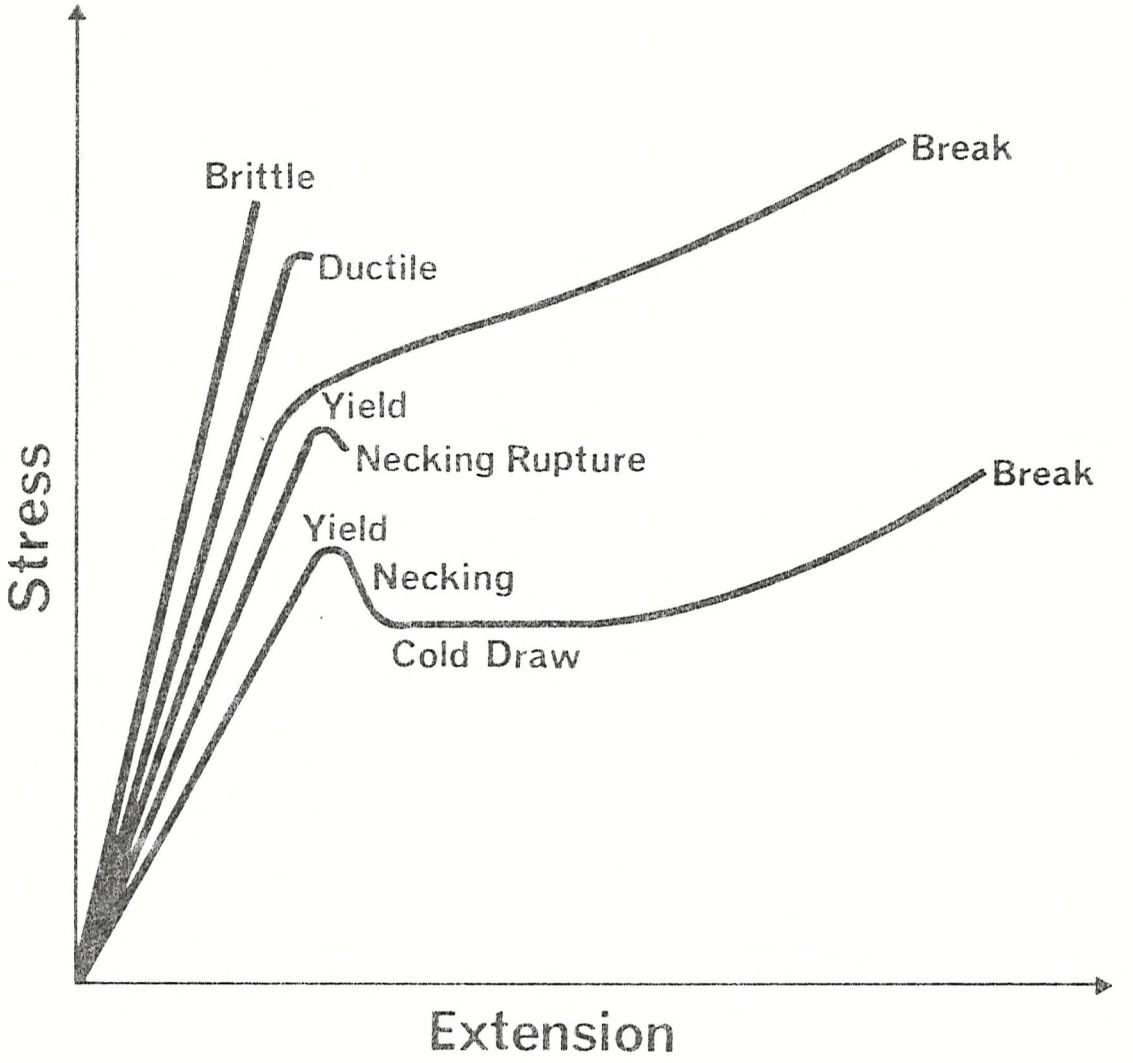

Figure III.13 SOME TYPICAL STRESS/EXTENSION CURVES

was controlled by inserting thickness gauges of 0.3 mm between the two plates. Several specimens (at least 3 for tensile measurements) are cut from the sheet with a specially designed punch. The shape obtained is represented in Figure III.13.a . Thickness and width have been measured precisely to introduce into the recorder area compensator the cross area section of each sample. Marks are drawn on the sample to follow its elongation while it is under test.

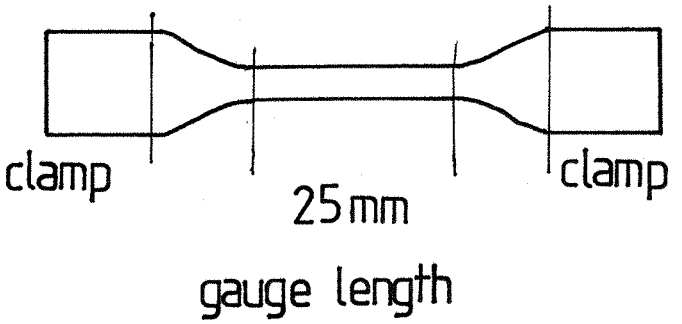

Figure III.13.a : SHAPE OF SAMPLES FOR TENSILE MEASUREMENTS

III.5.2.4 Observations and results

The samples were tested at a crosshead speed of 100 mm/min, and a temperature of 21°C. It has been observed since the beginning of this work that the quality of moulding is of real importance for such tests. If a defect is present within the gauge length of the specimen (air bubble, dust particle, ...) the sample will break soon after the yield point, and only characteristics up to the yield point could be obtained. It is reasonable to say that failure always occurs because of defects but one must differentiate between macroscopic defects such as air bubbles or dust particles, which are due to a 'bad' moulding (either by the moulding process or by the material itself) and microscopic defects, lamallae and chains arrangement, which are the consequence of the crystallisation process in the specimen.

Mouldings produced with care eliminate to a certain extent macroscopic defects, but do not change really the crystallisation phenomenon of polymers. It has been observed that some materials have the ability to be always well moulded and give similar results when several specimens are tested. In this case break occurs at failure stress and elongation within the experimental error, and it is possible to average the different stress values obtained from the stress-strain curves. The materials which belong to this category are Rigidex 2000 and samples 54-57.

Other materials did not show the same ability, and roughly one out of two specimens tested broke just after yield. In this case we retained only the curves corresponding to maximum elongations and an average has been made, from at

least three "successful" tests.

The different characteristics then obtained are listed in Table III.6.

From this set of data it can be seen that although the mouldability of Rigidex 2000 and sample 28 is different their tensile behaviour is very similar. Rigidex 9 has also similar characteristics except failure stress and elongation to break which are significantly higher. Different behaviour patterns are observed for samples 54 - 57. Although Rigidex 9 has a slightly higher yield stress than samples 54 - 57, (29 MN/m^2 compared to an average value of 25) the latter have a ratio yield stress/draw stress (σ_y/σ_D) = 1.1 which is fairly low and unexpected for H.D.P.E. There is also a difference between the elongations measured (550% compared to 980% for Rigidex 9) which is very noticable. Furthermore the tensile stress-strain curves for samples 54 - 57 indicates "work hardening" fairly soon after yield, an effect which is less accentuated in Rigidex 9 (see Figure III.14). Consequently the failure stress is significantly higher 46 MN/m^2 compared to 32 MN/m^2 for Rigidex 9. Here again as it has been shown from impact measurements, our own materials 54 - 57 seem to be significantly tougher than Rigidex 9.

Table III.6 Tensile stress-strain curves characteristics

Sample	Ability to be moulded	Yield stress y (MN/m^2)	Draw stress (MN/m^2)	Failure stress (MN/m^2)	Elongation %	σ_y/σ_D
Rigidex 2000	good	27	17	17	500	1.6
Rigidex 9	poor	30	19	32	980	1.6
28	poor	29	19	19	300	1.6
54	good	26	22	48	600	1.2
55	good	24	22	42	500	1.1
56	good	25	23	49	540	1.1
57	good	25	22	47	560	1.1

Experimental errors:

$\pm$ 1 MN/m^2 for stress values

$\pm$ 50% for elongation

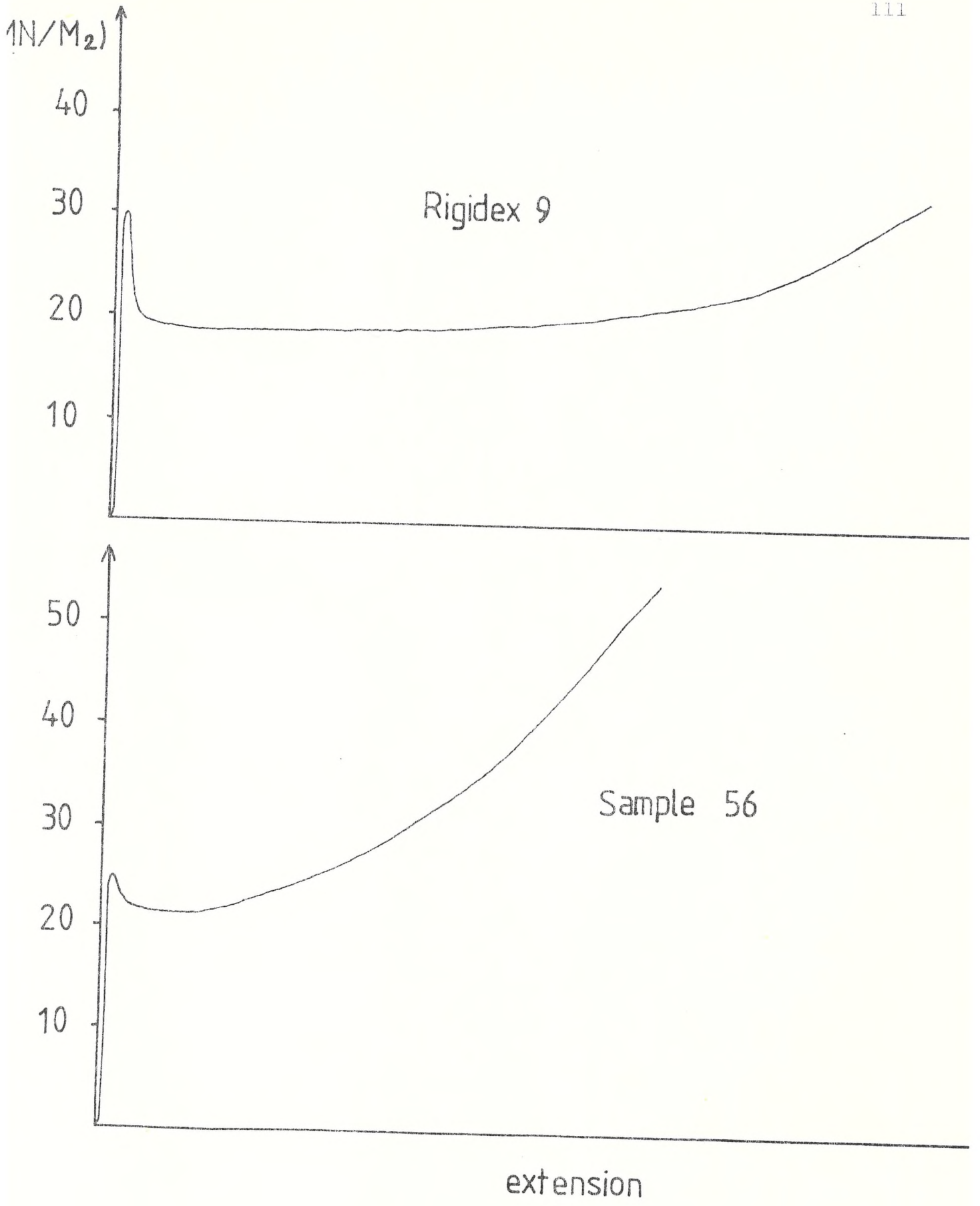

Fig III.14 STRESS-STRAIN CURVES FOR RIGIDEX 9 AND SAMPLE 56

III.6 Crystallisation characteristics

III.6.1 Crystallinity measurements

Crystallinity was calculated from measurements of the polymer density. Density measurements were made using a Davenport density gradient column by immersing the specimen in an ethanol/water column held at 23°C. The range of a typical column was 930 - 990 Kg/m^3. The column was calibrated such that densities could be measured to ± 0.2 Kg/m^3. Crystallinities were then estimated by assuming a value of 855.0 Kg/m^3 for the amourphous density and 1000.0 Kg/m^3 for the fully crystalline material (80). The error in crystallinity so derived is less than ± 0.1%.

It is obvious that density depends on the purity of the sample. High catalysts residues will also modify the density. It has been shown earlier that although a complete elimination of catalyst residues was not obtained, the contents for our sample are fairly low and comparable to commercial polyethylenes. Bubbles can also alter the density and give lower values than expected. This is not likely for our polymers which were "well moulded". Bubbles on the surface of the specimen in the density gradient column are easily seen and these specimens are ignored.

Density measurements were made on pieces of thin sheets of polymeric material made for tensile measurements (see Section III.5.2.3). All the samples measured had the same thermal history.

Results

Table III.7 Crystallinity measurements

Sample	Density Kg/m^3	% of crystallinity
Rigidex 9	959.2	72
28	958.7	72
54	945.4	62
55	938.8	58
56	939.8	59
57	943.6	61

Rigidex 9 is specified to have a density of 960 Kg/m^3 (81). Our determined value of 959.2 Kg/m^3 is a reasonably good match, which confirms the validity of our measurements. Table III.7 clearly reveals that samples 54 - 57 have a degree of crystallinity significantly lower than Rigidex whilst sample 28 which has the same value.
This observation, of real importance, will be discussed later.

III.6.2 Lamellar thickness

The lamellar thickness of the specimen was derived from the low frequency Raman spectrum as explained in Chapter II.

The samples used for lamellar thickness determination were pieces from thin moulded polymeric sheets made for tensile experiments as described previously.

Spectra were recorded using a Coderg T800 (triple monochromator) Spectrometer with a Spectra Physics model 170 argon ion laser operating at 514.5 nm as a source. The optical diagram of the Coderg T800 is shown in Figure III.15. The laser beam is focussed onto the sample and the light scattered at 90° is analysed by the triple monochromator and detected by a photomultiplier tube. The limiting spectral resolution of the spectrometer is better than 0.5 cm^{-1}. In order to achieve this sort of resolution, the instrument slitwidths must be very small. The power of the incident beam used was about 100 mW at the sample. Under a too powerful beam, polymers degrade and have been known to catch fire! The spectra obtained near the exciting line (from 4 - 40 cm^{-1}) were recorded at room temperature at a scan speed of 5 cm^{-1}/mn. They were deconvoluted by hand, by substracting the background to the spectra in order to get the true L.A. mode (see Figure III.17). The error made by deconvolution is certainly less than 0.5 cm^{-1}.

Lamellar thicknesses were derived from the frequencies of the L.A. mode using the formula (see Chapter II).

$$\nu = \frac{m}{2L}\sqrt{\frac{E}{\rho}}$$

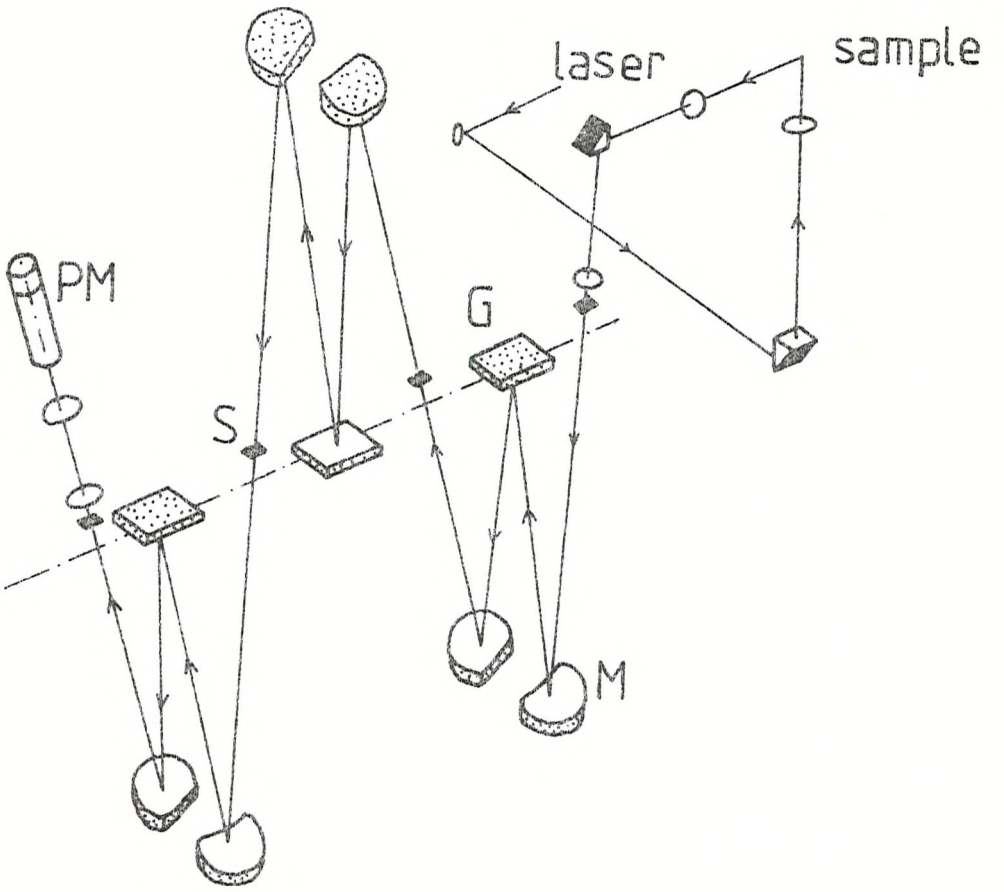

S: slit

M: mirror

G: grating

PM: photomultiplier tube

Figure III.15 OPTICAL DIAGRAM OF THE CODERG T800 SPECTROMETER

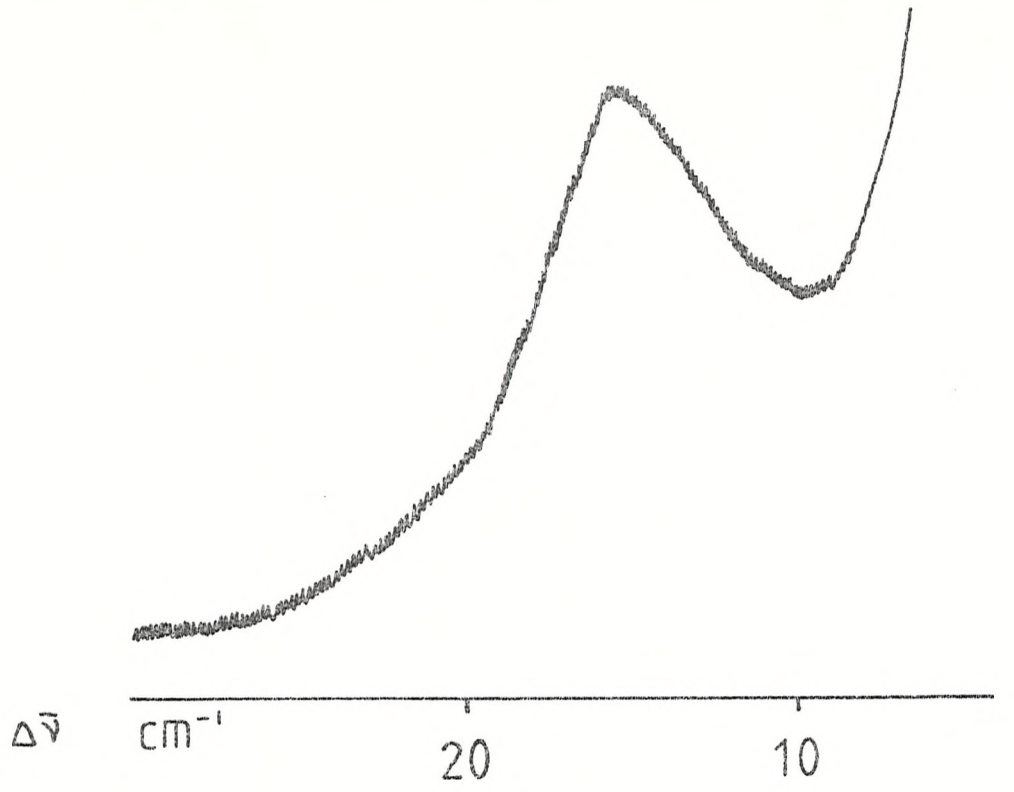

Fig III.16 THE LA MODE OF A LINEAR POLYETHYLENE

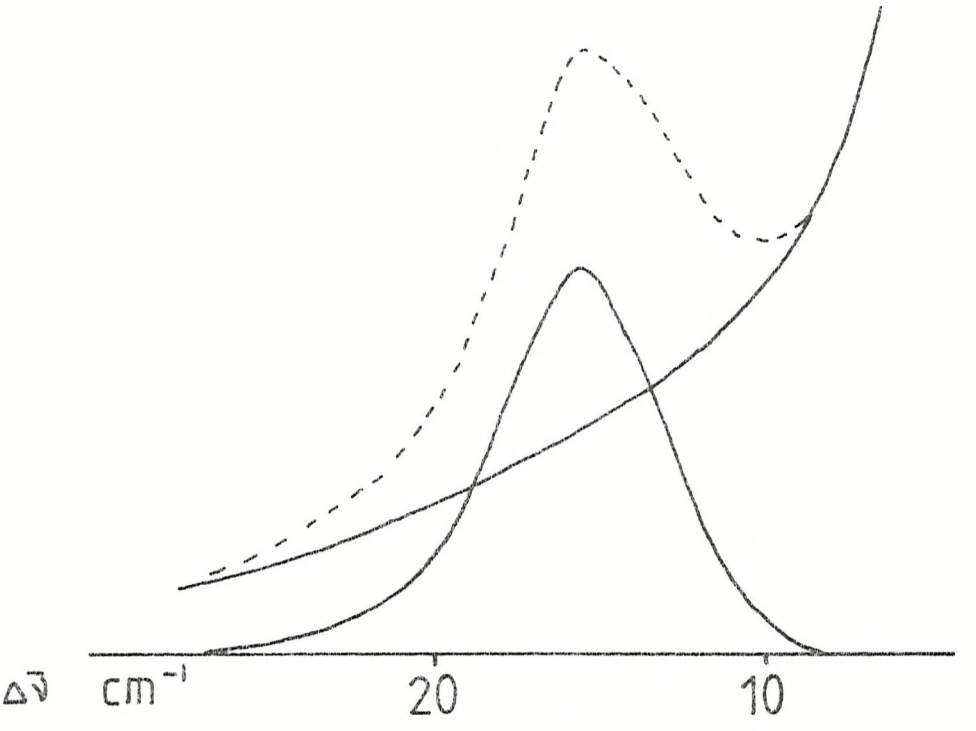

Fig III.17 DECONVOLUTION OF THE LA MODE

This relationship is controversial. Further there is doubt about the correct value of E to use (100). Usually ρ is the density of the crystalline phase (i.e. 1000 Kg/m^3) although Marsden (82) defines ρ as an "uniaxial density" term which is independent of the chain packing in the unit cell.

In this determination $E = 2.9$ dyne/cm^2 (100)

$\rho = 1$

$m = 1$ (order mode)

Results

Table III.8 Lamellar thickness measurement

Samples	L.A. mode $\pm$ 0.5 cm^{-1}	lamellar thickness nm	width of L.A. mode cm^{-1}
Rigidex 9	14	20.3	7
Sample 28	14	20.3	7
54	12.5	22.7	6
55	12	23.7	6
56	12.5	22.7	6
57	12.5	22.7	7

Table III.8 clearly shows evidence that samples 54 - 57 are significantly different to Rigidex 9 and sample 28. Lamellar thickness is greater suggesting that the crystals produced by melt crystallisation are more perfect. However, no significant differences appear regarding the lamellar thickness distribution; the width of the L.A. mode is in all cases very similar.

III.7 Acknowledgements

Many thanks are due to the following people from I.C.I. Plastics Division for their help in obtaining particular data:

M.L. SEARLE for polymerisation reactions

F. YEARSLEY for light scattering

A. TITTERTON for G.P.C.

M. SWERDLOW for melt viscosity

M.J. WILLIAM for mechanical properties

P. WILLCOX for density determination.

CHAPTER IV

DISCUSSION AND CONCLUSION

IV.1 Discussion

IV.1.1 Melt viscosity and molecular weight characteristics

It is well known that melt viscosity increases with molecular weight. To a first approximation one can relate melt viscosity (η) and molecular weight M by the following relationship:

$$\eta = KM^a \text{ where K and a are constants.}$$

These constants depend on several parameters. The most important of these are:

- the temperature of the melt considered
- the type of polymer
- its molecular weight characteristics
- the viscosity range.

A better approximation can be achieved by using the series suggested by Cross (84, 85)

$$\eta = K_1M + K_2M^3 + K_3M^5 + \ldots.$$

The dependence of viscosity and temperature is well known and has been measured for many types of polymers. This dependence is usually given as a relative fluidity index X for an increase in temperature of 10°C (86).

$$X = \frac{\text{viscosity at } T^\circ C}{\text{viscosity at } (T+10)^\circ C} \text{ at a constant shear stress.}$$

X is dependent on the temperature range. For linear polyethylene around 200°C X has a value of 1.2.

Molecular weight is certainly the parameter to take most into account when dealing with melt viscosity. Small variations in molecular weight lead to tremendous differences in viscosity. It is estimated that for linear polyethylene tested around 170°C an increase in molecular weight by a factor 2 results in an increase in melt viscosity by a factor 10 (88).

Molecular weight distribution has also to be taken into account. Figure IV.1 (87) shows the difference in viscosity for two polymers of different molecular weight distribution which have approximately the same viscosity under Melt Flow Index conditions defined in Chapter I (see also ref. (35)). It is clearly shown that the broader the molecular weight the steeper the curve of viscosity vs shear stress. This property is often used in industry when high viscosity is required at low stress for applications such as blow moulding, but broadening the molecular weight distribution is usually purchased at the expense of poorer strength properties.

Measurements of melt viscosity were carried out by cone and plate experiments, as described earlier. Experiments were made on virgin samples as well as on already melted ones. A study of the stability of the viscosity as a function of the time that the polymer has been held in the melt was also made. One sample (57) was extruded several times (in order to shear modify it) and tested.

Results are reported in Figure III.7 and in Table IV.1 where $\overline{Mw}$ values are also quoted.

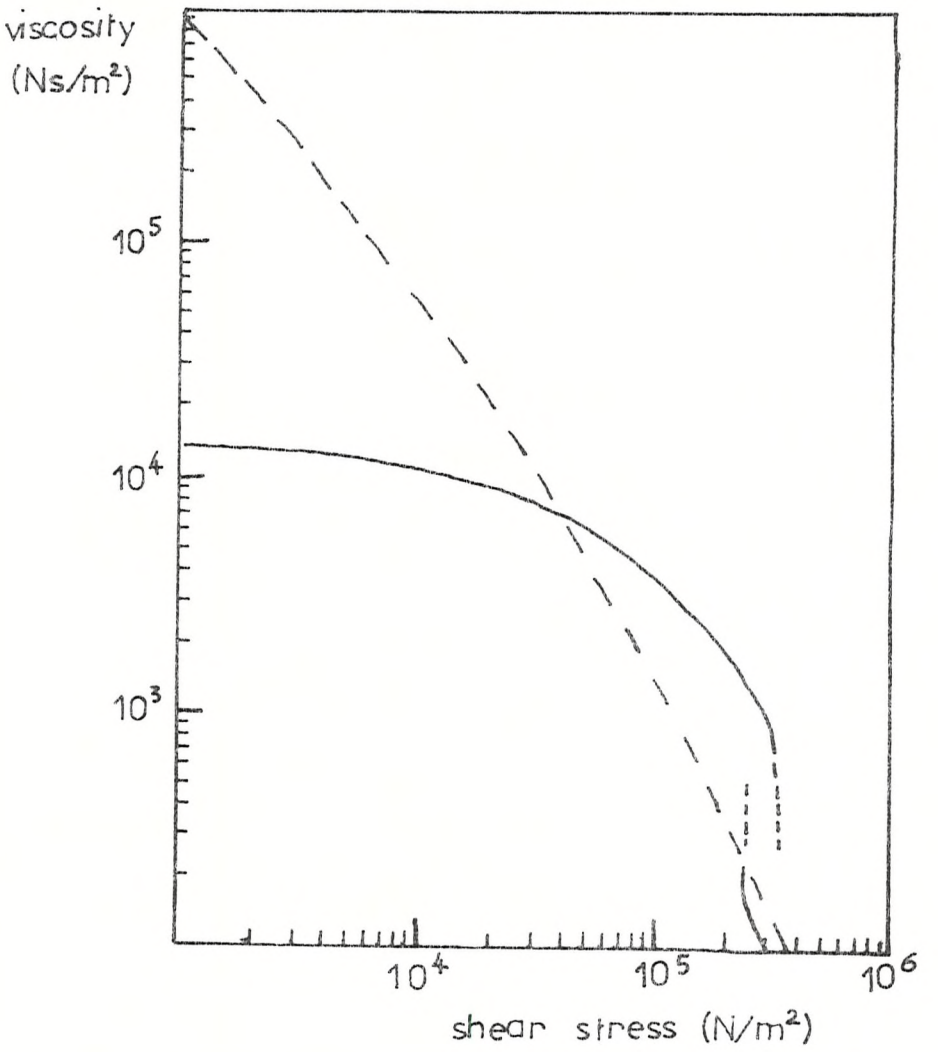

	$\overline{M_w}$	$\overline{M_n}$
– – –	185,000	15,000
———	120,000	30,000

Figure IV.1: MELT VISCOSITY OF LINEAR POLYETHYLENE AT 170°C

Table IV.1 Melt viscosity vs molecular weight at 170°C

Samples	$\overline{M}_w$	$\overline{M}_w/\overline{M}_n$	Melt viscosity at a shear stress of 1×10^4 N/m^2	
Rigidex 9	139,000	-	1.2×10^4	
Rigidex 2000	178,000	7.4	3×10^4	
28	99,000	2.7	1×10^3	estimated
54	1,160,000	-	1.5×10^7	
55	4,600,000	-	4×10^7	
56	800,000	-	1×10^8	estimated
57	960,000	-	2×10^7	

As was expected, viscosity increases with molecular weight and the set of samples tested can be divided in three groups: sample 28; Rigidex 9 and Rigidex 2000; and samples 54 to 57. However a closer examination reveals unusual results for sample 56 compared with samples 54, 55 and 57. Although sample 56 has the lowest molecular weight among these four, its viscosity is significantly greater than the others. The value given in the Table is estimated but cannot be lower than the one cited. This result is quite unexpected and reveals abnormal behaviour of the melt. The difference in viscosity between sample 28, Rigidex 9 and Rigidex 2000

can be attributed to molecular weight variations but it seems that for high molecular weight material it is not possible to relate molecular weight and melt viscosity directly (see Figure IV.2).

Due to their high viscosity, it was not possible to obtain wide-range melt flow curves for samples 54 - 57. However, since their shape and slope are identical it is reasonable to assume that their molecular weight distribution is very similar. M.F.I. measurements were not possible as the samples did not flow through the die of the extruder even with a 10 Kg load at 190°C. It has been found that for samples 54 - 57 viscosity is not time dependant since a sample held in the melt for various length of time always gave identical results. Sample 57 which was extruded several times was still very viscous and had the same melt flow curve as the virgin sample.

As a result viscosity anomalies in our samples cannot be explained fully through molecular weight and whatever the thermal and shear history of the sample, high viscosity is noticable and remains.

It would have been of interest to measure melt viscosity of our samples for higher shear stresses using capillary rheometers. Unfortunately, such equipment was not available when this project was carried out, but if this work is to be continued and enlarged, this type of measurement must be made.

On previously prepared samples similar to sample 54 - 57, but of slightly lower viscosity, melt elongation measure-

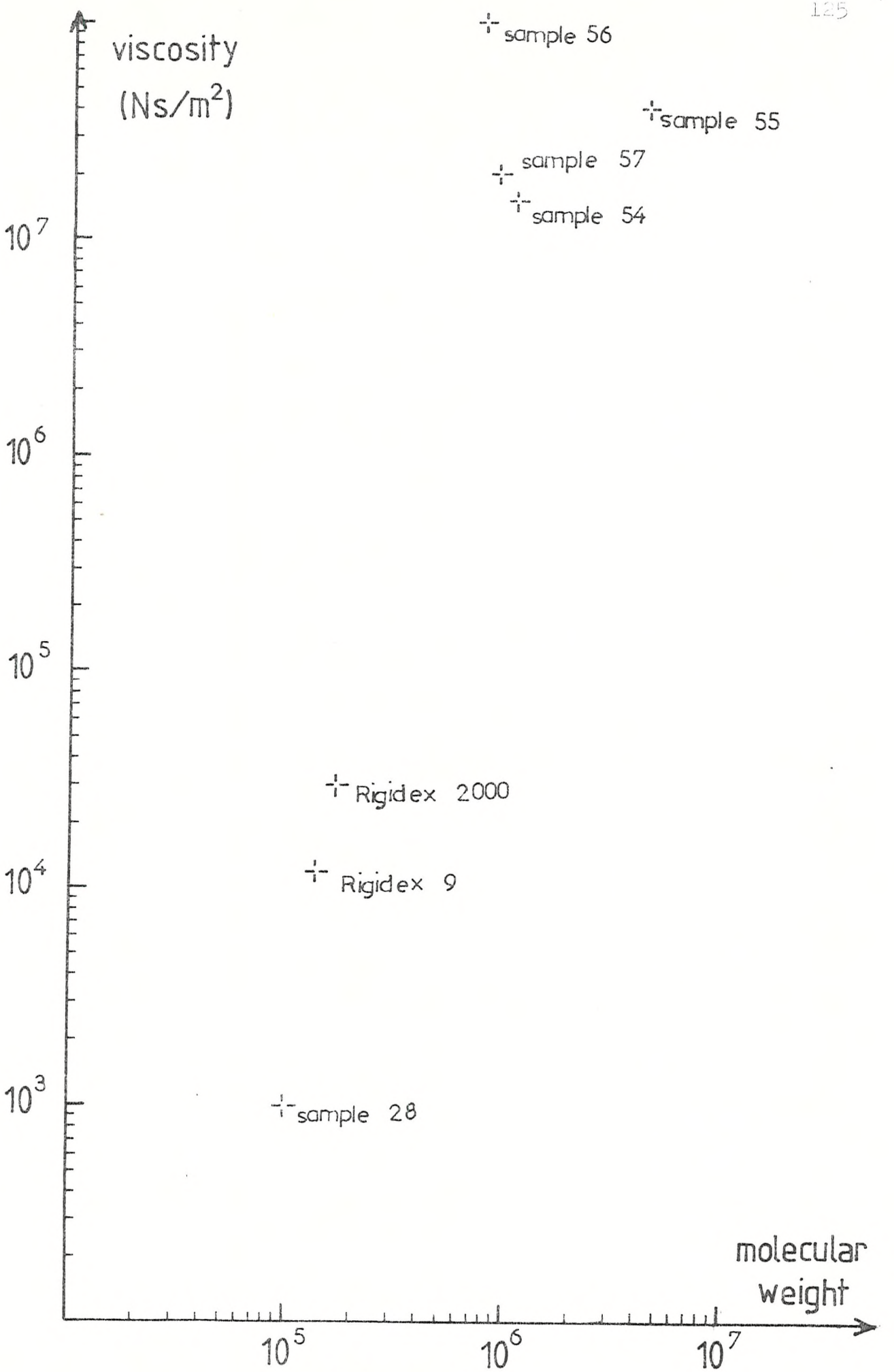
viscosity
(Ns/m²)
sample 56
sample 55
sample 57
sample 54
10⁷
10⁶
10⁵
Rigidex 2000
10⁴
Rigidex 9
10³
sample 28
molecular
weight
10⁵
10⁶
10⁷

Figure IV.2

ments were carried out. Polymer was extrudated through a grader with a 10 Kg load, and a weight was attached to the extrudate. Optimal results are obtained with the maximum weight (typically 12 g) at which the melt elongates without breaking; measurements were made at 150°C melt temperature. A complete description of the experiment has been published by Swerdlow et al (89). The value of the ratio of the diameter of the extrudate to the diameter of the elongated extrudate leads to the draw ratio, whereas the stress can be measured by the weight attached over the cross sectional area of the fibre.

Although this experiment seems very simple reproducibility is very bad and from one measurement to another, results can change dramatically. It requires considerable time and special care to obtain valuable results. We have found earlier (90) that it was possible to measure draw ratios of 1500 for our sample compared to the 100 obtained for Rigidex 2000. This difference is quite impressive and although these data may be of suspect reliability (because they come from few measurements) we can assume without any risk that the melt ductility of our samples are significantly improved compared with Rigidex, and further that this is not due to molecular weight.

To summarise, it is observed that:

- the relationship between melt viscosity and molecular weight seems very applicable for Sample 28, Rigidex 9 and Rigidex 2000. However, this relationship is not more valid for Samples 54 - 57.

- although melt flow curves for Samples 54 - 57 do not cover a wide range of shear stress it is reasonable to assume that their molecular weight distribution is very similar.

- whatever the thermal and shear history of the samples 54 - 57, they always exhibit very high viscosity.

- experiments reveal very high values of melt elongation.

IV.1.2 Crystallisation studies

During the few past years, the Southampton University polymer group has published results on numerous crystallisation studies of polymers. Such studies of crystallisation are normally based on crystallinity measurements and lamellar thickness determination. For the present work the former was carried out by density measurements, the latter by Raman spectroscopy.

The basic rules which govern crystallinity and lamellar thickness are now well established:

- branching is known to destroy crystallinity (3).

- thermal history (melt cooling procedure) greatly influences crystallinity and lamellar thickness.

a) it has been found that materials crystallised from high melt temperatures have thinner lamellae and are less crystallised (36)

b) the cooling rate is also very important: the

faster the cooling rate (quenching) the thinner the lamellae (36)

c) melt crystallisation is also pressure dependent (93).

- annealing (i.e. holding for a long time polymeric material just below its melting point) increases crystallinity and lamellar thickness (15)

- as the lamellar thickness rises so does the degree of crystallinity

- for a given polymer crystallinity and lamellar thickness is not molecular weight dependent (91).

All the samples described in this work are not branched since infrared analysis revealed less than 1 methyl group per 1000 carbon atoms.

The study of crystallisation versus thermal history was not undertaken in this project. Only a comparison of crystallisation characteristics was carried out on melt crystallised materials having rigourously the same thermal history. This is described in Section III.5.1.3.

This study clearly reveals that the degree of crystallinity is lower for samples 54 - 57 (average value 60%) than for samples 28 and Rigidex 9 (72%). Such a difference cannot be due to experimental errors which are better than 1%.

Spectroscopic measurements show evidence that lamellae are thicker for samples 54 - 57 compared with sample 28 and Rigidex (23 nm compared with 20 nm). Although this

difference seems small it is significant as the experimental error is less than 1 nm.

These results do not agree with what one would have expected. Effectively, since the cooling procedure was rigorously identical for each sample and since it is proved that no branching is present it was expected that crystallinity characteristics in all samples would be identical. They are not.

The fact that lamellar thickness rises whilst the degree of crystallinity decreases for samples 54 - 57 is also quite unexpected, and therefore suggested an increase in thickness of the disordered layers of polymers.

IV.1.3 Mechanical properties

It is well established that mechanical properties of melt-crystallised material depend on crystallisation characteristics. Further these characteristics depend on several other parameters as has been briefly reported earlier.

The mechanism of deformation of polymeric material under stress has been reviewed by Peterlin (92). He suggests that the deformation takes place in three stages:

- plastic deformation of spherulitic structure
- transformation of spherulitic into fibrous structure by fracture of lamellae and formation of micro-fibrils
- plastic deformation of fibrous structure.

The first stage takes place before necking proceeds by lamellar sliding motion, rotation and chain tilting. This stage is irreversible. The second stage corresponds to a complete change in morphology. Under stress the lamellae are transformed in fibres, and orientation of the chains takes place along the tensile direction. The third stage does not change the fibrous morphology; individual microfibrils and bundles of microfibrils slide past each other until failure occurs.

If the first stage is recognisable on a stress-strain tensile curve (the linear region before the yield point) the second and third stages are much more difficult to determine.

Trainor et al (93) have reported mechanical studies on very high molecular weight polyethylene of ca 4×10^6. They have noted that density (and therefore crystallinity) which is dependent of the moulding pressure greatly influence and modify the tensile behaviour of polyethylene. They also reported that necking behaviour (measured by the ratio of yield stress/draw stress) is more pronounced for high specific gravity values above 944 Kg/m^3; "work hardening", i.e. orientation of the polymeric chains along the tensile direction is very noticable after 200% extension and is more marked for high molecular weight material.

In this project mechanical properties were studied by impact and tensile measurements. They both demonstrate that samples 54 - 57 are tougher (50% to 90%) than Rigidex 9, Rigidex 2000 and sample 28 although slightly less stiff. It is known that stiffness increases with crystallinity and these results are in agreement with the respective specific

gravity values of our samples (see Table III.7).

Although impact measurements provide useful technical information the tensile stress-strain curve is more informative for the mechanism of deformation of samples under stress. Figure III.14 shows the typical behaviour of Rigidex 9 and sample 56 (identical for this experiment to 54, 55, 57) while they are under tensile stress.

The difference between the curves is obvious after the yield point. The necking behaviour (reported in Table III.6) is more pronounced for Rigidex 9 and sample 28 than for sample 54 - 57. This result is attributed to higher specific gravity values as reported by Trainor (93).

For sample 56 work hardening is very noticable. It sets in soon after yield, i.e. for extensions less than 100%, and increases all the time with extension until failure, whereas for Rigidex 9 the drawing stress remains constant for extension up to 900% and rises slightly before failure occurs. This change of behaviour is partly explained by molecular weight variation although identical behaviour is found for samples 54 - 57 where Mw varies from 800,000 to 4,600,000.

It is suggested from these curves that the re-orientation of the chains during deformation is much more difficult for sample 54 - 57 than for the others. If it is reasonable that one recognises a second stage of deformation as proposed by Peterlin for Rigidex 9 (part of the curve where the drawing stress remains constant) it is impossible to do so for samples 54 - 57. It is suggested

that the morphology of the latter polymers is so different that mechanical forces between the chains prevent the specimen becoming deformed.

It is reported in the literature that a similar deformation behaviour to the above is found in cross-linked linear polyethylene (101), and P.E.T. (102). In this case work hardening is explained through the network deliberately created by the high energy irradiation. It is known that the radiation causes crosslinking between chains in the random zones, i.e. between the lamellar cores (103, 104). The effects due to radiation crosslinking increase in importance with radiation dose.

Long chains are bound from statistical viewpoints to link lamellar cores more tightly than short ones. Further, long chains in melts, if they occur in random coil structures must entangle, the entanglements and entwinments being therefore related to molecular weight (see below). When made into crystalline solids these entanglements finish up in the interlamellar zones further changing the properties of the solid. Ward et al (105) have pointed out that work hardening is a characteristic much altered by network formation. Our measurements support this view since samples 54 - 57 perform like crosslinked polymers in their work hardening.

IV.1.4 Discussion

It has been shown in the previous sections of this Chapter that the rheological, crystallisation and mechanical

properties of samples 54 - 57 cannot be completely explained by their molecular weight characteristics, branching or other easily recognised characteristics of the polymers. It is suggested that the differences and unexpected results found for our samples 54 - 57 are due to molecular morphology different from Rigidex 9 and sample 28.

After due consideration of possible differences between the various grades of polyethylene described above and rejection of the more bizarre explanations it is concluded that entanglement is the most probable difference between them.

It is first of importance to define clearly what is meant by an entanglement: publications about entanglement are not numerous and one does not know how to measure the property precisely mainly because there is no accepted definition of the phenomenon. Workers refer often to "entanglement" without precisely stating what they mean by the word.

In the melt, molecules adopt a random configuration as they do when they are in solution, but the chains are not entirely excluded from interfering with each other and they form a very confused mass. It is reasonable to suggest that in this confused mass chains make loops between themselves; we define an "entanglement" as the phenomenon which results in the chain breaking if one, as it were, tries to pull chains out from polymer. This is different from "entwinment" which is an overlapping of several chains in a portion of volume and which can be destroyed without involving rupture of the chains (Figure IV.3).

It is widely accepted that in the melt the chains tend to an equilibrium configuration which involves a statistical number of entanglements per unit volume: this statistical

number is related to the chain length therefore to the molecular weight of the material. Although relationships between the degree of entanglement and molecular weight are widely accepted they are not quantified. However, it is suggested that a small increase in molecular weight will result in a very noticable increase in the degree of entanglement.

Of course due care has to be taken to guarantee that the entanglement defined in this thesis is the same as that quoted in the literature. It is likely that other authors mean entanglement and entwinment. Many authors seem to feel that this entanglement effect becomes important in chains longer than 10^3 C atons. Obviously, if this problem is to be properly controlled and understood it is insufficient to know only the $\overline{Mn}$ and $\overline{Mw}$ values, one urgently needs G.P.C. data. Unfortunately, as explained earlier, these were not available in this research on our new samples.

The number of entanglements can only be varied by chain rupture or if a chain is able to move over long distances along its axis. In the melt it is well established that this motion is negligible. If there is a wriggling motion of chain sectors (Brownian motion) the centre of gravity of the chain does not translate. It has to be pointed out here that the reptation model proposed by De Gennes (30) has been lately challenged by the same author (31).

The only possibilities of a chain to become more or less entangled occurs when this chain is able to move along its axis. This may happen in several different cases:

i) during its creation (polymerisation) chains can grow from active centres of catalyst by insertion reactions. As they are formed, the chains may form loops between themselves and become entangled.

ii) during the working up of polymer, cooling or introduction of non-solvent may modify the morphology of the polymer network. This will be outlined later.

iii) when polymer is dissolved in a solvent the first stage corresponds to a swelling of the chains. This

swelling, in fact, corresponds to an overall negative propagation of a chain along its axis and may therefore disentangle itself from others. Evaporation of solvent causes the reverse phenomenon.

iv) during crystallisation either from solution or from melt molecules must move to form crystalline lamellae. This phenomenon may also involve modification of entanglements.

The effect of entanglements on polymer properties is very readily envisaged:

i) melt viscosity measures the ease of flow and the ability of polymer chains to slide past each other. Entanglements which act as a sort of physical cross-linking will restrict molecular motion of chains which are trapped between themselves by "knots". Hence the viscosity will be increased.

ii) during melt crystallisation, if the chains are entangled they will have more difficulty in alligning themselves around a nucleus; it is therefore expected that the degree of crystallinity will become lower. The crystal morphology will remain unchanged but the amo rphous phase is then supposed to be more confused and entangled. Flory (29) reported that during melt crystallisation entanglements, as any other defect, are rejected into the amo rphous phase. Scerri (94) also suggested that entanglements prevent to some extent crystallisation from taking place.

iii) mechanical properties will of course be very

sensitive to this phenomenon. As they depend greatly on the amourphous phase, the change in its morphology will modify the mechanical behaviour of polymers. It is suggested that entanglements will restrict the re-orientation of chains and that greater energy will be required to draw the material as more ruptures of chains will be necessary. (Ward (95) reported that in high molecular weight materials, the network relates primarily to physical entanglements and further deformation requires that these be destroyed or that chain scission occurs).

As a result, it is reasonable to assume that differences in the level of entanglements between samples 54 - 57 and 28 and Rigidex may well explain the various observed results in melt viscosity, crystallisation and mechanical properties which cannot be fully explained by molecular weight variations.

However, the fact that lamellar thickness rises whilst crystallinity decreases is not easily explainable. It would have been expected that a decrease in both lamellar thickness and crystallinity would have occurred. It is also expected that entanglements will modify the behaviour of polymers in solutions. It has been reported (96) that solution viscosity increases with entanglement; in some cases it is presumed that polymers cannot fully be dissolved. This phenomenon was observed in dissolving samples 54 - 57 for light scattering measurements. It was suggested at that stage that data obtained could refer to groups of molecules closely entangled rather than to individuals. Why do we

think that our polymers 54 - 57 are more entangled than the other grades studied here (28 in particular)? This is a question to which an answer is proposed below.

As discussed previously, for very high molecular weight materials entanglements are inevitably present modifying greatly the morphological structure of the polymer. In other words it is suggested that if samples 54 - 57 are more entangled than the others, this may be due to higher molecular weight values.

Despite the molecular weight effect causing some of our samples to be entangled, another explanation may be derived from the polymerisation reactions and the working up procedure.

All our prepared polymers were made under fairly similar conditions. The polymers obtained, however, do not have identical characteristics and properties. Variations of molecular weight are noticable and it is known that exact reproducibility cannot be maintained from one polymerisation to another. Nevertheless, it has been shown that variations of molecular weight cannot completely explain the differences observed in rheological and mechanical properties.

The main difference between the polymerisations of sample 28 and samples 54 - 57 was not the polymerisation conditions themselves but rather the cleaning and working up procedures.

After its creation, sample 28 was allowed to cool down when it was still in the presence of its solvent. It was then washed with HCl and methanol at room temperature as described in Section III.1.2. On the other hand, sample 54 - 57 were held at 65°C with their polymerisation solvent and

the cleaning procedure took place at this temperature.

When monomer polymerises, chains grow from an active centre of the catalyst following a mechanism as described by Cossee (97, 98)(cis-ligand insertion). It is thought that at a temperature of 65°C and with an aliphatic solvent (i.e. a good solvent) the polymer produced forms a structure similar to that of the "fringed micelle" model. In other words, chains meander through crystals and amourphous phases all surrounded by a solvent which tends to exclude chains from each other and to swell the polymer.

If a mixture is allowed to cool down, as for sample 28, it is suggested that the chains reorganise themselves by a reeling-in process and that the fringed micelle structure is partially destroyed. However the introduction of alcohol into the still hot mixture may prevent reorganisation of the chains from taking place. If this is so, the polymer then obtained still has a fringed micelle structure and it is suggested that entanglements between chains are more numerous in this case.

As a result, it is assumed that entanglements are created during the polymerisation (as the chains grow) but that they can be partially destroyed during the cleaning and working up procedure. Downs (99) has indicated that properties of polymeric materials have been found to depend on the purification treatment after polymerisation.

It is suggested that this project has to be enlarged in order to study more carefully and to improve the creation of entanglements by polymerisation processes. This could

lead to the creation of very highly entangled materials which will behave identically to cross-linked polymers. It is reasonable to assume that if the polymer is extremely entangled it will become a gel in the molten phase.

IV.2 Conclusion

The challenge of various theories regarding semi-crystalline polymer morphology lead us to investigate the correlation between properties (melt, crystallisation and mechanical) and morphology. Because of its structural simplicity this study was made on linear polyethylene.

In order to carry out this research programme, polymers had to be made under unusual polymerisation conditions and compared with commercial ones. A lot of time was expended in finding acceptable conditions to produce polymers in sufficient quantity and with acceptable molecular weight characteristics. Material restrictions which were beyond our control prevented us from carrying out further unusual polymerisations and therefore considerably limited the field of this research.

Nevertheless, it has been found that among our specially produced polymers some of them exhibited remarkable properties and unusual crystallisation characteristics. It has been proved that these cannot be explained fully by any readily measured polymer characteristics such as molecular weight and branching; only a change in morphology of the polymer chains could explain the behaviour of our materials.

The presence of entanglements, as defined previously, is the most plausible suggestion which explains the observed properties of our polymers. It is suggested that although some entanglements are created as the polymer chains grow during the polymerisation process, the cleaning and working-up procedure may well modify the content of entanglement, merely by diminishing it.

Although this research programme is far from complete it reveals that the morphology of the polymer molecule can be modified and that in favourable cases better properties can be obtained without increasing molecular weight.

In order to investigate in greater depth and to complete this research programme some suggestions are now given:

i) more work should be undertaken in polymerisation reactions. It is of importance to bear in mind that it is at that stage that entanglements are created because the chains are able to move along their axes; if the growth rate (propogation rate) of each chain could be controlled by polymerisation conditions (temperature, nature of monomer, catalyst, etc.) this could control the degree of entanglement. Effectively, it is thought reasonable to assume that when chains grow slowly they have time to meander and meet other growing chains to form entanglements; if they grow very quickly the chance of forming an entanglement is diminished because the chains will form a bunch of mass within themselves. It is also of importance to adjust the concentration of active centres. If they are very near each other the nascent chains must entangle. This requires more knowledge about catalysis and the creation of catalysts in which all the active centres are effectively active and produce polymeric chains. It is suggested that to create very different materials using entanglements, polymerisation conditions must be drastically varied from one experiment to another. This also implies a more complete study of the effect of solvent (good or bad solvent) and the effect of

temperature. Polymerisation in total solution (high temperature in Xylene or decalin) could be of considerable interest.

ii) studies should be made on cleaning and working up procedures. It is there that entanglements may disappear if a proper working up method is not found. The aim of this procedure is to remove the solvent and dry the polymer without destroying the structure created, by allowing the polymer chains to reorganise themselves.

Further work is also required to reveal the presence of entanglements and hopefully to estimate the degree of entanglement.

This could possibly be achieved by determining the various properties of virgin polymers and those of polymers which have been dissolved up several times in an appropriate solvent (Xylene or decalin for example). Solutions must be very dilute and this requires large amounts of solvent in order to dissolve several grammes of polymer to be able to carry out mechanical testing or viscosity measurements afterwards. It has been suggested earlier that dissolution involves an overall negative motion of chains which could therefore lead to disentanglement. A diminution of molecular weight may then also be observable; this would not correspond to degradation but to disentanglement, as light scattering measurement would correspond on individual molecules rather than groups. In order to complete the study of polymers in solution, solution viscosity measurements should be also undertaken.

It has been assumed that entangled polymers which are tested on tensile experiments will lead to more chains ruptures than unentangled ones. If this is so the number of free radicals created could be related to entanglement. A suitable experiment has to be found in order to confirm this hypothesis. E.S.R. Spectrometry seems very adequate if tensile experiments could be achieved in the area sample of the Spectrometer.

It is also suggested that several extrusions of polymer melt would break down the structure of the polymer and consequently that molecular weight reduction would be noticable.

REFERENCES

1. P.J. HENDRA and H.P. JOBIC, J.Polym.Sci., Polym. letters Ed., 13, 365, (1975)

2. M. SELWOOD, B.Sc. Dissertation, Southampton University, (1979)

3. A.V. TOBOLSKY, Properties and Structures of Polymers, Ed. John Wiley & Sons, Inc. (1967)

4. C.W. BUNN, Trans. Faraday Soc., 35, 482, (1939)

5. K. HERRMANN and O. GERNGOSS, Kantschuk, 8, 181, (1932)

6. W.M.D. BRYANT, J.Polymer Sci., 2, 547, (1947)

7. A. KELLER, Phil.Mag., 2, 1171, (1957)

8. E.W. FISHER, Z Naturforsch, 12A, 753, (1957)

9. P.H. TILL, J.Polym.Sci., 24, 301, (1957)

10. B.G. RANBY, F.F. MOREHEAD and N.M. WALTERS, J.Polym.Sci., 34, 349, (1960)

11. M. KOJIMA, J.Polym.Sci., A2, 5, 397, (1967)

12. P.H. GEIL, N.K.J. SYMONS and R.G. SCOTT, J.Appl.Phys., 30, 1516, (1959)

13. P.H. GEIL, J.Polym.Sci., 44, 449, (1960)

14. Y. YAMASHITA, J.Polym.Sci., A3, 81, (1965)

15. A. KELLER and A. O'CONNORS, Disc. Faraday Soc., 25, 119, (1958)

16. P.H. GEIL, Polymer Single Crystals, Interscience, (1963)

17. D.H. RENEKER, J.Polym.Sci., 59, 532, (1962)

18. P. DREYFUSS and A. KELLER, J.Polym.Sci., 138, 253, (1970)

19. A. KELLER, Rept.Progr.Phys., 31, (11), 623, (1968)

20. H.F. KAY and B.A. NEWMAN, J.Appl.Phys., 38, 4105, (1967)

21. R.P. PALMER and A.J. COBBOLD, Die Makromol. Chem., 74, 174, (1964)

22. D.C. BASSET, F.C. FRANK and A. KELLER, Phil.Mag., 8, 1753, (1963)

23. E.W. FISHER and R. LORENZ, Kolloid-Z., Z. Polymere, 189, 97, (1963)

24. J.B. JACKSON, P.J. FLORY and R. CHIANG, Trans. Faraday Soc., 59, 1906, (1963)

25. T. KAWAI, Makromol. Chem., 90, 288, (1966)

26. H. HENDUS and K.H. ILLERS, Kunststoffe, 57, 196, (1967)

27. E.W. FISCHER and G.F. SCHMIDT, Angew.Chem.Int.Ed.Engl., 1, 488, (1962)

28. P.J. FLORY, Principles of Polymer Chemistry, Cornell University Press, Ithaca, New York, (1953)

29. P.J. FLORY and D.Y. YOON, Nature, 272, 226, (1978)

30. P.G. DE GENNES, J.Chem.Phys., 55, 572, (1971)

31. P.G. DE GENNES, Journ.Chem.Phys., 76, 763, (1979)

32. P.J. FLORY, Pure Appl.Chem. Macromol.Chem., 8, 1-15, (1973)

33. W.M.D. BRYANT, J.Polymer Sci., 2, 547, 564 (1947)

34. RICHARDS, J.Appl.Chem., (1951)

35. ASTM D 1238, BS, 2782

36. D.J. CUTLER, P.J. HENDRA and R.D. SANG, Faraday Discussion 68/10 (1979)

37. M. GLOTIN, Ph.D Thesis, Southampton (1979)

38. H. BENOIT, J.Chem.Phys., 63, 1507, (1966)

39. J.C. MOORE, J.Polym.Sci., A2, 835, (1964)

40. Waters : Waters Associates, Inc., Framingham, Mass., 01701

41. Lord RAYLEIGH, Phil.Mag., (4), 41, 447, (1871)

42. Lord RAYLEIGH, Phil.Mag., (5), 12, 81, (1871)

43. P. DEBYE, J.Appl.Phys., 15, 338, (1946)

44. P. DEBYE, J.Phys. & Coll.Chem., 51, 18 (1947)

45. B.H. ZIMM, J.Chem.Phys., 16, 1099, (1948)

46. K.A. STACEY, Light Scattering in Physical Chemistry, Butterworths, London, (1956)

47. P.M. DOTY and R.S. STEINER, J.Chem.Phys., 18, 1211, (1950)

48. J.M.G. COWIE, Polymers: Chemistry and Physics of modern materials, published by International Textbook Company Limited, Aylesbury, Bucks., England, (1973)

49. F.W. PEAKER, Chap 5, Techniques of Polymer Characterisation, Butterworths, London (1959)

50. H. BENOIT, J.Chem.Phys., 65, 23, (1968)

51. P.J. HENDRA, Chapter in "Polymer Spectroscopy" (D.O. HUMMEL editor) Verlag Chemie, Germany (1974)

52. G. HERZBERG 'Infrared and Raman Spectra of polyatomic molecules', D. Van Nostrand Co., Princeton, N.J. (1945)

53. G. HERZBERG 'Spectra of diatomic molecules', D. Van Nostrand Co., Princeton, N.J. (1945)

54. P.J. HENDRA and T. GILSON, 'Laser Raman Spectroscopy', J. Wiley, Interscience, London, (1970)

55. A. SKEMAL, Die Naturwiss, 11, 875, (1923)

56. C.V. RAMAN, J.Opt.Soc.Am., 15, 185 (1923)

57. S. MIZUSHIMA and T. SHIMANOUCHI, J.Chem.Phys., 71, 1320 (1949)

58. W.L. PETICOLOS, G.W. HIBBERT, J.L. LIPPERT, A. PETERLIN and H.G. OLF, J.Appl.Phys. Letters, 18, 87, (1971)

59. P.J. HENDRA, E.P. MARSDEN, M.E.A. CUDBY and H.A. WILLIS, J. Makromol. Chem., 176, 2443 (1975)

60. H.G. OLF, A. PETERLIN and W.L. PETICOLOS, J.Polym.Sci., Letters Ed., 12, 359, (1974)

61. D.H. RENEKER and B. FANCONI, J.Appl.Phys., 46, 4144, (1975)

62. B. FANCONI and J. CRISSMAN, J.Polym.Sci. Poly. Letters Ed., 13, 421, (1975)

63. G.A. MORTIMER, J.Appl.Polym.Sci., 20, 55 (1976)

64. A.D. CAUNT, I.C.I. Plastics U.K. (Private communication)

65. P.J.M. MATHIEU, 1st year Dissertation, University of Southampton, (1979)

66. Polymer Handbook

67. A. TITTERTON, I.C.I. Plastics U.K. (Private communication)

68. F. YEARSLEY, Industrial Polymers: Characterisation by molecular weight p 39, Edited by J.H.S. Green and R. Dietz, Transcripta Books, London (1973)

69. A. TITTERTON, ibid p 83

70. F. YEARSLEY (Private communication)

71. J. HASLAM, H.A. WILLIS, D.C.M. SQUIRREL, Identification and analysis of plastics, 2nd Edition, Illffe books, London (1972)

72. M.V. VOLAROVICH and N.V. LAZOSKAYA, Colloid J. U.S.S.R., 28, 166, (1966)

73. J.J. BENBOW Lab. Practice, 12, 533, (1963)

74. R.S. HIGGINBOTHAM, J.Sci.Instrum., 27, 139 (1950)

75. K. WEISSENBERG, Principles of rheological measurement (London: Nelson) p 36 (1949)

76. see 77

77. S. RAMA, M.J. WILLIAMS and P. LAMB, Journal of Sci. Instrum. (Journal of Physics E) series 2, volume 1, 1113, (1968)

78. C.J. HOOLEY, M.J. WILLIAMS, Internal manual, I.C.I. Plastics U.K. (1978)

79. Notice relative to the Model 1101 - Instron Limited England

80. Polymer Handbook, ed. J. Brandrop and E.H. Immergent Interscience Publishers, London (1967)

81. Technigramm on Rigidex 9, British Petroleum Chemicals, U.K.

82. E.P. MARSDEN, Ph.D. Thesis, University of Southampton (1977)

83. I.N. MESHKOUA, N.G. KUDRYAKOUA and N.M. CHIRKOU, Polym.Sci., U.S.S.R., 15, 1220, (1974)

84. M.M. CROSS Polymer 11, 238, (1970)

85. M.M. CROSS Pheologica Acta, 10, 3, 368 (1971)

86. F.N. COGSWELL Polymer melt precessing rheology, p 40, I.C.I. Plastics U.K. (1980)

87. ibid p 83

88. M.S. SWERDLOW (Private communication)

89. M.S. SWERDLOW, et al "Plastics and Rubber processing" p 11 (March 1980)

90. P.J.M. MATHIEU, P.J. HENDRA and R.R. RAMALKAR (unpublished results)

91. D.J. CUTLER, Ph.D. Thesis, Southampton University (1980)

92. A. PETERLIN, Advance in Polym. Sci. and Eng.

93. A. TRAINOR, R.N. HAWARD and J.N. HAY, J.Polym.Sci. Polym.Phys.Ed., 15, 1077 (1977)

94. E.R. SCERRI, M.Phil. Thesis, Southampton University (1979)

95. I.M. WARD

96. F. BUECHE, C.J. COUEN and B.J. KINZIG, J.Chem.Phys., 39, 1, 128 (1963)

97. P. COSSEE J. of Catalysis, 3, 80 (1964)

98. E.J. ARLMAN and P. COSSEE, ibid p 100

99. G. DOWNS, British Petroleum Chemicals Ltd., (Private communication)

100. G.R. STROBL and R. ECKEL, J. of Polym. Sci., 14, 913, (1976)

101. G. CAPACCIO, I.M. WARD and M.A. WILDING, J.Polym.Sci. Polym.Phys.Ed., 16, 2083 (1978)

102. I.M. WARD, Text Res. J. 31, 650 (1961)

103. R. SALOVEY, J.Polym.Sci., 61, 463 (1962)

104. L. MANOELKERN, D.R. ROBERTS, J.C. HALPIN and F.P. PRICE, J.Am.Chem.Soc., 82, 46 (1960)

105. G. CAPACCIO, T.A. CROMPTON and I.M. WARD, J. of Polym. Sci.Polym.Phys.Ed., 14, 1641 (1976)